Journal of Analytical and Applied Pyrolysis 163 (2022) 105479

Contents lists available at ScienceDirect

Journal of Analytical and Applied Pyrolysis

journal homepage: www.elsevier.com/locate/jaap

Review on the catalytic effects of alkali and alkaline earth metals (AAEMs) including sodium, potassium, calcium and magnesium on the pyrolysis of lignocellulosic biomass and on the co-pyrolysis of coal with biomass

Wei Wang [a,b], Romain Lemaire [a,*], Ammar Bensakhria [b], Denis Luart [c]

[a] Department of Mechanical Engineering, École de Technologie Supérieure, Montreal, Quebec H3C 1K3, Canada
[b] Université de Technologie de Compiègne, Centre de recherche de Royallieu, EA 4297-TIMR, BP20529, 60205, Compiègne, France
[c] École Supérieure de Chimie Organique et Minérale, 1 Rue du Réseau Jean-Marie Buckmaster, 60200 Compiègne, France

ARTICLE INFO

Keywords:
Wood
Coal
Catalytic pyrolysis
Alkali and alkaline earth metals
Mechanism
Kinetics

ABSTRACT

Alongside the development of pyrolysis processes aimed at converting solid biomass into upgraded biofuels and biochemicals, interest has been growing in the analysis of the catalytic effects induced by inherent or externally added alkali and alkaline earth metals (AAEMs). These AAEMs greatly affect the thermal conversion of biomass, although their effects are only partly understood. Furthermore, while coal currently plays a major role in global energy demand, its massive use in a carbon-constrained world has prompted the need to identify alternative and carbon-neutral energy sources. In this context, the co-pyrolysis of biomass with coal has been shown to be a promising way to support the transition from fossil to renewable energy carriers. Because AAEMs can significantly impact such a co-processing approach, there is therefore the need for a firm understanding of their catalytic role. Consequently, and to examine and summarize the main research advances that have been made in this field, the present review first covers a description of the main properties of lignocellulosic biomass and coal, along with their decomposition processes. It then focuses on AAEM catalysts and on their impact on pyrolysis reaction pathways and kinetics. In terms of highlights, the review illustrates that the presence of inherent or impregnated AAEMs shifts the decomposition of biomass to lower temperatures while increasing the char and gas yields at the expense of bio-oil. Moreover, these effects depend significantly on the nature of the catalyst considered and on the way it is mixed with biomass. As examples, potassium tends to favor the production of low molecular weight compounds and gaseous species, magnesium promotes dehydration reactions, whereas calcium and magnesium oxides allow to upgrade volatiles by deoxygenation and deacidification. A discussion of pyrolysis reaction mechanisms is also proposed by reviewing the different pathways involved in the decomposition of the main components of biomass and coal, noting that the emphasis is particularly on the changes induced by AAEM catalysts. The synergistic effects between coal and biomass which are likely to enhance the co-pyrolysis process are then discussed. Eventually, a comprehensive reaction pathway is proposed to better explain the important role played by AAEM catalysts during primary and secondary pyrolysis reactions.

1. Introduction

Given the ever-growing environmental concerns related to global warming, biomass, a carbon- neutral fuel, is attracting more and more attention not only for the production of electricity and heat, but also for the synthesis of biochemicals and biomaterials [1]. Raw biomass, which is characterized by a high oxygen content, however, generally needs to be converted into biogas, bio-oil or biochar prior to being used as a convenient energy carrier for energy applications and/or to produce specific value-added chemicals [2,3]. The advantages associated with the use of biomass-derived fuels include a reduced dependence on fossil energies, a decrease in net carbon dioxide emissions and the mitigation of agricultural and household solid waste problems [4,5]. Biochemical and thermochemical processes currently appear to be the most promising routes when it comes to converting biomass into biofuels [6,7]. In short, biochemical methods consist in converting biomass through the enzymatic activity of micro-organisms. On the other hand, thermochemical processes involve the conversion of dried biomass (whose

* Corresponding author.
E-mail address: romain.lemaire@etsmtl.ca (R. Lemaire).

https://doi.org/10.1016/j.jaap.2022.105479
Received 12 September 2021; Received in revised form 15 February 2022; Accepted 18 February 2022
Available online 23 February 2022

moisture content is less than 10%) through the action of heat, which can be achieved by different methods, including pyrolysis, gasification, hydrothermal liquefaction, hydrothermal carbonization, etc. [2,7,8].

As far as pyrolysis is concerned, it is the first step (and thus a critical one) in the thermochemical conversion of biomass. It plays a key role in the estimation of fuel conversion rates and kinetics, in addition to influencing the prediction of the nature and distribution of pyrolysis products, while being an essential process to be considered for the proper design of reactors [2,9–11]. Basically, pyrolysis consists in decomposing biopolymers present in biomass as a result of heating under an inert atmosphere, which leads to the release of a wide variety of products formed in three states: a carbon-rich solid residue called char, a condensable vapor fraction composed of a complex mixture of water and organic species, and a non-condensable gaseous phase [1]. However, pyrolysis products obtained directly from raw biomass usually present certain disadvantages, due to their high oxygen content, which leads to high corrosiveness and a low heating value [12]. Besides, the pyrolysis of raw biomass is often affected by limited conversion yields and selectivity. Therefore, additional upgrading processes, including catalytic pretreatments, are often necessary to improve the quality and the target product yields [13]. Within this framework, the use of zeolites as catalysts has been widely investigated [14–17]. It allows to directly convert pyrolysis-derived volatile molecules into value-added chemicals such as aromatics and olefins [18]. However, zeolite micropores are easily deactivated by the coke and liquid products deposits, which usually contain a large quantity of carcinogenic polycyclic aromatic hydrocarbons (PAHs) [19]. Another possible means of improving the conversion efficiency of biomass through pyrolysis relies on the use of metal components as catalysts to treat biomass feedstocks, either in situ or ex situ. Such catalysts are typically classified into three categories (natural, primary and secondary) depending on the specific reactions on which they act [20]. Apart from the three main biopolymer components, namely, cellulose, hemicellulose and lignin, lignocellulosic biomass also contains traces of extractive and mineral ash. The mass percentage of mineral ash generally varies from less than 1–15%, depending on the considered feedstock [21]. Despite such low concentrations, the presence of mineral ash in biomass is still considered as an important factor influencing the pyrolysis process [22]. It must therefore be taken into account, although many early modeling works focused on the pyrolytic behavior of the three main biopolymer components while neglecting the impact of inorganic species [23]. To address this issue, the catalytic effect of inherent and added metal compounds on biomass pyrolysis has been increasingly investigated during the last decades. Among these metal elements, alkali and alkaline earth metals (AAEMs) are largely present in raw lignocellulosic biomass and can drastically influence the yields and composition of bio-oils [20,24]. Their use in industrial processes is considered as extremely promising due to their low price and toxicity, along with their ready availability for industrial needs. Furthermore, the addition of AAEMs to biomass feedstocks usually allows to promote biomass degradation, shifting the pyrolysis process to lower temperatures and improving the yield and quality of high-value products.

Despite the growing interest in the use of biomass as an energy carrier, coal remains one of the most widely used resources worldwide for producing electricity and heat. Indeed, it currently accounts for around 40% of global electricity generation. It is, moreover, considered as a very convenient feedstock for the production of chemicals. Thanks to large reserves and low exploitation prices, coal currently covers about one-third of global primary energy needs, and will remain an important energy source for the foreseeable future [25]. This solid fuel is classified into the following categories, in increasing rank order: peat, lignite, subbituminous and bituminous coals, and anthracite. The use of a coal type for a given application mainly depends on its coalification level as well as on resultant factors, including the quantity of volatiles contained within the fuel or its heating value [26]. The pyrolysis of coal consists in the thermal decomposition of the carbonaceous material forming the fuel at 200 °C or above in an atmosphere deprived of oxygen. As in the case of biomass, pyrolysis is the initial step in almost all coal conversion processes. It thus has a critical influence on the subsequent reaction stages, and determines the yields and properties of pyrolytic products (e.g., volatiles, tar, char) as well as their reactivity and conversion efficiency [27]. Coal pyrolysis typically involves a wide variety of mechanisms, including desorption, gasification, distillation, hydrogenation, hydrocracking, condensation and carbonization [26–30]. It is thus quite a complex process, basically decomposed into two competing phenomena. The first one corresponds to depolymerization, which induces the breakage of chemical bonds, along with the release of water and tar, while the second consists in repolymerization reactions leading to the formation of solid char. Different factors can affect coal thermal decomposition, including the conversion temperature, the fuel heating rate, the reactor configuration, etc. [31–33]. As a consequence, a good understanding of coal pyrolysis is required in order to be able to properly design and optimize industrial coal conversion units [28,34]. As far as the composition of coal is concerned, it essentially contains carbon, with other elements such as hydrogen, oxygen, sulfur, nitrogen and some mineral matters. Among these mineral matters, alkali and alkaline earth metals (mainly Na, Mg and Ca) are important components which can play a catalytic role that can have an impact on pyrolysis product distribution and yields [35]. The catalytic effect of AAEMs increases globally with the decreasing coal rank [27]. When released with gaseous volatiles, AAEM species can induce corrosion, slagging and ash deposits on the surface of superheaters [36–39]. Alternatively, when contained in the char, AAEMs will act as catalysts for the subsequent gasification and conversion processes [38]. A comprehensive characterization of the role and efficiency of AAEMs on reaction mechanisms and kinetics is thus necessary to facilitate the industrial deployment of coal pyrolysis. This notwithstanding, and even though coal is widely used worldwide for electricity production, a major drawback with such an intensive utilization, as mentioned earlier, is the release of massive amounts of carbon dioxide into the atmosphere [40,41]. With the ever-growing consciousness of the threats posed by global warming and air pollution, coal processing is therefore regarded with increasing caution [27]. In this respect, the co-pyrolysis of coal with lignocellulosic biomass is considered as one of the most promising strategies to alleviate carbon dioxide emissions resulting from coal conversion in industrial systems. Various works, moreover, have highlighted the fact that synergistic effects are likely to increase the yield of emitted volatiles when coal is co-pyrolyzed with biomass, and thus enhance the overall efficiency of the conversion process [42]. Furthermore, the increase of the H/C ratio induced by the addition of biomass to coal also tends to inhibit the yield of heavy oil and tar produced [42] while the presence of AAEMs has a remarkable influence on co-pyrolysis reactions and products. As an example, the reactivity of char issued from co-pyrolysis is generally higher than that of char obtained from the pyrolysis of only one feedstock, which can be attributed to the fact that the retained and concentrated AAEM species in co-pyrolysis-derived char can act as catalysts during the subsequent char conversion stages [42].

When conducting a preliminary survey of the literature devoted to the analysis of the impact of alkali and alkaline earth metals on pyrolysis, it can be noted that a wide variety of parameters (e.g., type of feedstock and catalyst, impregnation mode, reactor configuration, operating conditions, etc.) have been considered to elucidate, through both analytical and kinetic approaches, the effect of AAEMs on the conversion efficiency, as well as on the nature and quantities of pyrolytic products released. Without loss of generality, one can cite, among recently published works, the 2014 study by Veses et al., who used an auger reactor to investigate the catalytic effects of calcium and magnesium oxides on the pyrolysis of wood [43]. Zhang et al. subsequently used Fe/CaO catalysts to prevent calcium oxide (CaO) deactivation and to thus upgrade biomass fast pyrolysis vapors by reducing the quantity of oxygenated species [44,45]. In a 2015 paper, Wang et al. used the integral Coats-Redfern kinetic method to study the catalytic effect of

potassium and calcium chlorides on the pyrolysis of lignin [46]. Notably, that led the authors to note a decrease in the activation energy associated with the main stage of the degradation process when adding potassium chloride (KCl) or calcium dichloride ($CaCl_2$) to lignin. Later, Dalluge et al. compared the influence of seven AAEM salts on char and volatile yields issued from the fast pyrolysis of lignin [47]. For their part, Deng et al. investigated the release and transformation of inherent potassium during the pyrolysis of different types of biomass, including wheat straw, corn stalk and rice hull [48]. Meanwhile, Liu et al., Wang et al., Leng et al. as well as Zhang et al. proposed possible pathways allowing to explain the mechanisms at play during the AAEM-catalyzed pyrolysis of biomass [4,46,49,50]. In parallel, many investigations of the influences of AAEM catalysts on the pyrolysis of coal and on the co-pyrolysis of coal with biomass have been conducted. For example, it has been shown that the use of CaO additive enhances the pyrolysis of coal and the co-pyrolysis of coal/biomass mixtures by favoring cracking reactions that increase the content of high-valued tar products while inducing a higher quantity of gaseous species produced [26,51–53]. By investigating the role of four AAEMs impregnated on raw coals and demineralized coals, Yan et al. confirmed the good catalytic activity of alkali and alkaline earth metals in the decomposition of condensed aromatics into light aromatic hydrocarbons [35]. Furthermore, the authors traced the catalytic role of cations in the reduction of tar yields to their ability to prevent the diffusion of large tar molecules while catalyzing the repolymerization and condensation of these compounds as well as increasing the stability of surface groups [54,55]. Within the framework of an analysis relying on the use of a reactive molecular dynamic simulation method, Hong et al. showed that calcium rarely affects the primary pyrolysis of coal, but significantly promotes the secondary reactions of tar, which results in an increase of gas and char yields [36]. Zhao et al. subsequently proposed an infrared structural parameter method to analyze the impacts of intrinsic AAEMs on the chemical structure of low-rank coal char [27]. Some authors additionally explored the role of inherent mineral matters in coal by comparing the pyrolytic results issued from the analysis of acid-washed coals with those obtained with raw fuels [27,35]. Tian et al. eventually analyzed the kinetics and products issued from the co-pyrolysis of various coals with biomass (i.e., *Miscanthus sacchariflorus*) and showed the important role of inherent mineral matters (iron oxide (Fe_2O_3), CaO and potassium oxide (K_2O)) on the synergistic effects that influence the thermal decomposition and the nature of the vapor phase species released [5].

This brief overview of the literature on the effects of AAEMs on the pyrolysis of lignocellulosic biomass and on the co-pyrolysis of coal/biomass blends clearly shows how this topic has attracted the attention of many research groups, with hundreds of articles published during the last two decades. Nevertheless, during the same period, a few works still tried to compare all reported results with a view to better determining the roles of AAEMs on pyrolysis mechanisms and kinetics. In addition, inconsistent trends or contradictory conclusions sometimes emerge from published studies, which may be traced to differences in the selected feedstocks, experimental conditions, catalyst loading, demineralization pretreatments, etc. [27]. The literature review proposed herein thus aims at summarizing and comparing experimental/numerical results and conclusions that have been reported regarding the catalytic effects of AAEMs on the pyrolysis of biomass. Furthermore, and as explained above, the co-pyrolysis of blends composed of coal with lignocellulosic biomass has proven to be a relevant option to improve the conversion of these energy carriers while reducing the adverse effects on the environment induced by the sole use of fossil resources. Consequently, and even though the present review deals predominantly with the catalytic pyrolysis of biomass, co-pyrolysis cannot be overlooked, and will indeed be examined. That is why information regarding the main features of coal will be colligated in the first section of this document in addition to a thorough presentation of the characteristics and properties of biomass. A detailed description of the mechanisms governing the pyrolysis process will then be given, after which the focus will be directed to the pretreatment strategies currently adopted to prepare the feedstocks before their processing. Similarly, the fundamental effects of AAEMs on the main conversion pathways and kinetics will be addressed. As a deep understanding of the phenomena involved at the molecular level is essential for a proper development of the processes relying on the catalytic thermal conversion of solid fuels, a concluding section aimed at summarizing the role of AAEM catalysts on major decomposition routes will finally be proposed. Of note, unresolved questions laying out avenues for future works to be undertaken will be highlighted throughout the paper.

2. Feedstock composition and properties

2.1. Biomass characteristics

There are three main natural polymeric constituents composing the lignocellulosic biomass: cellulose, hemicellulose and lignin (see Fig. 1). The rest are comprised of non-structural low molecular weight extractives, along with inorganic ash. Although the mass fractions of cellulose, hemicellulose and lignin widely vary depending on the type and origin of the biomass feedstock, they typically reach values of 38–50%, 23–32% and 15–25%, respectively [23]. These main components contain many functional groups, such as -OH, C═C (aromatic ring), C═O, C-O-C, C-O-H, -OCH_3 and -COOH, all connected together via hydrogen and covalent bonds [56]. Cellulose is essentially coated with hemicellulose, whereas lignin fills up the empty space (see Fig. 2).

Cellulose, the most abundant natural polymer in plant cells, consists of linear chains of glucose units linked by β-1,4-glycosidic bonds that are relatively weak and thus tend to cleave under heating or within acid media [8]. The degree of polymerization (noted n) of cellulose, whose chemical formula is denoted $(C_6H_{10}O_5)_n$, can reach values higher than 5000 [2] and possibly as high as 15,000 [8] in the case of woody fiber. By using Fourier transformed infrared spectroscopy (FTIR), Yang et al. showed that cellulose exhibits higher contents of OH and C-O as compared to hemicellulose and lignin [56]. The presence of numerous hydroxyl groups on the cellulose chain notably enables the formation of intra- and inter-molecular hydrogen bonds, contributing to the stabilization of a three-dimensional network composed of cellulose flat sheets [57,58]. The cellulose ultrastructure can be classified into crystalline and amorphous regions based on the arrangement pattern of the chain molecules. The crystalline region is characterized by a packed cellulose structure enabling a better thermal stability as compared to the amorphous region, which is loose and disordered [59]. The crystallinity index denoting the relative amount of crystalline material in cellulose is globally comprised between 30% and 60% for biomass fibers. Regarding the temperature range of cellulose degradation during pyrolysis, it is

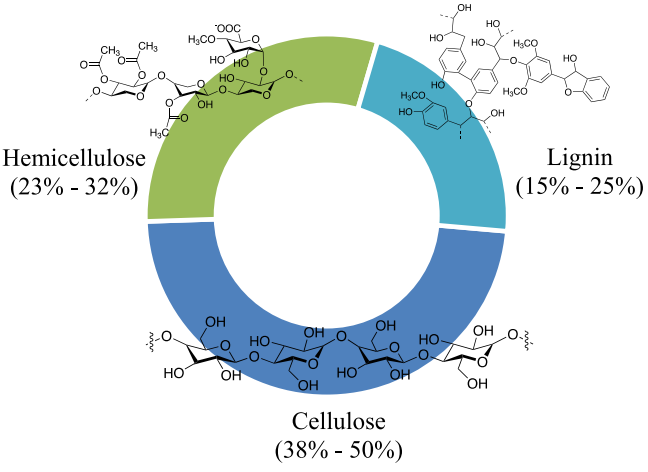

Fig. 1. Composition of the three main biomass components.

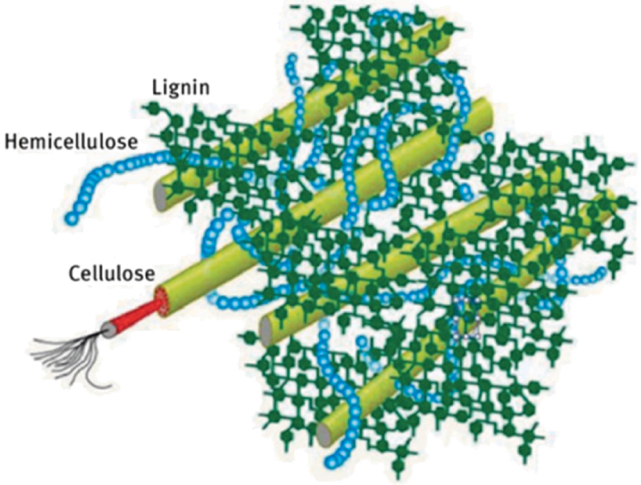

Fig. 2. Schematic representation of the structure of lignocellulosic biomass. Reprinted from Wang et al. [8].

typically comprised between ~260 and ~400 °C [56,60].

As far as hemicellulose is concerned, it corresponds to an amorphous and branched structure made up of a mixture of short-chain hetero-polysaccharides. The principal chain of hemicellulose is usually composed of branched five-carbon or six-carbon monosaccharide units (such as glucose, mannose, galactose, arabinose or xylose) with uronic acids, acetyl groups or monosaccharides that complete the structure. The polymerization degree of hemicellulose is usually less than ~200. Hemicellulose can more easily be cleaved than cellulose or lignin by depolymerization under heating conditions because of its amorphous, branched and random structure [56,60]. This in turn leads to the degradation of hemicellulose at lower temperatures comprised between ~190 and ~350 °C, with a maximal mass loss at around 290 °C [56,60].

Lignin globally corresponds to an amorphous complex made up of a three-dimensional polymer composed of three so-called phenylpropane units, that contain a phenyl group and a propyl side chain. These basic elements, which include p-hydroxyphenyl (H-type), guaiacyl (G-type) and syringyl (S-type) units, differ from one another, depending on the number of methoxy groups attached to the aromatic ring (see Fig. 3). The relative proportion of H-, G- and S-type units in lignin largely depends on the type of biomass involved. For instance, softwood lignin mainly contains guaiacyl units, hardwood lignin is typically made up of both syringyl and guaiacyl components, while grass lignin consists of a mixture of the three types of phenylpropane units [8]. In addition to methoxy groups, lignin also contains hydroxyl, carboxyl or carbonyl fragments, which directly impact its reactivity. Lignin base units are linked through covalent bonds such as ether, carbon-carbon and ester ones, with the most common linkages being β-O-4 (the main one accounting for 43–65%), α-O-4, 4-O-5, 5–5, β-1 and β-5 [2,8,19] (see Fig. 4). The relative proportion of each of these linkages differs

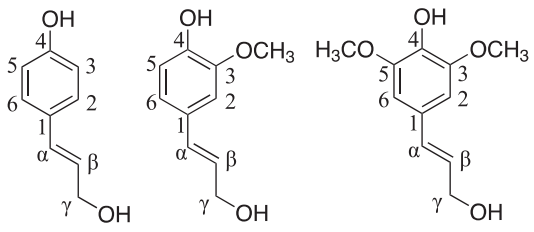

Fig. 3. Basic units of lignin.

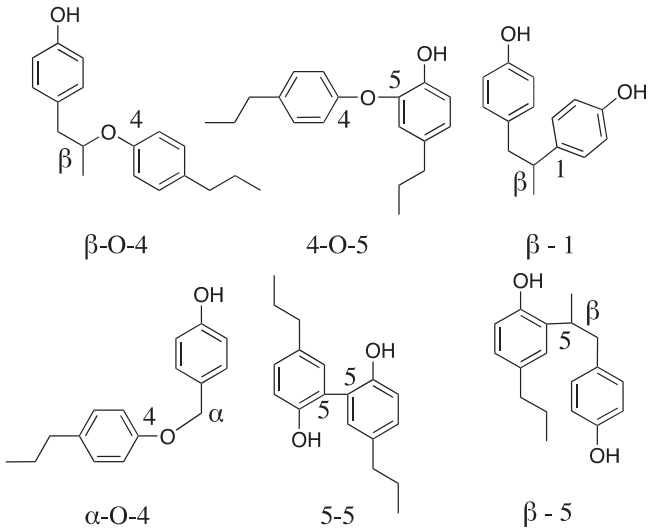

Fig. 4. Examples of linkages present in the lignin structure.

according to the biomass resource, with hardwood lignin having generally higher ether linkages and lower carbon-carbon bonds than softwood, as an example. This can be attributed to the structure of the monomer units, as hardwood contains more syringyl units where two methoxy groups are connected to an aromatic ring, while softwood lignin is composed mainly of guaiacyl lignin. These connections directly affect the pyrolysis behavior of lignin. In fact, ether linkages such as the above-mentioned α-O-4 and β-O-4 are relatively weak, and can easily be broken, unlike carbon-carbon linkages, which tend to enhance the rigidity of lignin, thus making it more difficult to degrade under heating. As a result, the lignin degradation temperature range is broader than that of the other biomass components, and typically extends from ~150 to ~900 °C [12,19,56,61].

In addition to the above-listed components, biomass also contains some extractives and inorganic compounds. Regarding extractives, they consist of organic species that can be soluble in polar or non-polar solvents, and include waxes, fats, sugars, starches, pectin, proteins, gums, etc. [8,61]. Inorganic elements in biomass essentially include aluminum, calcium, iron, potassium, magnesium, sodium, phosphorus, silicon, and some other heavy metals whose concentration is dependent upon the type of biomass (see Table 1). Such species are present in water-soluble inorganic salt (mainly sodium and potassium) as well as under mineral and/or organically-bonded states (mainly calcium and magnesium) [23,65,68–70], noting that metal ions bonded in the organic structure are ion-exchangeable with protons that can thus be eliminated by acid washing [70–72], as discussed in Section 4.1.1. Their relative quantity is usually assessed using Inductively Coupled Plasma Mass Spectrometry (ICP-MS) or Inductively Coupled Plasma Atomic/Optical Emission Spectrometry (ICP-AES/OES). Moreover, the ash fraction, which is one of the main proximate analysis parameters (see Table 2), allows characterizing the solid inorganic residues issued from the oxidation of biomass, given that the minerals are present therein in the form of oxides such as silicon oxide (SiO_2), CaO and K_2O. Generally speaking, agricultural and herbaceous biomass contain more ash (up to 30% ash) than woody biomass (<0.5%) [8,61,69]. Besides, and as depicted in Table 2, the volatile content of biomass remains quite high (>50%) regardless of the feedstock, contrary to the percentages of C or O issued from the ultimate analyses, which tend to significantly differ as a function of the raw material.

Finally, it should be noted that alkali and alkaline earth metals (especially calcium, potassium and magnesium) are significantly present in forestry plants and agricultural harvests [4,20,24,69,91]. Here again, their content in biomass is a function of a series of factors, including the type of plant, the soil properties and the surrounding weather conditions

Table 1
Composition of mineral matter in raw biomass.

Biomass feedstock	Inorganic content (ppm (except for ash content) - dry basis)										
	Ash content (wt%, db)	Al	Ca	Fe	K	Mg	Na	P	S	Si	Reference
Woody biomass											
Moso bamboo	–	–	346	61	1 000	188	15	197	370	–	[62]
Poplar wood (*Populus albaglandulosa*)	0.7	19	783	12	769	282	15	117	–	14	[63]
Pinewood	0.3	10	600	20	200	100	30	6	–	50	[64]
Pinewood	–	520	540	–	710	100	60	–	–	5 380	[65]
Mango tree wood	1.5	–	1 683	–	5 025	675	78	–	–	–	[66]
Beechwood	1.4	10	2 000	10	3 600	600	100	150	100	200	[64]
Agricultural waste											
Alfalfa straw	7.4	600	12,900	–	28,000	1 400	1 000	1 900	300	2 000	[64]
Sugarcane bagasse	–	3 740	790	–	1 000	730	40	–	–	20,500	[65]
Wheat straw	6.8	500	3 900	–	10,460	1 100	–	400	2 500	12,200	[48]
Wheat straw	4.1	150	2 500	200	11,000	750	150	550	1 000	8 500	[64]
Rice hull	14.2	nd	900	–	2 010	nd	–	300	600	59,900	[48]
Rice straw	13.9	65	6 400	300	22,600	2 100	900	1 000	2 600	41,400	[24]
Corn stalk	7.1	1 100	3 500	–	12,210	1 900	–	300	2 500	11,900	[48]
Corncob	2.0	–	300	500	6 300	400	300	–	–	–	[67]

Note: db: dry basis; nd: not detected.

Table 2
Summary of proximate and ultimate analyses of different types of raw biomass.

Biomass feedstock	Proximate analysis (wt%)				Ultimate analysis (daf.wt%)					Heating value (db)	Reference
	Moisture (ad/ar)	Ash content (db)	Volatile Matter (db)	Fixed Carbon (db)	C	H	O[a]	N	S	(MJ/kg)	
Biomass component											
Cellulose	–	1.1	92.8	6.1	–	–	–	–	–	–	[73]
Lignin	–	3.1	55.4	41.5	–	–	–	–	–	–	[73]
Alkali lignin	–	6.2	66.4	27.4	62.4	6.1	29.4	0.26	1.77	23.3[b]	[46]
Xylan	–	2.3	76.1	21.6	–	–	–	–	–	–	[73]
Woody biomass											
Pinewood	8.0	0.4	87.6	12.0	50.1	6.2	43.6	0.00	0.00	20.4 (HHV)	[74]
Pinewood	8.3 (ad)	2.2	82.0	15.9	–	–	–	–	–	19.9	[75]
Pinewood	9.2	0.6	80.2	19.2	49.4	6.1	44.2	0.08	0.19	19.9 (HHV)	[76]
Pinewood	6.1	2.2	84.6	13.2	50.3	6.0	43.0	0.69	nd	18.4	[77]
Poplar wood	4.2 (ad)	5.8	78.9	15.4	46.0	6.3	41.9	0.18	0.13	17.7[b]	[78]
Rubberwood	5.0	1.9	82.9	15.2	46.6	6.0	47.2	0.14	–	17.1 (HHV)	[57]
Fir wood	7.5 (ad)	2.0	80.9	17.2	–	–	–	–	–	21.8	[75]
Fern stem (*Dicranopteris linearis*)	10.3	0.7	92.9	6.4	46.7	5.5	47.0	0.27	0.46	18.0 (HHV)	[76]
Saltree wood	8.9	1.2	83.3	15.4	49.8	6.0	43.6	0.58	nd	18.2	[77]
Areca nut husk	7.4	2.7	80.4	16.9	48.8	5.8	43.5	1.95	0.10	18.2	[77]
Mango tree wood	–	1.5	81.2	17.3	46.6	6.1	46.2	0.11	–	18.8[b]	[66]
Agricultural waste											
Corn stalk	7.8 (ad)	9.7	74.9	16.3	44.0	6.8	46.3	2.69	0.22	16.4[b]	[79]
Corncob	2.0 (ad)	2.0	79.9	18.1	50.8	3.6	44.2	0.90	0.50	19.3[b]	[67]
Rice straw	–	17.6	69.8	12.7	50.2	6.5	42.2	1.05	0.12	16.8[b]	[80]
Rice straw	7.6 (ad)	11.4	72.1	16.5	–	–	–	–	–	–	[81]
Rice husk	5.6	17.8	62.6	14.0	43.4	6.6	48.3	1.06	–	16.7	[82]
Rice husk	–	25.2	56.4	18.4	35.6	7.2	56.7	0.40	0.10	11.2[b]	[83]
Rice husk	5.6	15.5	60.9	23.5	38.5	5.8	54.1	1.68	< 0.01	15.5 (HHV)	[84]
Cotton stalk	7.7 (ad)	7.5	74.8	17.7	–	–	–	–	–	18.7	[75]
Wheat stalk	5.9	8.5	76.3	15.2	42.2	6.0	51.0	0.21	0.14	16.1 (HHV)	[76]
Wheat straw	10.1 (ar)	7.0	76.2	16.8	50.0	5.3	43.8	0.67	0.23	18.9 (HHV)	[85]
Sugarcane bagasse	3.6	7.0	84.9	8.1	45.0	6.2	48.5	0.21	0.14	18.0 (HHV)	[76]
Sugarcane leave	10.0 (ar)	8.4	77.2	14.3	51.8	9.3	38.0	0.90	–	20.3[b]	[86]

Note: ar: as received basis; ad: air dry basis; db: dry basis; daf: dry and ash free basis; nd: not detected; HHV: higher heating value.
[a] Calculated by difference
[b] Higher heating value (HHV) calculated based on average values obtained using three empirical correlation formulas (in which elemental compositions are expressed on a dry basis) [87]: Tillman (1978) [88]: HHV(MJ/kg) = 0.4373C – 1.6701 / Jenkins (1985) [89]: HHV(MJ/kg) = –0.763 + 0.301C + 0.525H + 0.064O / Grabosky (1981) [90]: HHV(MJ/kg) = 0.328C + 1.4306H – 0.0237N + 0.0929S – (1 – A/100)(40.11H/C) + 0.3466 where A denotes the ash content.

[68]. Calcium, for instance, can be fixed in the plant structure in the form of insoluble salts, with a content typically comprised in a 0.03–1.3% range on a dry basis (see Table 1). Regarding potassium, it is an essential element for plant growth. It is especially considered as one of the most important fertilizers for crops, which additionally prevents disease and pest damage. When used as a fertilizer for agricultural use, potassium is commonly applied in the form of potassium chloride (KCl) and sulfate (K_2SO_4). It is usually the most abundant AAEM element, with a mass percentage going up to ~3% on a dry basis (see Table 1). As far as magnesium is concerned, it is a component of chlorophyll cells which are involved in the photosynthesis process allowing producing energy for the whole plant. For the sodium (another alkali metal present in biomass) concentration, it is very limited according to the analyses reported in the literature, thus making it a so-called trace element. The

presence of these AAEM elements in biomass enhances the cohesion of the biopolymers [92,93]. Moreover, both inherent and added AAEMs significantly modify the pyrolytic behavior of biomass, as discussed below (see Section 5).

2.2. Coal characteristics

Coal is a combustible black or brown material issued from the conversion of biomass over a geologic time scale. The slow metamorphosis here arises from temperature and pressure gradients inherent to the burial of animal and/or vegetable residues that are ultimately converted

Table 3
Summary of proximate and ultimate analyses of different coal types.

Coal type	Source	Proximate analysis (wt%)				Ultimate analysis (daf wt%)					Heating value (db/daf) (MJ/kg)	Reference
		Moisture (ad/ar)	Ash content (db)	Volatile Matter (db)	Fixed Carbon (db)	C	H	O[a]	N	S		
Lignite	Inner Mongolia, China	36.8 (ar) / 13.7 (ad)	10.8	57.9	32.4	63.8	5.6	29.2	1.0	0.4	25.3[b]	[79]
Lignite	Shanxi, China	–	25.5	36.0	38.5	73.0	5.5	19.6	1.2	0.7	29.9[b]	[97]
Lignite	–	11.7 (ad)	17.3	38.4	44.2	69.0	4.3	24.7	1.2	0.7	26.0[b]	[35]
Lignite	Inner Mongolia, China	10.6 (ad)	9.4	40.9	49.8	69.0	4.3	23.1	1.2	2.5	26.4[b]	[67]
Lignite	Inner Mongolia, China	29.1 (ad)	13.0	41.9	45.1	71.3	4.1	22.4	1.4	0.8	26.8[b]	[98]
Lignite	Inner Mongolia, China	–	16.6	42.3	41.1	67.6	4.6	26.5	1.0	0.3	25.6[b]	[99]
Lignite	Greece	–	16.6	47.2	36.2	56.5	5.6	35.1	1.5	1.2	18.4 (HHV, db)	[100]
Lignite	Greece	–	20.4	37.9	41.7	55.4	4.1	37.7	1.5	1.4	20.5 (HHV, db)	[100]
Lignite	Greece	–	32.4	35.8	31.8	53.2	4.4	38.7	1.6	2.1	16.8 (HHV, db)	[100]
Lignite	Greece	–	27.8	32.4	39.8	55.9	4.9	36.3	1.3	1.6	18.1 (HHV, db)	[100]
Subbituminous coal	Alberta, Canada	9.7 (ar)	9.5	11.8	78.7	76.5	5.2	15.6	0.4	0.0	31.2[b]	[31]
Subbituminous coal	Inner Mongolia, China	–	7.0	34.3	58.7	82.0	4.8	11.4	1.0	0.9	33.2[b]	[97]
Subbituminous coal	–	14.8 (ad)	3.5	32.6	63.9	75.9	3.0	19.9	0.7	0.5	27.2[b]	[35]
Subbituminous coal	Wyoming, USA	20.9 (ar)	7.4	43.3	49.3	73.3	3.4	21.6	1.2	0.6	27.2	[101]
Bituminous coal	Shanxi, China	8.7	4.7	35.3	60.0	80.6	4.5	13.6	1.1	0.3	31.9[b]	[102]
Bituminous coal	Shanxi, China	–	8.2	36.7	55.1	76.8	4.5	17.1	1.0	0.5	30.1[b]	[99]
Bituminous coal	NSW, Australia	2.8	13.9	35.3	50.8	83.3	5.8	8.0	1.8	1.1	28.7 (HHV, db)	[74]
Bituminous coal	Shanxi, China	–	6.3	35.4	58.3	84.5	2.3	11.3	1.2	0.8	30.4[b]	[103]
Bituminous coal	–	0.5 (ad)	9.0	20.8	70.1	86.1	4.7	7.1	1.7	0.4	35.0[b]	[35]
Bituminous coal	Guizhou, China	1.5 (ad)	25.9	23.7	50.4	84.2	4.9	4.2	1.0	5.8	24.0 (ar)	[104]
Bituminous coal – lvb	Queensland, Australia	9.7 (ar)	9.5	11.8	78.7	90.8	4.3	2.7	1.5	0.6	36.7[b]	[31]
Bituminous coal – mvb	Middelburg, South Africa	3.2 (ar)	14.5	22.7	62.8	86.6	4.3	7.2	1.4	0.5	34.6[b]	[31]
Bituminous coal – mvb	Mexico	–	21.1	23.7	55.2	86.2	5.5	5.9	1.6	0.8	27.8 (HHV, db)	[105, 106]
Bituminous coal – hvb	Pennsylvania, USA	2.5 (ar)	13.7	34.4	51.9	83.3	5.4	8.0	1.6	1.6	31.5	[106, 107]
Bituminous coal – hvb	South Africa	–	15.0	29.9	55.1	81.5	5.0	10.5	2.1	0.9	27.8 (HHV, db)	[105, 106]
Bituminous coal – hvb	Cesar, Colombia	5.0 (ar)	4.2	38.0	57.8	83.5	4.6	10.1	1.3	0.4	30.5 (HHV, db)	[108, 109]
Bituminous coal – hvb	West Virginia, USA	7.5 (ar)	12.9	34.1	53.0	85.6	5.1	7.2	1.4	0.7	35.5[b]	[31]
Bituminous coal – hvb	Ukraine	10.1 (ar)	9.8	39.0	51.2	84.3	5.2	7.6	2.2	0.7	35.1[b]	[31]
Bituminous coal – hvb	Freyming, France	1.6 (ar)	4.8	34.2	61.0	86.2	5.2	6.9	0.9	0.9	33.1 (HHV, db)	[109, 110]
Anthracitic coal	Guizhou, China	–	19.0	7.6	73.5	94.5	2.6	0.5	1.4	1.0	35.9[b]	[103]
Anthracitic coal	Shanxi, China	–	14.4	8.9	76.7	95.1	2.3	0.6	1.2	0.8	35.6[b]	[99]
Anthracitic coal	Asturias, Spain	–	14.2	3.6	82.2	94.7	1.6	2.0	1.0	0.7	29.2 (HHV, db)	[105]

Note: ar: as received basis; ad: air dry basis; db: dry basis; daf: dry, ash free basis; HHV: higher heating value, lvb: low volatile bituminous; mvb: medium volatile bituminous; hvb: high volatile bituminous.

[a] Calculated by difference

[b] Higher heating value (HHV) calculated based on four empirical correlation formula (in which element compositions are expressed on a dry, ash free basis) [87]: Dulong (1880) [111]: HHV(MJ/kg) = 0.3383C + 1.443(H – O/8) + 0.0942S / Strache and Lant (1924) [112]: HHV(MJ/kg) = 0.3406C + 1.4324H – 0.1532O + 0.1047S / Vondracek (1927) [113]: HHV(MJ/kg) = (0.373 – 0.00026C)C + 1.444(H – 0.1O) + 0.1047S / Grummel and Davis (1933) [114]: HHV(MJ/kg) = (0.0152H + 0.9875)((C/3) + H – (O – S)/8)

into coal [42]. This so-called coalification process itself involves various sub-processes (dehydration, bituminization, debituminization and graphitization [94]), which induce chemical, physical and structural changes of the organic matter. Actually, a systematic description of the coal structure and composition is rather impossible due to the wide variety of fuels in existence and to the significant heterogeneity that can be observed within a given coal type. Nevertheless, it can still be noted that every coal contains an organic fraction (essentially composed of carbon associated with hydrogen, oxygen, nitrogen and sulfur atoms), mineral components (silicates (quartz, kaolinite, illite), oxides and hydroxides (haematite, lepidocrocite, corundum), carbonates (calcite, dolomite, siderite), sulfides and sulfates (pyrite, gypsum)) and volatiles, including water (H_2O), carbon monoxide and dioxide (CO and CO_2), light hydrocarbons such as methane (CH_4) or ethylene (C_2H_4) and tars [95,96]. As illustrated in Table 3, the main coal elemental components are carbon, oxygen and hydrogen (sulfur and nitrogen being present in very low quantities, for their part). The mass fractions of these elements vary significantly depending on the coal rank as depicted in Table 3. As compared to biomass (see Table 2), coal contains more carbon and less oxygen or hydrogen, regardless of the considered fuel type (i.e., lignite, subbituminous and bituminous coals or anthracite). On the other hand, the greater the coalification, the greater the mass fraction of carbon, as shown in Table 3. This can be explained by the decreases of the O/C and H/C ratios undergone by the organic matter during its slow decomposition. As a consequence, lower-rank fuels (e.g., lignite and sub-bituminous coals) contain less carbon, as well as more volatiles and ash than higher-rank fuels (e.g., anthracite). Besides, and based on ^{13}C nuclear magnetic resonance (NMR) analyses conducted on a lignite and three bituminous coals, Yan et al. showed that lower-rank fuels tend to contain a larger proportion of protonated aromatic carbon, aliphatic carbon, carbonyl carbon, carboxyl carbon and aliphatic carbon bonded to oxygen, as well as less phenolic carbon and alkylated aromatic carbon [115]. This observation is in fact very consistent with the higher mass fractions of oxygen and hydrogen observed in lignite [115]. As far as the structure of coal is concerned, it can be regarded as a heterogeneous mixture of fused aromatic rings combined by means of cross-linking bonds and side chains, including hydroxyl, carboxyl, ether and aliphatic functional groups [116] (see Fig. 5). The size and molecular weight of aromatic clusters tend to increase with the coal rank, while the side chains are gradually shortened and even eliminated [115].

Due to some similarities between biomass and coal in terms of elemental composition and structure, AAEMs (mainly Na, Mg and Ca) can also be found in coal through the three above-mentioned categories, (i.e., ion-exchangeable state (mainly calcium and magnesium), water-soluble state (mainly sodium and magnesium) and insoluble state [27] (see Section 2.1)). Ion-exchangeable calcium and magnesium exist in large amounts within low-rank coals [27,39,117,118] (see Table 4). According to Zhao et al., ion-exchangeable Ca and Mg specifically account for nearly 69% of the total AAEMs present in the three states

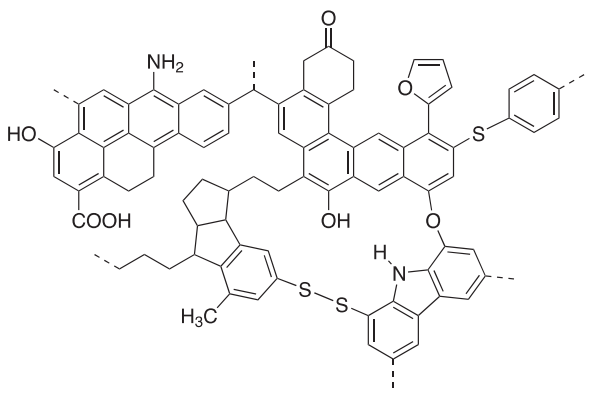

Fig. 5. Example of typical coal chemical structure.

within a low-rank coal. On the other hand, the proportion of water-soluble and insoluble AAEMs are only 24% and 7%, respectively [27]. Divalent Ca and Mg cations are chemically attached to oxygen-containing groups, such as carboxylates and phenolates, and can be removed by hydrogen ions during acid washing [100,117]. Water-soluble salts, such as sodium chloride (NaCl), are mostly found within the coal moisture [39]. For insoluble AAEM minerals such as kaolinite, which are present in very low proportions in coal, they can only be dissolved through some extreme conditions involving the use of concentrated hydrochloric acid/hydrofluoric acid (HCl/HF) solutions, for instance [118]. The total AAEM content in a given coal can be quantified by calculating a so-called alkali index (AI), which is expressed as a function of the mole ratio of basic compounds (sodium oxide (Na_2O), K_2O, CaO, magnesium oxide (MgO) and Fe_2O_3) and acidic compounds (SiO_2, aluminum oxide (Al_2O_3)) multiplied by the fuel ash content [100,119–121]. Skodras et al. notably used this indicator to illustrate that the gasification rate of various lignites could be reasonably correlated to their alkali index, whose values were comprised between 0.11 and 0.32 [100]. With increasing fuel rank, higher AI values can be determined, as exemplified in [121], where values comprised between 4.2 and 6.5 were estimated for bituminous medium-rank coals against 2.93 in [119] in the case of a low-rank bituminous coal.

3. Decomposition mechanisms

3.1. Biomass decomposition

The processes involved in biomass decomposition, as well as the composition and partition between pyrolytic products, are significantly influenced by numerous experimental factors, including the temperature, the residence time, and the heating rate [7]. For long residence times, low and high temperatures will respectively favor the production of char and gaseous products, whereas pyrolytic oils will be promoted at medium temperatures for short residence times (i.e., for high heating rates). According to Collard et al. [2], the primary pyrolysis reaction can be summarized as the superposition of three principal pathways: char formation, depolymerization and fragmentation (see Fig. 6). In short, the first pathway (i.e., char formation) occurs at low temperatures and slow heating rates. It involves the conversion of biomass into a solid polycyclic aromatic structure called char [122–124]. It is, moreover, accompanied by the release of water and incondensable gaseous species issued from dehydration and rearrangement reactions [2,125–127]. For its part, the depolymerization process consists in the cleavage of the bonds between the monomer units of biomass leading to volatile molecules [128] (see the example of cellulose in Fig. 7). As far as fragmentation is concerned, it corresponds to the linkage of covalent bonds of the polymer, which results in the formation of condensable low molecular compounds, together with incondensable gaseous species [7,129,130]. Both of these pathways (i.e., depolymerization and fragmentation) occur at higher temperatures than the char formation process [2]. Further secondary reactions, including cracking or recombination of emitted volatile compounds, can also occur, depending on the thermal conditions within the medium [7,131]. While cracking reactions involve the breaking of chemical bonds to form lower molecular weight species, the recombination of volatiles inversely gives birth to higher molecular weight compounds. Under fast pyrolysis conditions (i.e., when the heating rate is higher than 100 °C/s), many linkages are cleaved nearly simultaneously. Volatile species are thus rapidly released, which prevents secondary reactions from occurring [19,61]. On the other hand, the low heating rate pyrolysis (<10 °C/min) only induces the breakage of the less stable bonds of the polymer. Rearrangement reactions are then favored, thus limiting the release of volatiles.

The nature of the gas products emitted during the pyrolysis of biomass directly depends on the type of chemical structures present in hemicellulose, cellulose and lignin which are cleaved by heating. As an

Table 4
Composition of mineral matter in raw coal.

Coal type	Inorganic content (ppm (except for ash content) - dry weight)												
	Ash content (wt%, db)	Al	Ca	Fe	K	Mg	Na	P	S	Si	Ti	Alkali Index (AI)	Reference
Lignite	10.8	10,600	12,700	2 400	790	5 000	1 600	440	5 100	15,100	500	–	[79]
Lignite	13.0	11,200	4 200	5 600	1 340	3 800	2 600	–	–	34,800	–	–	[98]
Lignite	25.5	26,600	7 200	8 800	3 390	1 000	1 200	–	200	77,600	1 100	–	[97]
Lignite	16.6	12,700	12,300	6 200	1 410	2 800	1 100	190	1 500	45,700	800	–	[99]
Lignite	9.4	–	12,200	3 500	600	4 300	1 000	–	–	–	–	–	[67]
Lignite	16.6	12,300	39,200	9 300	800	1 300	700	0	14,200	21,500	100	0.19	[100]
Lignite	20.4	14,600	59,500	8 600	800	4 400	800	0	8 000	24,000	200	0.32	[100]
Lignite	32.4	33,600	45,600	20,000	2 700	8 700	1 200	0	14,600	52,600	400	0.22	[100]
Lignite	27.8	24,900	55,200	15,400	1 400	3 800	600	0	18,800	40,600	500	0.24	[100]
Subbituminous coal	7.0	5 000	4 200	5 200	910	600	1 100	–	800	18,400	200	–	[97]
Subbituminous coal	7.4	5 600	13,900	3 100	490	2 800	900	380	2 000	10,600	400	–	[101]
Bituminous coal	4.7	9 000	1 400	1 400	180	800	100	80	400	10,300	400	–	[102]
Bituminous coal	13.9	19,500	7 800	7 300	–	500	100	790	3 400	31,100	1 600	–	[74]
Bituminous coal	8.1	6 000	9 300	5 200	620	700	1 300	100	2 800	17,800	300	–	[99]
Bituminous coal	15.3	16,000	2 200	8 000	3 400	1 000	2 300	–	–	38,800	–	2.93	[119]
Anthracite coal	14.4	28,200	2 800	2 400	990	400	1 300	550	600	34,900	1 300	–	[99]

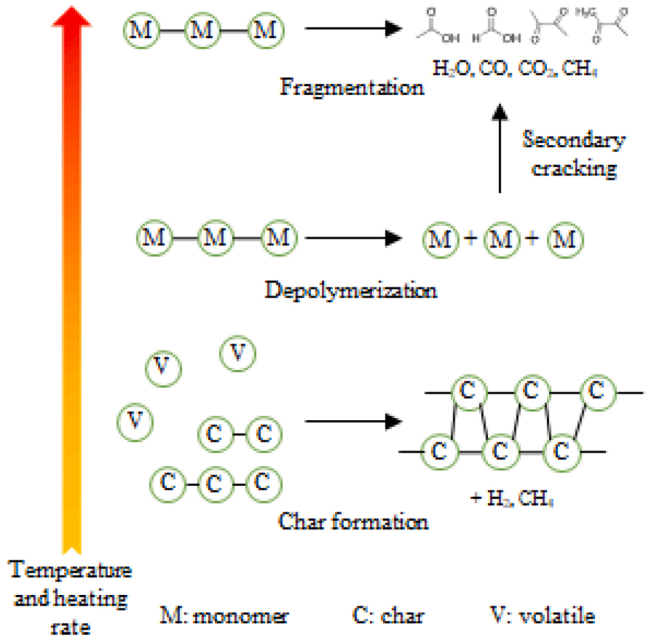

Fig. 6. Pathways involved in the primary mechanisms of the conversion of biomass constituents.
Adapted from Collard and Blin [2].

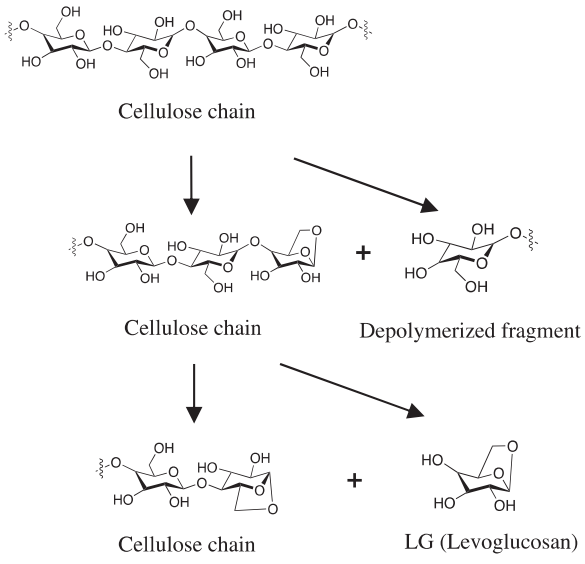

Fig. 7. Cellulose decomposition mechanism.

example, CO_2 is typically derived from the cleavage of carboxyl groups present in hemicellulose [132,133]. As regards CO production, it especially originates from the cracking of carbonyl groups contained in cellulose [134]. On the other hand, the deformation and cracking of lignin containing aromatic rings and methoxy groups, as explained in Section 2.1, will preferentially lead to the release of H_2 and CH_4 [56]. In terms of condensable liquid products, the major components of pyrolytic oils are acids, ketones, esters, furans, phenols, anhydrosugars and hydrocarbons [135]. Note that organic compounds are mainly issued from the decomposition of hemicellulose and cellulose, whereas only limited amounts of organic compounds result from the pyrolysis of lignin [56]. Due to the high H/C and O/C ratios of biomass, the liquid tar typically has a low heating value and is highly corrosive, which explains why upgrading deoxygenation processes are usually required.

To complement this brief overview of the biomass decomposition processes, the mechanisms governing the conversion of cellulose, hemicellulose and lignin will be further addressed in Sections 3.1.1 to 3.1.3. At this stage, it should, however, be noted that the decomposition of biomass cannot be represented as being a simple addition of the conversion processes related to the three above-listed biopolymers due to the intrinsic interactions existing between these components [136], in addition to the role of inherent minerals, which will be addressed more specifically in Section 5.1.3.

3.1.1. *Cellulose conversion*

Due to its abundant presence in all kinds of lignocellulosic feedstocks, cellulose is the biopolymer that has attracted the most attention in studies dealing with catalytic pyrolysis [20]. Generally speaking, cellulose is relatively stable under heating as compared to hemicellulose because of its well-arranged structure, which allows it to decompose at higher temperatures (see Section 2.1). The composition and yields of products issued from the pyrolysis of cellulose are influenced by different structural features, including its degree of polymerization, its crystallinity index, crystalline size and allomorph [8]. For instance, a higher crystalline index and crystallite size tend to shift the cellulose

degradation to higher temperatures [2,59]. In addition, a high crystallinity is likely to enhance depolymerization reactions, producing more levoglucosan and less char. Indeed, dehydration reactions that promote reticulation to form cellulose char are lessened in such cases. It can, moreover, be added that the solid residue left from cellulose pyrolysis is generally quite low, especially for thermal treatment at temperatures higher than 400 °C [2,56].

Regarding pyrolysis mechanisms, cellulose is first depolymerized to produce active cellulose. According to Mamleev et al. [137], the subsequent stages can be represented by means of a two-competing reaction scheme, including a so-called E_i-elimination [138–140], leading to the production of light gases and a transglycosylation process producing cellobiosan and levoglucosan (LG). The latter does not break down in the absence of metal ions or other co-reactants [20], and is the most abundant product issued from the pyrolysis of cellulose, with yields reaching up to 60% [137]. To account for the formation of LG from cellulose, a well-admitted mechanism relies on the succession of depolymerization steps as represented in Fig. 7 [141]. In short, a glucosyl cation is first produced from the scission of the glycosidic bond. The so generated free primary hydroxyl group at C-6 then forms a stable 1,6-anhydride, while the subsequent cleavage of another glycosidic bond allows monomeric LG to be liberated together with another glucosyl cation, which also reacts, etc. A higher degree of polymerization of cellulose is therefore attributable to higher LG yields as the cleavage of glycosidic bonds prevails during pyrolysis reactions. In addition to LG, anhydro-oligosaccharides and anhydro-saccharides such as levoglucosenone can be produced during the fast pyrolysis of cellulose, together with 5-(hydroxymethyl) furfural or furfural [129,142]. Further fragmentation will ultimately result in the production of lighter linear carbonyls such as hydroxyacetaldehyde and acetol (or 1-hydroxy-2-propanone) in addition to incondensable gaseous species. Different possible pathways have been proposed to account for the formation of these compounds. They notably involve dehydration, ring scission, ring opening, cyclization and tautomerization reactions [8,20]. As for the charring process, which consists in the organization of the benzene rings in a polycyclic structure, it takes place at higher temperatures when the char structure progressively becomes more thermally stable while exhibiting fewer aliphatic and oxygenated groups.

3.1.2. Hemicellulose conversion

Although the composition of hemicellulose depends directly on the considered feedstock, it is built mainly upon two major polysaccharides, namely, xylans and glucomannans [56]. As previously reported in Section 2.1, the decomposition of hemicellulose takes place at temperatures lower than those related to the thermal degradation of cellulose. Besides, and while almost all cellulose is pyrolyzed above 400 °C, around 20% in solid residue still remains at 900 °C during the conversion of hemicellulose [56]. For pyrolytic products, water will first be produced through dehydration within polysaccharides at around 200 °C [143]. Furthermore, oxygenated compounds such as methanol (CH_3OH), formic acid (HCOOH) or acetic acid (CH_3COOH) will also be released through the fragmentation of the methoxy group, the rupture of the carboxylic acid function of the hexuronic acids and the fragmentation of acetyl substituents, respectively [133]. Regarding the depolymerization of hemicellulose, it follows a mechanism similar to the one described in the case of cellulose, with the cleavage of glycosidic linkages yielding different anhydro-saccharides [132], while the released pyran rings tend to shift to furan rings, which are more thermally stable under heating conditions [2]. Finally, is should be noted that the amount of pyrolytic char is higher during the pyrolysis of hemicellulose as compared to cellulose [2,144]. This is mainly attributable to factors such as the presence of minerals in higher proportions [143,144], the higher propensity of xylan and glucomannan to produce char [145], in addition to the fact that hemicellulose, contrary to cellulose, is only composed of an amorphous phase [2,144]. This latter will thus undergo rearrangement reactions before depolymerization, and therefore promote the char yield [2,144].

3.1.3. Lignin conversion

As compared to cellulose and hemicellulose, lignin is the most thermally stable component of biomass. It therefore decomposes very slowly [56]. The variety of linking bonds in lignin polymers results in a large pyrolysis temperature range, as explained in Section 2.1. It, moreover, also induces the release of very different pyrolytic products, although lignin depolymerization leads mainly to phenolic compounds as this biopolymer is the primary origin of aromatic rings in biomass [146]. Regarding the chemical bonds linking the basic units of lignin, their reactivity is influenced by the presence of substituted functional groups. Within the framework of a study conducted with different model dimers, Kawamoto et al. reported that their reactivity follows the order: α-O-4 (phenolic, nonphenolic), β-O-4 (phenolic) > β-O-4 (nonphenolic), β-1 (phenolic, nonphenolic) > 5–5 (phenolic, nonphenolic) [147]. Prior to the release of volatile species, lignin first undergoes a glass transition with a fluidity starting at 150 °C to reach 100% at 200 °C before decreasing when the temperature rises above 325 °C [148]. During pyrolysis, hydroxyl groups on side chains are involved in dehydration reactions and ether bonds (α-O-4 and β-O-4) typically break at temperatures of ~200 and ~250 °C [149]. Their cleavage provokes the depolymerization of lignin monomers and the production of gaseous molecules (such as CO and CO_2) through recombination reactions among aromatic rings. At this stage, the release of phenolic compounds usually containing alkyl chains having 2–3 carbon atoms also occurs [150]. C-C bonds in alkyl side chains react when the temperature reaches 300 °C and small chain compounds like methane, acetaldehyde or acetic acid can be formed. For their part, methoxy groups on aromatic rings become reactive when the temperature is higher than 400 °C [151,152]. As a result, an evolution from S-type lignin to H-type lignin [153], as well as a higher production of methanol and methane [8] can be observed with increasing temperatures. Lignin with low methoxy groups like softwood produces more char as the empty C3 and C5 positions in the aromatic ring favor condensation, and thus, the formation of pyrolysis lignin char [8]. Besides, demethylation and cross-linking reactions above 500 °C result in the formation of methane and a higher reticulated aromatic structure of the char [2]. To conclude, it is noteworthy that linkage cleavages are likely to form new crosslinking bonds yielding lignin char. It is therefore difficult to completely decompose lignin under pyrolysis, which thus explains why the solid residue is the highest, as compared to cellulose and hemicellulose (around 46% at 900 °C) [56].

3.2. Coal decomposition

Coal pyrolysis involves a series of complex physical and chemical processes that result in the formation of gaseous volatiles, tar and char. When being heated, the structure of coal, which consists of a heterogeneous mixture of organic polymer networks (see Section 2.2), undergoes significant changes characterized by the release of oxygen and hydrogen, and to a much smaller extent, of carbon. This in turn generates coal char having a significant carbon content, a compact structure and a high aromaticity [99]. The nature and composition of pyrolytic products issued from coal pyrolysis depend primarily on the relative rates of bond-breaking, cross-linking and mass transport phenomena [117]. In fact, the fragmentation of coal particles during rapid pyrolysis may occur following three different processes, namely: exfoliation, denoting the breaking up of the coal outer shell generating fine particles, fragmentation at the outer zone involving the separation of this zone from the rest of the particle, and fragmentation at the center zone, leading to a decrease in the particle size, with significant morphological restructuring [154]. According to Cui et al. [155], exfoliation and fragmentation at the outer zone are the most important modes governing the decomposition of lignin and bituminous coals, respectively, while no fragmentation at the center zone has been evidenced in [155] regardless of the coal rank. Fuel volatile content is another important feature that influences the nature of emitted species, as well as the

intensity of thermal decomposition during pyrolysis. Indeed, as low-rank coals are quite rich in volatile matters as compared to bituminous coals and anthracite (see Section 2.2), they will therefore lead to the emission of more gaseous products. For identical operating conditions, the extent of pyrolysis will moreover tend to weaken with an increase in the degree of fuel coalification, as exemplified in a study by Cui et al. [99]. Operating conditions, such as the temperature and the heating rate, are obviously other essential parameters that directly drive the pyrolysis process and the composition of the pool of pyrolytic products emitted. In this respect, high pyrolysis temperatures and long heating durations will typically contribute to increasing the fuel weight loss while favoring the growth of aromatic monomers within the char [99,155]. Besides, a high heating rate and a low pyrolysis temperature correspond to the most favorable conditions for producing volatile tars. Alternatively, a low heating rate and a high pyrolysis temperature will favor the formation of char and gas. Higher yields and release rates of pyrolysis gases are indeed generally associated with increasing temperatures (see [98], for instance), which are likely to promote secondary cracking reactions favoring tar conversion [98,156]. As far as the impact of the heating rate is concerned, an increase of this parameter tends to facilitate the release of larger aromatic ring systems [38,157]. Such an effect can, however, be hindered by the presence of AAEM species [38] that may enhance cross-linking reactions, thus leading to lower tar, extractables and liquids yields, while lowering the average tar molecular weight [117,155].

Reactions at play during pyrolysis are directly related to the thermostability of coal organic structures, which is determined by the bond energy between atoms (the thermal stability of hydrocarbons increasing in the following order: alkanes < olefins < cyclic hydrocarbons < aromatics < condensed aromatics [158]). Consequently, and due to a wide variety of bond energies, coal pyrolysis intrinsically takes place over a large temperature range going from 200 °C up to 1600 °C. During non-isothermal thermogravimetric analysis (TGA), it can be observed that the pyrolysis process exhibits three to four different stages, namely: dehydration and degassing stage (< ~240 °C), initial pyrolysis (~240 – ~350 °C), main pyrolysis (~350 – ~700 °C) and secondary degassing with polycondensation (> ~700 °C) [26,79,118]. During the first stage, only moisture and some physically adsorbed gases like carbon dioxide or methane are released. Above ~200 °C, aliphatic bonds begin to break down while decarboxylation reactions can occur. The main pyrolysis stage is characterized by the decomposition and depolymerization of the coal matrix, which generates gaseous species, including dihydrogen (H_2), CO, CO_2 and CH_4, as well as large-molecule (e.g., aromatic) volatile matter and char. Ultimately, gases like H_2 and CH_4, together with a little tar, are generated through polycondensation reactions in the char, whose aromatization continues to proceed [79,98,118]. The temperature ranges associated with each of the above-mentioned pyrolysis stages strongly depends on the coal rank, however. Indeed, the cleavage of carboxyl groups, which promotes the yield of CO_2 and cross-linking reactions, begins to occur at 200 °C in the case of lignite, while no cross-linking can be observed before 400 °C for bituminous coals [117]. In terms of major pathways, the formation of CO stems from the cleavages of carbonyl, aldehyde and methoxy groups below 700 °C, and from ether linkages, oxygen-containing heterocyclics and phenolic hydroxyl above 700 °C [98,103,156,159]. With regard to the production of CO_2, it mainly originates from carboxyl and carboxylate groups at low temperatures and from ether linkages, quinones or oxygen-bearing heterocycles at higher temperatures [98,103]. As far as CH_4 is concerned, its formation is correlated to demethylation reactions, such as the cracking of aliphatic and aromatic hydrocarbons, along with the rupture of methyl, oxy-methylene and poly-methylene components [98,156,159]. Since the carbonation reaction of CH_4 begins above 1000 °C, the quantity of methane emitted hence reaches its maximum around this temperature [98]. The different pyrolysis stages described above can be easily highlighted during differential scanning calorimetry (DSC) analyses as the devolatilization process can be identified through several endothermic peaks between 150 and 570 °C, while polycondensation reactions are highlighted through an obvious exothermic event occurring between 570 and 1000 °C [78].

4. Methods and strategies adopted in the literature

4.1. Water and acid washing

4.1.1. Biomass

As explained in Section 2.1, biomass contains an ash fraction in addition to the three main biopolymers (namely, cellulose, hemicellulose and lignin). This solid inorganic residue comprises a variety of elements, such as potassium (K), silicon (Si), calcium (Ca), sodium (Na), and magnesium (Mg), along with some trace elements like iron (Fe), aluminum (Al), manganese (Mn), sulfur (S) and phosphorous (P), among others. Despite their relatively small quantities, these inherent inorganic compounds, including AAEMs, are known to substantially influence biomass pyrolysis [22]. They are therefore likely to affect the distribution of products issued from catalytic pyrolysis as well. Consequently, and to isolate the effect of catalysts on thermal conversion processes, inherent inorganic contents are usually removed from biomass before pyrolysis tests are conducted. To this end, pretreatments consisting in washing out metals or converting them into thermally stable salts through acid infusion are commonly implemented. As such, their interactions with biopolymers can be eliminated or inhibited which allows focusing the attention solely on the impact of AAEM species added as catalysts [91]. The above-mentioned pretreatment approaches can, however, also modify the chemical structure of biomass, thus resulting in changes in the nature and quantity of pyrolytic products. As an example, demineralization by acid washing usually results not only in a decrease in inorganic content, but also in a non-negligible destruction of the biomass structure [70]. It is therefore relatively difficult to distinguish between the intrinsic role of inherent AAEMs and the impact of acid washing in such cases [21,81,93]. This is notably why Persson et al. used mild acetic acid (CH_3COOH) solutions for the leaching of inorganic matter in softwood biomass while avoiding reducing its volatile matter [71]. Since water and acid washing are commonly implemented in studies aiming at elucidating the intrinsic role of AAEMs on the catalytic pyrolysis of biomass [49,58,160–163], covering such an aspect is therefore quite essential within the framework of the present literature review. Nevertheless, only the changes induced by these treatments on biomass content, structure and morphology will be discussed in the present section. The effects of AAEMs on pyrolysis processes and pyrolytic products will indeed be addressed more specifically in Section 5, which is entirely-devoted to the subject.

Various studies have shown that demineralization can significantly eliminate the AAEM content of biomass, with removal efficiencies strongly dependent on the nature of the deashing agents used [9,48,62,63,70,71,80,160]. For instance, Eom et al. compared the effect induced by demineralization with distilled or tap water, as well as with HCl and HF, on the pyrolysis behavior of poplar wood powders [63]. They concluded that the demineralization effects of water were negligible while the use of tap water even tended to increase the calcium content of the analyzed samples. As far as the two tested acids are concerned, they have been shown to significantly decrease the biomass ash content as well as the concentration of major metallic constituents such as potassium, magnesium, and calcium. Eom et al. also noted that the amount of low molecular weight compounds was significantly reduced in demineralized biomass, while the use of HCl allows hydrolyzing hemicellulose and pectic materials, thus suppressing some monomeric sugars. In a subsequent study, Jiang et al. compared the efficiency of six demineralization agents (deionized water, CH_3COOH, HCl, sulfuric acid (H_2SO_4), nitric acid (HNO_3) and orthophosphoric acid (H_3PO_4)) used to remove inorganics from rice straw [70]. They concluded that only strong acids (HCl, and H_2SO_4) were able to efficiently remove most minerals, albeit while inducing more notable impacts on the physicochemical

structure of biomass (i.e., surface structure and functional group changes) than water or weak acids. Dong et al. then compared four types of dilute acid washings on the pyrolysis of moso bamboo [62]. They noted that such treatments can remove a large portion of inorganic species, although they can also disrupt the chemical structures of biomass, thus influencing the subsequent pyrolysis processes (the formation of levoglucosan (LG) being particularly more promoted heavily by an HCl washing, as an example). For their part, Persson et al. observed that the higher the acidity of the leaching solution (CH_3COOH at 5 and 10 wt% being considered), the greater the amount of inorganics removed [71]. Similarly, the longer the treatment duration, the greater the amount of extracted AAEMs at lower acidity [71]. Compared to alkali metals, alkaline earth metals are more difficult to remove through water washing because of their low solubility. Divalent cations are, moreover, more difficult to leach than monovalent ones due to their stronger interactions with carbon surfaces [9,81,93,161]. Furthermore, the walls of biomass cells tend to separate into fibers after water washing, which can be explained by the extraction of AAEM species (especially the monovalent alkali metals such as K and Na) as the AAEM cations ensure the cohesion of the biomass structure through electrostatic and van der Waals interactions.

To conclude, it is noteworthy that the removal of ash by acid or water washings before pyrolysis represents an efficient way to decrease the release of AAEMs in the gas phase as well. This aspect is all the more important when considering that such species are a major cause of fouling, slagging and corrosion on the surface of superheaters [70,164,165]. In this regard, Deng et al. notably demonstrated that the yield and the proportion of potassium released in gaseous species were largely reduced after a removal of ash through water washing [48]. More recently, Niu et al. investigated the possible use of rainwater or snow for the removal of ash and inorganic species in ash from corn straw by using a laboratory scale leaching apparatus simulating rainfall [164]. It has been shown that such a practical and economical procedure could efficiently reduce the formation of KCl and K_2SO_4 in biomass ash, thus resulting in higher ash fusion temperatures due to the reduced formation of low-melting $K_2O{\cdot}nSiO_2$ (with $n = 1$–4) and to the enhanced content of high-melting SiO_2 [164]. Besides, demineralization through both acid and water washings have been demonstrated to decrease the nitrogen content in biomass. On the other hand, it tends to increase the selectivity of ammonia (NH_3), isocyanic acid (HNCO) and nitric oxide (NO) while decreasing the hydrogen cyanide (HCN) selectivity [81]. Despite a satisfactory demineralization efficiency, it is finally worth noting that the addition of strong acids such as HCl, HNO_3 or H_2SO_4 is likely to introduce undesirable elements (Cl, N or S) in the generated pyrolysis products [70].

4.1.2. Coal

As was the case in Section 4.1.1, only the changes induced by water and acid washings on the composition, structure and morphology of coal will be discussed here. That being the case, it is first of interest to note that both acid and water washings can reduce the water-soluble mineral content of coal. Nevertheless, acid washing can additionally remove ion-exchangeable AAEM species such as calcium and magnesium, while the use of highly concentrated acid solutions can further remove some insoluble minerals [38,118]. In a study examining the impact of advanced demineralization on coal properties and combustion characteristics, Rubiera et al. notably showed that the use of a mixture of hydrofluoric and fluorosilicic acids (HF/H_2SiF_6) followed by a secondary washing with HNO_3 reduced the fuel ash content, which went from 6.2% to 0.3% [166]. This pretreatment additionally led to increases in the volatile matter, oxygen and nitrogen contents, with a reduction of nearly 52% of the total sulfur content [166]. More recently, Zhao et al. compared the efficiency of different pretreatment approaches and noted that deionized water, dilute H_2SO_4 and concentrated HCl/HF washings allowed reducing the ash content of a low-rank coal by 22.00%, 74.25% and 91.32%, respectively [27]. Besides, it has also been demonstrated that SiO_2 can be dissolved in HF with acid washing as exemplified in [159].

While water washing induces almost no change in the organic structure of coal, acid washings may inversely substitute hydrogen ions for AAEM cations, thus increasing the production of carboxyl and phenolic species by the protonation of carboxylate and phenolate groups [118]. Acidic environments can additionally cause esters to undergo hydrolysis [118]. Furthermore, the removal of AAEM species leads to breakage of the ionic bonds connecting macromolecular clusters, which are then replaced by weak hydrogen bonds that are less stable under heating [27]. As part of a research work examining the impacts of intrinsic AAEMs on the structure of low-rank coal char, Zhao et al. showed that the aliphatic side chains and bridge bonds of demineralized coal shorten after an HCl/HF washing, which also induces a lower degree of fusion and a higher degree of substitution of the aromatic ring system [27]. On the other hand, other authors have argued that the organic matter of coal could be considered to be hardly impacted by acid washings as only a small degree of depolymerization in demineralized coal can be observed after such a pretreatment [117,159].

4.2. AAEM salt impregnation

Salt impregnation usually consists of different successive operations, including grinding and sieving, washing of samples to remove mineral compounds, impregnation of the feedstock in an aqueous solution or through dry mixing, filtration and final drying in an oven to suppress the residual humidity. A summary of impregnation procedures implemented in a series of works from the literature is summarized in Table 5. Particular attention should be paid to the molar ratio between the catalyst and the feedstock used. In the case of biomass, and due to the similarity of molar mass among the three main monomers (~162 g/mol for cellulose, ~173 g/mol on average for hemicellulose and between ~150 and ~210 g/mol for lignin), a proximate calculation (relying on the assumption that the average molar mass of monomers is 180 g/mol and that all biomass monomers are equivalent to glucose) allows to investigate the efficiency of catalysts. As shown in Table 5, this ratio is comprised between 0.001 and 0.45 mol cation/mol glucose (generally less than 0.2) and reflects the strong catalytic characteristics of AAEMs by the impregnation method.

Concerning coal, similar impregnation procedures are sometimes implemented in order to investigate the influence of added cations on pyrolysis. In such cases, it is, however, not possible to achieve a proximate calculation similar to the one described above for biomass due to the complexity and wide variety of coal structures in each considered rank. On the other hand, it can still be seen that cation mass ratios generally lower than 15 wt% are applied in the literature (see Table 5). As an example, one can refer to a recent study by Sun et al., who investigated the impact of salt impregnation on coal pyrolysis reactivity and kinetic characteristics [169]. To that end, they de-ashed a low-rank fuel by HCl/HF washing before impregnating it using a methanol/tetrahydrofuran (CH_3OH-THF) mixed solvent, together with different solutes, including $CaCl_2$ with a mass ratio of metal ions, to coal of 0.05 [169]. Nevertheless, and even though different works involving coal impregnation can be found in the literature (see [119,170], for instance), these latter will not be further discussed herein as they do not directly deal with pyrolysis, which is the core of the present document.

To conclude on salt impregnation, it is noteworthy that only some metal cations are likely to be bonded in biomass by ion-exchange reactions after impregnation, whereas non-bonded cations and most anions are still present in the solution. Therefore, filtration is sometimes included in the impregnation procedure to remove these extra anions in order to suppress their effects [20].

4.3. Strategies associated with the use of solid catalysts

In addition to impregnation methods, pretreatment procedures

Table 5
Summary of impregnation methods and procedures for biomass and coal pretreatment.

Feedstock	Particle size	Catalyst	Acid / water washing	Impregnation			Drying		Reference
				Ratio cation/feedstock	Stirring duration	Filtration	Duration	Temperature (°C)	
Biomass				**(mol/mol glucose)**					
Yellow poplar	< 0.5 mm	$MgCl_2$	3 wt% HF for 1 h	0.009 – 0.036	48 h	Yes	Overnight	75	[161]
Rubber wood	125–250 μm	K_2CO_3	–	0.004 mol/L - 0.036 mol/L (Concentration of solution)	1 h	Yes	24 h	105	[57]
Cellulose	75–106 μm	KCl, NaCl, $MgCl_2$ and $CaCl_2$	Deionized water	0.025	–	–	–	–	[162]
Cellulose, xylan and lignin	< 0.4 mm	K_2CO_3	–	0.13	Physically mixed	–	–	–	[167]
Pine wood	–	NaOH, Na_2CO_3, Na_2SiO_3, NaCl,	–	0.15 – 0.45	5 min	No	Until constant weight	105	[6]
Rice husk	< 0.16 mm	NaCl	–	0.03 – 0.15	Physically mixed	–	–	–	[82]
Sawdust of pin wood, fir wood and cotton stalk	< 1 mm	Na_2CO_3, NaOH, NaCl, Na_2SiO_3	–	0.15 – 0.45	5 min	No	Until constant weight	75	[75]
Alkali lignin	20–45 μm	KCl, $CaCl_2$	–	0.004, 0.022	Ultrasonic immersion for 0.5 h and static immersion for 12 h	(Yes)	6 h	105	[46]
Cellulose	(filter paper)	KCl, NaCl, $MgCl_2$ and $CaCl_2$	–	0.005, 0.05, 0.09, 0.27, 0.45	–	–	48 h	Ambient temperature	[168]
Cellulose	106 – 150 μm	KCl and $CaCl_2$	Deionized water	0.025	–	–	Overnight	105	[49]
Willow coppice	150 – 180 μm	CH_3COOK	HCl	0.046	–	Moistened by 1 mL of water	Until constant weight	60	[160]
Wheat straw	–	KCl	HCl	0,04	–	–	–	–	[163]
Pine wood	90 – 140 μm	CH_3COOK	HCl	0.03 – 0.12	2 h	No	Until constant weight	70	[58]
Coal				**(wt%)**					
Lignite	< 75 μm	KCl and $CaCl_2$	–	6%	24 h	–	6 h	105	[98]
Lignite	< 75 μm	KCl	HCl + HF	6%	24 h in HCl + 24 h in HF	Yes	12 h	80	[159]
Subbituminous	< 75 μm	$CaCl_2$	HCl + HF	5%	24 h in a CH_3OH-THF mixed solvent	Evaporation	Until constant weight	–	[169]
Bituminous and anthracite coal	80 – 120 μm	Na_2CO_3	–	5%, 10%, 15%	Until the liquid changes into a thickened mass	–	24 h	80	[103]
Bituminous coal	< 200 μm	$NaNO_3$, KNO_3, $Ca(NO_3)_2$	–	1%, 3%, 5%	–	–	–	–	[119, 170]
Coal (not specified)	100 – 120 μm	KCl	–	0.5%, 1.0%, 1.5%, 2.0%	15 min	–	4 h	105	[171]

involving solid AAEM catalysts have also been reported in the literature. Such methods rely on the use of metal oxides or zeolites whose efficiency can be improved by metal loading, surface modification or the introduction of mesopores, etc. [19]. Solid catalysts, which are assumed to be inert with the feedstocks, are typically introduced by dry mixing (in situ configuration) or by means of a catalytic bed (ex situ configuration) on which released vapors are driven (see Fig. 8). Here again, the physicochemical characteristics, including the surface properties of the selected catalyst, will directly influence the conversion efficiency of biomass or coal. As an example, Zhang et al. showed that both basic oxides (such as CaO and MgO) and acid oxides influence the composition and yield of bio-oils and gaseous species far differently [172].

Alkaline earth metal (AEM) oxides exhibiting a high surface area present a high number of basic sites and can thus be directly used in pyrolysis processes to favor deoxygenation and a reduction of acids and gaseous species released (see Sections 5.2.1.1 and 5.2.2). Furthermore, various physicochemical treatments can also be applied to catalysts based on AEM oxides in order to improve their activity, as detailed in Table 6. For instance, Zhang et al. prepared a Fe(III)/CaO catalyst with 5–15 wt% of iron [44,45]. Through X-ray diffraction (XRD) analyses, they observed that a new dicalcium diiron pentaoxide ($Ca_2Fe_2O_5$) phase was formed because of the strong reaction between Fe and CaO, which can prevent the deactivation of CaO and inhibit the sintering of Fe. On the other hand, with an increase in the Fe loading, it has been noted that more $Ca_2Fe_2O_5$ phase could spread over the CaO support and then reduce the number of active sites, reducing the amount of oxygenated compounds [45]. In a more recent study, Stefanidis et al. compared the efficiency of naturally derived basic MgO materials to be used as catalysts for the production of pyrolysis oil from the catalytic fast pyrolysis of lignocellulosic biomass [177]. The authors produced MgO samples from natural magnesite mineral by implementing different calcination conditions in terms of duration and temperature. They notably found that a longer calcination time and a higher temperature could promote the sintering of MgO and thus increase the crystal size. Alternatively, the use of mild calcination conditions has been shown to result in a smaller crystal size and a larger surface area. Zhu et al. then prepared a Ni/MgO

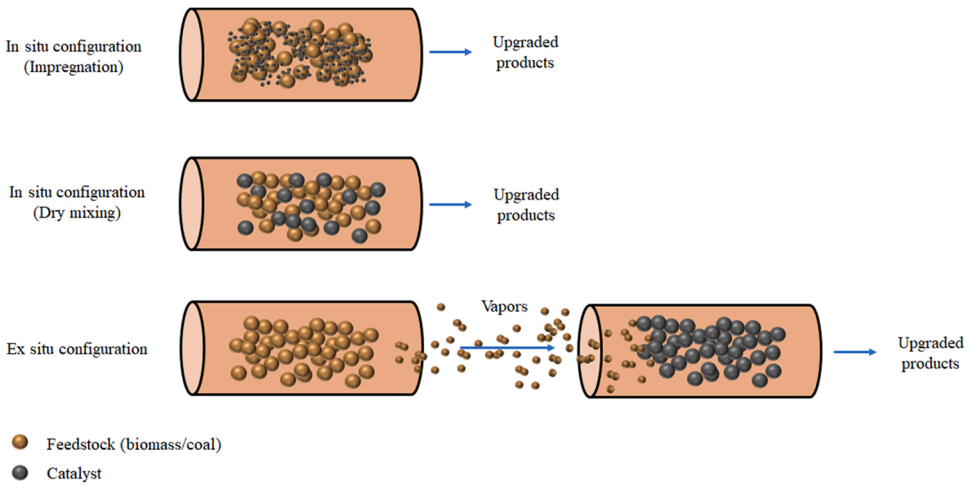

Fig. 8. Three configurations of in situ and ex situ pyrolysis.

Table 6
Summary of experimental methods related to the use of alkaline earth metal oxides for the pyrolysis of biomass and coal.

Feedstock	Feedstock size	Catalysts	Ratio feedstock/catalyst	Reacting medium	Configuration	Reference
Biomass						
Corncob	200 mesh (74 μm)	CaO obtained by calcination of $CaCO_3$	5 mg corncob + 5 mg catalyst (quartz sand for blank test)	TA[a]	Dry mixing	[173]
Lignin, nanocellulose and xylan	< 1.5 mm	CaO	100 g biomass + 60 g CaO (0.43 g calcium / g biomass component)	Fluidized bed reactor	Dry mixing	[174]
Wheat straw	150–210 μm	CaO obtained by calcination of $CaCO_3$	8 mg wheat straw + 0, 7.4, 14.9 and 18.6 mg CaO, corresponding to mole ratios of carbon in wheat straw to calcium in additives of 2, 1 and 0.8 respectively	TA[a]	Dry mixing	[85]
Sawdust	200–300 μm	CaO and Fe(III)/CaO	0.5 mg sawdust + 0.5 mg catalyst	CDS Pyroprobe 5200 HP Pyrolyzer	Dry mixing	[44]
Poplar, lignin and cellulose	100–200 mesh (74–149 μm)	CaO	4.5 g feedstock	Fixed bed reactor	Ex situ	[172]
Sawdust	200–300 μm	CaO and Fe(III)/CaO	0.5 mg sawdust + 0.5 mg catalyst (with Fe contents of 5, 10 and 15 wt%)	CDS Pyroprobe 5200 HP Pyrolyzer	Dry mixing	[45]
Rice hull	< 710 μm	CaO obtained by calcined limestone and eggshells	5 mg rice hull + 0.5 mg catalyst (10 wt% of the total weight of biomass)	TA[a]	Dry mixing	[175]
Bamboo residual and waste lubricating oil (co-pyrolysis)	0.15 mm	MgO and HZSM-5 (dual catalytic beds)		CDS Pyroprobe 5200 HP Pyrolyzer	Ex situ	[146]
Cellulose and LLDPE (co-pyrolysis)	–	MgO/C, MgO/Al_2O_3, MgO/ZrO_2	Mixture of 0.5 mg cellulose and 0.5 mg LLDPE blended + 5 mg catalysts	Frontier Lab RX-3050TR micro-reactor	Dry mixing	[176]
Beech wood	–	MgO	1.5 g biomass + 0.7 g catalyst	Fixed bed tubular reactor	Ex situ	[177]
Rice husk, herb residue and wood residue	–	CaO, $CaCO_3$, calcined $CaCO_3$ and eggshell	Blended with a mixing ratio of 1:1	TA[a]	Dry mixing	[178]
Coal						
Bituminous coal	200–450 μm	CaO	Blended with a mixing ratio 9:1	Fixed bed reactor	Dry mixing	[26]
Subbituminous coal	50 μm	CaO and $Ca(OH)_2$	0.5 g coal + 1 g CaO / 1.5 g $Ca(OH)_2$	Fixed bed reactor	Dry mixing	[51]
Bituminous coal and cow dung (co-pyrolysis)	150–180 μm	CaO	coal:cow dung:CaO mixing ratio of 5:5:1	TA[a]	Dry mixing	[52]
Lignite and bituminous coal	120 mesh (125 μm)	CaO	Blended with a mixing ratio of 9:1	TA[a]	Dry mixing	[97]
Coal (not specified)	100–120 μm	CaO	0.5%,1.0%,1.5%,2.0% of loading ratio	TA[a]	Dry mixing	[171]
Bituminous coal	250–550 μm	Ni/MgO	100 g coal + 10 g catalyst	Fixed bed reactor	Dry mixing or Ex situ	[179]

Note: TA: thermogravimetry analyzer

catalyst by impregnation in order to increase the yield of tar issued from the pyrolysis of a bituminous coal. Results obtained then showed the propensity of the so produced catalyst to favor methanation of CO and CO_2 as well as the CO_2 reforming of methane. Furthermore, Zhu et al. noted that a higher tar yield could be obtained from coal pyrolysis under CO/H_2, CO_2/H_2, and CO_2/CH_4 atmospheres when using the Ni/MgO

catalyst, which has been traced to the formation of intermediate radical species such as H or CH_x, which are issued from the above-mentioned methanation and reforming reactions [179].

Surface-modified base catalysts consisting of AAEMs dispersed on a support (alumina, activated carbon and silica) have also attracted attention since the combination of both acid and basic sites allows improving the fuel properties of biomass pyrolysis oil through a synergistic effect. In such a case, the metal cations (such as Na^{2+}, Mg^{2+} and Ca^{2+}), characterized by a strong tendency to donate an electron, lead AAE metal ions dispersed and sintered on support particles to act as heterogenous base catalysts [12]. Moreover, by implementing consecutive impregnation and calcination treatments that tend to shift metal cations into a more thermally stable state, one can modify the physicochemical properties of the support on which they are coated, namely, acidity and basicity, the total pore volume, the pore size or the surface area [157,180–183]. As an example, Rizkiana et al. loaded ultra-stable Y type zeolites with Mg cations [181]. In so doing, they observed that the formation of formate and carboxylate intermediates at the surface of the catalyst due to the slight basicity of MgO allows reducing the amount of deposited coke. In addition, they also reported an increased hydrocarbon content in the pyrolytic oil during the co-pyrolysis of coal and biomass catalyzed by means of the Mg-modified zeolite. In another study focusing on the catalytic co-pyrolysis of cellulose and LDPE (low-density polyethylene), Ryu et al. prepared three magnesium-impregnated support materials as catalysts (MgO/C, MgO/Al_2O_3 and MgO/ZrO_2) by calcination and found that the catalytic activity of MgO/C was higher due to a large amount of acid and base sites, together with a larger surface area [176]. Other studies have also confirmed an upgraded catalytic efficiency of AAEM-coated zeolites that are likely to influence carboxylation, dehydration and aromatization mechanisms during biomass pyrolysis [182,184,185]. Sun et al. recently used a mixing method aided by an ultrasonic treatment to improve the dispersing uniformity of CaO on a ZSM-5 zeolite [186]. N_2 adsorption and desorption analyses conducted therein with ZSM-5 zeolite, CaO, and CaO/ZSM-5 samples showed a uniform distribution of mesopores along with higher pore volume and area in the case of the alkali-treated CaO/ZSM-5 catalyst. This latter therefore appeared to be more efficient in promoting the gas diffusion ability as well as the catalytic performance with respect to CO_2 capture, oil selectivity and biomass conversion. Nevertheless, and as the catalytic effect of zeolite does not represent the main topic tackled in the present review, this upgrading pathway will not be further addressed. However, additional information on the matter can be found in [12,187], among others.

5. Catalytic effects of AAEMs on pyrolysis (composition, distribution and characteristics of pyrolytic products)

5.1. Catalytic effects on the pyrolysis of biomass

5.1.1. Alkali and alkaline earth metal salts

In the studies reviewed in the present section, pyrolysis experiments have typically been conducted after the biomass samples are impregnated into aqueous solutions of AAEM salts, so that the ionized metal cations can form coordination bonds with the biopolymer molecules [161,188]. Therefore, even when it is not specifically mentioned, the reader should consider that the analyzed biomass has been pretreated using such a wet impregnation approach. With this clarification done, it should first be noted that as it is difficult for the salts to migrate into the crystalline structure of cellulose, metal cations are expected to only change the reactivity of the surface molecules [161,168]. In this context, there is a strong tendency for impregnated salts to break existing chemical bonds due to their affinity to polymer organic groups. Moreover, the absorbed metals are particularly believed to induce homolytic cleavage of pyranose rings during the decomposition of cellulose, while their interaction with oxygen atoms is likely to contribute to the weakening of the hydrogen bonds. Furthermore, AAEMs tend to decrease the stability of glycosidic bonds and hydroxyl groups during impregnation and pyrolysis, which results in glycosidic bond cleavage, dehydration reactions, as well as ring scission reactions producing smaller molecular species and suppressing the formation of LG [6,10,20–22,49,50,92,160,168,188–193]. Yang et al. and Mahadevan et al. further explained that the nature of the products issued from the pyrolysis of cellulose can be related to the positions of the bond cleaving with CO_2, glycolaldehyde, acetol and levoglucosan, which result from homolytic cleaving at positions C1 or C5, C2 or C4, C3 and C6, respectively [189,192]. Apart from intramolecular bonds, intermolecular linkages are also influenced by the addition of impregnated salts. Of note, cellulose is connected to hemicellulose and lignin via hydrogen bonds, while hemicellulose is linked to lignin through hydrogen and covalent bonds [8]. In a study aimed at better apprehending the influence of potassium chloride (KCl) on wheat straw pyrolysis, Jensen et al. analyzed the thermal degradation of the three main biopolymers composing such a feedstock (i.e., cellulose, xylan and lignin) in the presence and absence of KCl [163]. The TGA results they obtained showed that potassium chloride impregnation does not significantly decrease the decomposition temperature of cellulose, xylan and lignin [163]. In a 2007 study, Nowakowski et al. also found that impregnation with potassium has a greater impact on the pyrolysis of natural biomass as compared to a synthetic biomass that consists of a mixture of cellulose, hemicellulose and lignin [160]. These results therefore suggest that minerals influence the interaction between the biopolymers such that the morphology and structure of biomass can be modified [160]. It has, moreover, been shown in a study by Safar et al., who analyzed the behavior of rubber wood impregnated by potassium carbonate (K_2CO_3), that the crystallinity of cellulose decreases with increasing potassium concentration, which enhances the biomass reactivity during pyrolysis [57]. Finally, Jiang et al. proposed that the AAEMs released in gaseous phase can also promote the catalytic cracking of tar molecules [194,195]. As they did not provide any further experimental results to support this conclusion, additional investigations are therefore required on the matter since the homogeneous interactions between gaseous AAEMs and volatile species are seldom documented in the literature.

The presence of salt in biomass usually shifts the decomposition process to lower temperatures, promotes such a process and increases the char and gas yields at the expense of bio-oil [20,47,57,91,160,161,188,193,196]. Moreover, it increases the carbon-to-oxygen (C/O) ratio of bio-oils produced, which are thus more valuable for use as biofuels, notwithstanding the decrease of the bio-oil yield [20]. When studying the primary pyrolysis of pure cellulose (containing a negligible amount of mineral impurities) impregnated with different inorganic salts (NaCl, KCl, magnesium chloride ($MgCl_2$), $CaCl_2$, etc.) and switchgrass ash, Patwardhan et al. noted that inorganic salt concentrations as low as 0.005 mmoles/g of cellulose were sufficient to induce significant reductions of levoglucosan yields, along with an increased formation of low molecular weight species such as formic acid, glycolaldehyde and acetol [22]. Such a decrease in the LG yields induced by the catalytic reactivity of added metal salts has been explained by Kawamoto et al. as being induced by a polymerization of volatile LG, which enhances primary char formation, and by the same token, inhibits secondary char formation [10].

Biomass impregnation with metal salts, however, inevitably brings anions, which remain in the treated feedstock and decompose at higher temperatures during the pyrolysis process. The emission of volatile species such as hydrochloric acid in the non-condensable gases can thus occur and contribute to air pollution [197]. Some volatile AAEM metals, such as potassium and sodium, can lead to the formation of high mass loadings of aerosols and to the deposition of potentially corrosive components on the surfaces of reactors [24]. Efficient removal systems are therefore required to avoid the above-mentioned environmental and technical issues [197]. Furthermore, pretreatment methods such as washing or wet impregnation require that biomass is dried before being pyrolyzed, which also causes water and energy waste as well as

pollution. Consequently, the economic aspects of wet impregnation should be carefully considered for industrial applications [19], hence the need for works to be undertaken with a view to improving and optimizing current processes.

5.1.1.1. Sodium additives. Among AAEMs, sodium chloride (NaCl) is expected to be mild while being one of the most common and inexpensive catalysts. During pyrolysis experiments conducted in a fixed bed reactor with rice husk, Zhao and Li showed that the addition of NaCl as a catalyst with mixing ratios comprised between 1 and 5 wt% allowed increasing the bio-oil yield, decreasing the percentage of organic acids, esters, ketones, guaiacols and aldehydes and increasing the percentage of alcohols, phenols, furans and anhydrosugars [82]. Furthermore, the authors showed that adding NaCl to rice husk allowed to obtain bio-oils with a higher heating value and a lower acidity. These results can be explained by the fact that small sodium cations can penetrate biomass textures, break intermolecular hydrogen bridges, and thus favor the degradation of biomass [82]. Such actions directly influence the pyrolysis reactions of cellulose, hemicellulose and lignin through ring scission, depolymerization, dehydration and rearrangement to form small decomposition products [75,82]. Besides, the impact of the basicity of sodium containing inorganic compounds on pyrolysis has also been investigated due to the good solubility of such compounds. Highlighted trends show that a strong sodium base can extract low molecular compounds from biomass (species such as sodium hydroxide being particularly likely to react with functional groups of biopolymers through active alcohol groups of cellulose as an example) [75]. By comparing the catalytic effects of sodium hydroxide (NaOH), sodium carbonate (Na_2CO_3), sodium silicate (Na_2SiO_3) and NaCl on the pyrolysis of impregnated biomass samples (including pine wood, cotton stalk and fir wood), Wang et al. demonstrated that all the sodium compounds caused the tested feedstocks to devolatilize at lower temperatures [75]. Interestingly enough, the observed temperature reductions have been found to follow the compounds' basicity sequence (i.e., NaOH > Na_2CO_3 > Na_2SiO_3 > NaCl). Furthermore, the differential thermogravimetric analysis (DTG) curves obtained in [75] exhibited a peak at ~120 °C for the samples treated with NaOH and Na_2CO_3, which has been related to the basic feature of these compounds that would allow extracting low molecular compounds from biomass that vaporize at this specific temperature. Using the same four sodium catalysts, Chen et al. investigated the pyrolysis of pine wood sawdust by microwave heating under dynamic nitrogen atmosphere [6]. Significant increases in the yields of solid products and decreased yields of gaseous products have been reported regardless of the considered additive while no major change in the liquid products yields has been noted. As in [75], the sodium additives caused the non-condensable gaseous products (essentially H_2, CH_4, CO and CO_2) to evolve earlier. In addition, alkaline sodium catalysts have been shown to favor the production of hydrogen and acetol while restraining the formation of furfural, 2-furanmethanol, 4-methyl-2--methoxyphenol and LG. While the deoxygenation efficiency of the tested catalyst was not analyzed in [6], Peng et al. investigated this aspect in a recent work dealing with the effect of alkaline additives, including NaOH and Na_2CO_3, on the production of phenols by lignin pyrolysis in a fixed bed reactor [13]. The authors concluded that decarboxylation or decarbonylation reactions as well as the removal of unsaturated alkyl branch chains were promoted by the use of alkaline catalysts. They finally noted that NaOH, which has the strongest basicity among the additives, favors deoxygenation of methoxy groups, thus leading to phenols free of methoxy groups in the so derived pyrolysis products.

5.1.1.2. Potassium additives. A far as the impact of potassium additives on bio-oils is concerned, two main effects have been evidenced in the literature as being significant. These are the formation of fewer oxygenated compounds through enhanced deoxygenation reactions and the production of smaller molecular species originating from catalytic cracking. Nowakowski et al. notably showed that char and methane yields were increased during experiments conducted with short rotation willow coppice and synthetic biomass [160]. They also noted that the pyrolysis of K-impregnated samples tends to produce much less LG which would be induced by heterocyclic ring opening and cracking reactions favoring the production of low molecular weight species together with char, as also highlighted in [21,22,50]. Within the framework of an analysis focusing on the catalytic effect of K_2CO_3 on the pyrolysis of pine wood, Wang et al. reported increased yields of gaseous and char products originating from secondary reactions involving liquid products whose yields consequently decreased [198]. While suppressing the formation of saccharides, aldehydes or alcohols and reducing the formation of acid, furans and guaiacols, potassium has also been shown to increase the alkanes and phenols yields, which is in line with the increased productions of phenol and phenol derivates reported in the above-mentioned work from Nowakowski et al. [160]. In a study pertaining to the production of bio-oils issued from the pyrolysis of wood biopolymers impregnated with K_2CO_3, Rutkowski noted that the liquid products obtained were characterized by higher proportions of aliphatic hydrocarbons, in conjunction with reduced contents of monocyclic aromatic hydrocarbons, phenols and compounds with carboxyl groups [167]. According to these authors, such a reduction in the proportion of oxygen-containing groups would be related to dehydration and demethoxylation reactions occurring during the pyrolysis of the main wood components in the presence of potassium carbonate. The intrinsic importance of the two above-mentioned reaction pathways (i.e., dehydration and demethoxylation) has, moreover, been confirmed by Hwang et al. who noted increased contents of water and guaiacyl-related compounds in bio-oil issued from the pyrolysis of poplar wood with KCl-impregnated samples [190]. Meanwhile, Lu et al. highlighted the relevance of impregnating poplar wood with potassium phosphate (K_3PO_4) as a catalyst to produce phenolic-rich pyrolysis bio-oils notably containing phenol and 2,6-dimethoxy phenol [199]. These different studies therefore tend to illustrate the specific deoxygenation ability of K_2CO_3 and potassium hydroxide (KOH), which favor demethoxylation reactions. Nevertheless, potassium-containing additives can additionally promote decarboxylation or decarbonylation reactions, along with the removal of unsaturated alkyl branch chains, as demonstrated by Peng et al. during an analysis focusing on the effects of several alkalis (including K_2CO_3 and KOH) on the pyrolysis of lignin [13]. While K_2CO_3 has been shown to promote the production of methoxy-phenols, the strong alkalescence of KOH has been pointed out as favoring the deoxygenation of methoxy-phenols and the production of alkyl-phenols. More recently, possible reaction pathways accounting for the influence of potassium on the pyrolysis of different feedstocks (camphor branch, corn cob and walnut shell) impregnated with potassium nitrate (KNO_3) have been proposed by Zhang et al. [50]. Following the observations made by these authors, anhydrosugars issued from the dehydration of LG would be converted by ring scission into linear aldehydes, themselves converted into 5-(hydromethyl)furfural via a dehydration reaction accelerated by K catalysis. Additional fragmentation would then lead to furfural, while cyclic ketones would be alternatively issued from the catalytic conversion of active cellulose. On the other hand, the depolymerization and dehydration reactions of hemicellulose in the presence of potassium are believed to induce the production of furans, while depolymerization and cracking reactions of lignin are expected to be responsible for the formation of monophenols and polyphenols. Regarding gaseous species, their yields are typically increased during pyrolysis conducted in the presence of K additives. This behavior was observed in the above-referenced works by Patwardhan et al. [22] or Leng et al. [49], for instance, as well as in a former study by Jensen et al., who measured CO, CO_2 and H_2O yields about 4, 5 and 3 times higher, respectively, during the pyrolysis of cellulose impregnated with KCl [163]. Similarly, Wang et al. observed that physically mixing K_2CO_3 with pine wood allows increasing the cumulative CO, CO_2 and H_2 yields [198]. In this regard, Shah et al. [196] explained that the higher yields of

gases (such as CO and CO_2) and light volatiles could be induced by the effect of potassium additives on temperature histories, secondary tar reactions and pyrolysis kinetics, as they observed that the timings of the temperature maximum and gas generation were both significantly affected by the addition of potassium, which is consistent with the observations in [46]. To conclude, it has also been demonstrated that the light aromatic hydrocarbons content in gaseous phase was increased through catalytic cracking in the presence of potassium additives [191].

5.1.1.3. Calcium additives. Compared to other AAEMs, the attention paid to the catalytic effects of calcium components on the pyrolysis of biomass is somewhat limited in the literature, since alkaline earth metal catalysts are more commonly used in the form of oxides. Nevertheless, and similarly to other AAEMs, calcium ions promote the pyrolysis of biomass by enhancing its degradation through different mechanisms, including depolymerization, dehydration, ring opening and repolymerization reactions. In an analysis dealing with the different actions induced by alkaline earth metal chlorides on the thermal conversion of cellulose, Shimada et al. concluded that $CaCl_2$ allows to substantially reduce the pyrolysis temperature while accelerating the depolymerization of cellulose [168]. In their investigation of the pyrolysis of pine wood physically mixed with calcium hydroxide ($Ca(OH)_2$), Wang et al. reported, for their part, that the aldehyde and acid yields were inhibited by the addition of a calcium-based catalyst, whereas the formation of alcohols and H_2 was significantly increased [198]. They also noted that calcium hydroxide promotes the decomposition of cellulose (as noted above) and lignin constituents while leading to liquid and char yield trends running opposite to those mentioned in Section 5.1.1.2 when using K_2CO_3 as a catalytic additive. By comparing the effect of 5 calcium salts ($CaCl_2$, $Ca(OH)_2$, calcium nitrate ($Ca(NO_3)_2$), calcium carbonate ($CaCO_3$) and calcium hydrogen phosphate ($CaHPO_4$)) on the pyrolysis of cellulose, Patwardhan et al. found that the counter anion of the metal ions influences the chemical speciation during pyrolysis, with a decrease in the LG yield in the following order: $Cl^- > NO_3^- \sim OH^- > CO_3^{2-} \sim PO_4^{3-}$ [22]. In addition, calcium chloride has also been shown by Wang et al. to influence the pyrolysis of alkali lignin by decreasing the activation energies of the main pyrolysis stage (between 200 and 560 °C), by shifting the degradation of lignin to lower temperatures and by promoting its thermal cracking [46]. It is finally noteworthy that calcium ions are more active than magnesium ones in promoting the primary formation of char, the conversion of LG into light oxygenates and furans, together with the conversion of 5-(hydroxymethyl)furfural into smaller furans such as furfural [20]. This was notably demonstrated by Zhu et al. in a study focusing on the catalytic effect of AEMs on cellulose pyrolysis. The authors, moreover, showed that bio-oils with higher C/O ratios were obtained when adding calcium or magnesium ions to cellulose, which is consistent with the deoxygenation phenomenon previously reported in the case of other AAEMs [20].

5.1.1.4. Magnesium additives. The interaction between magnesium and oxygen-containing functional groups of biomass is known to facilitate the decomposition of biopolymers by weakening the strength of intramolecular bonds. In this respect, the Mg^{2+} cation in hydrated $MgCl_2$ salt would be particularly capable of coordinating with glycosidic oxygen, as a Lewis acid, to catalyze the cleavage of glycosidic bond, resulting in the solid-state hydrolysis of cellulose and the decrease of its degree of polymerization [161,168,188,200]. Besides, magnesium cations are also known to enhance the cracking of oxygen rings, thus promoting the formation of volatiles with lower molecular weights [10,22]. As a dehydration agent, $MgCl_2$ quite logically has a catalytic effect on the primary dehydration of cellulose by favoring the degradation of hemicellulose, which results in the formation of furans [201]. Furthermore, the addition of magnesium additives to biomass can significantly reduce the decomposition temperature and the maximum degradation rate. For instance, while the decomposition of cellulose begins at around 260 °C (see Section 2.1), Yu et al. still detected the presence of sugar and anhydrosugar oligomers resulting from the pyrolysis of $MgCl_2$-impregnated cellulose at temperatures as low as 150 °C [188]. Similarly, Santana et al. also reported initial degradation temperatures as low as 172 °C during the pyrolysis of $MgCl_2$-impregnated soybean bull samples [197]. As far as bio-oils are concerned, the above-mentioned dehydration and cleavage processes related to the presence of magnesium tend to increase the yield of water in the liquid pyrolytic products. Due to the strong hydration ability of Mg^{2+}, its combination with water is difficult to break, which explains why water can still be produced in the bio-oil at temperatures higher than 500 °C [161,168]. Furthermore, and as noted in [161], the presence of magnesium is likely to reduce the benzene, toluene, ethylbenzene, xylene and styrene (BTEXS) yields, which could be related to an enhanced char formation from lignin and/or to a combination of the metal with oxygen-containing fractions derived from the cleavage of ether linkages in the lignin complex. Similarly, a reduction of the amount of LG in bio-oil can be noted and traced to the primary decomposition of the biomass as well as to a secondary repolymerization by magnesium. On the other hand, and despite the above-mentioned higher water content, the viscosity of bio-oil produced from magnesium-doped biomass tends to increase due to an enhanced formation of oligomers and char fines [161]. Besides, and as concluded by Zhu et al. in their investigation of the alkaline-earth-metal-catalyzed pyrolysis of cellulose, the magnesium ions are able to catalyze secondary pyrolysis reactions, leading to the conversion of anhydrosugar into secondary char, even though Mg seems to have less of an effect on primary pyrolysis products than does Ca [20]. As a divalent cation, magnesium is finally believed to catalyze reactions between volatile molecules and to enhance char formation through recombination reactions [161]. After fast pyrolysis, magnesium is present as metal oxide or in an ionized state and mainly remains in the bio char, which can be further used for soil applications [202].

5.1.1.5. Comparison between the four AAEM additives. Both alkali and alkaline earth metals are able to weaken the hydrogen bonding network in cellulose, although AEMs, which are stronger Lewis acids, show a better ability to catalyze dehydration reactions. This leads to the formation of more cross-linked cellulose, and eventually, char [20,162,188]. Compared to alkali metals, alkaline earth metals accelerate the bulk cellulose pyrolysis more significantly and decrease the related decomposition temperature in the following order: $Mg^{2+} < Ca^{2+} < K^+ < Na^+$ [168]. It should be noted that this phenomenon is more easily influenced by the catalyst loading for alkaline earth metals. In this respect, Shimada et al. explained that Mg^{2+} and Ca^{2+}, as Lewis acids, have a better affinity to the oxygenated ring of LG, and thus promote solid-state hydrolysis at elevated temperatures [168,200]. While the effect of alkali metals and alkaline earth metals on the decomposition of LG during the pyrolysis of cellulose is globally well-documented, no consensus, however, truly emerges from the literature regarding the relative catalytic efficiency of the different AAEMs. Shimada et al. [168] and Hu et al. [9] have reported that the effect of AEMs on the decomposition of LG is greater than that of alkali metals. Similar trends have also been observed by Kawamoto et al., who demonstrated that the catalytic activities of $MgCl_2$ and $CaCl_2$ on the polymerization of LG are much higher than those of KCl and NaCl [10]. They also linked the reduction of the amount of volatile LG to the inhibition of secondary char, as pointed out in Section 5.1.1. Nevertheless, Patwardhan et al., who examined the primary pyrolysis products of cellulose, alternatively found an inverse trend with a reduction of LG yields in the following order: $K^+ > Na^+ > Ca^{2+} > Mg^{2+}$, without giving any further explanation [22]. This observation therefore paves the way for further investigations to better understand these seemingly contradictory results. In a subsequent analysis focusing on the comparative effects of AAEMs (used in the form of acetate salts) on cellulose pyrolysis, Wang et al. found that all tested additives decreased both the aromatic and olefin yields, with

an AAEM effect on the reduction of hydrocarbon yields in the following order: $K^+ > Na^+ > Ca^{2+} > Mg^{2+}$ [91]. According to this work, the presence of AAEMs in biomass enhances cracking and dehydration reactions, which increase thermally-derived CO_x and char. It also reduces the yield of condensable vapors that can be converted into hydrocarbons by deoxygenation reactions. Overall, AEMs are characterized by higher catalytic activities than are alkali metals. As a result, AEMs significantly contribute to increasing the primary and total char yields during the pyrolysis of cellulose [10]. On the other hand, Dalluge et al. still observed increased char yields when adding alkali metals to lignin instead of AEMs [47]. By comparing the electropositivity of four alkali metals (Li, Na, K and Cs) and three alkaline earth metals (Mg, Ca, and Ba), Dalluge et al. concluded that increased electropositivity increases the catalytic activity of metal cations toward char production. To conclude, it has also been shown that magnesium and calcium have a stronger inhibition ability with respect to the formation of N-containing species as compared to potassium, which can thus have strong impacts on flue gas denitrification in biomass power plants [81]. Moreover, as alkaline earth metals reduce the activation energy of the main pyrolysis stages more significantly, they therefore reduce the pyrolysis thermal degradation temperature, which in turn helps save energy in the context of industrial applications [46,81,197].

5.1.2. Alkaline earth metal oxides

5.1.2.1. Calcium oxide. Calcium oxide is a stable chemical compound that can be used as a catalyst under high temperature conditions. It is an abundant, renewable and nontoxic component which can be obtained from the calcination of $CaCO_3$, $Ca(OH)_2$ or natural resources, including calcite, dolomite and eggshell. In the literature, CaO is usually physically mixed with biomass with Ca loading up to 100 wt% (see Table 6). It has often been used for coal pyrolysis with a view to decreasing the viscosity and oxygen content of pyrolytic oils. It is, moreover, a promising base catalyst for cracking pyrolytic vapors in order to produce high-quality bio-oils from biomass [43]. Due to its above-mentioned thermal stability, CaO can ultimately be recycled at the end of the thermal treatment by combusting the char issued from the pyrolysis process.

In addition to fixing the CO_2-like compounds, calcium-based catalysts also promote dehydration, decarbonylation, decarboxylation and cracking reactions. In doing so, they contribute to reducing the oxygen content of pyrolytic oils [43,45,135,203]. This deoxygenation capability of CaO can be exemplified by the elimination of acid compounds, the decrease of aldehydes and ketones yields, the increase of light and aromatic hydrocarbons, the higher production of H_2O by dehydration of oxygenated species, and the reduction of heavy substituted phenols yields [43,45,135]. As a base catalyst, calcium oxide can largely decrease the yields of acids which are converted into ketones by ketonization [135] as well as into hydrocarbons and CO_2 by means of three major pathways, consisting in neutralization, thermal cracking and catalytic cracking [85,173]. As such, it is possible to decrease the acidity and oxygen content of the bio-oils obtained while increasing their heating value. This, therefore, makes these pyrolytic products more suitable for use in pipes and engines as high acidity decreases the stability and increases the corrosiveness of bio-oils [43,45,85,135,203,204]. Veses et al. particularly noted, through analyses conducted in an auger reactor, that the use of calcium-based catalysts during wood pyrolysis allows reducing the relative amount of phenolic compounds having a high oxygen content (such as ethylmethoxyphenol, creosol or guaicol) and increasing the relative quantity of phenolic species with a lower oxygen content (including cresol and phenol) [43]. This is consistent with the observations by Sun et al., who showed that impregnating sawdust with Fe/CaO catalysts increases both the light phenols and heavy substituted phenols yields, as mentioned above [45]. This phenomenon is in fact due to the ability of the catalyst to favor the cracking of the oligomers derived from lignin to generate monomeric phenolic compounds while further converting them without the carbonyl group and unsaturated C-C bond on the side chain [44,205]. Moreover, Sun et al. concluded that the catalyst exhibiting the lowest Fe content among those tested showed the best activity in removing the methoxy group and hydrotreating the unsaturated C-C bonds, leading to deoxygenated phenolic vapors [45]. On the other hand, the use of calcium oxide has also been demonstrated to increase the PAH yields, which should be carefully considered due to the carcinogenic and mutagenic potential of such compounds [174,206]. Eventually, and to prevent the catalyst deactivation during the pyrolysis processes, CaO can be advantageously loaded with iron, as was done in [44] and [45] for example. Note here that Zhang et al. notably showed that a Fe (III)/CaO catalyst was more effective than CaO in reducing the oxygen content of bio-oil due to the synergistic effect between Fe and CaO support [44].

As far as the formation of gaseous species is concerned, CaO has been demonstrated to promote the CO, H_2, H_2O and CH_4 yields via different mechanisms. As an example, when analyzing the composition of the gaseous products obtained from biomass pyrolysis in the presence of CaO, it has been noted that the greater the calcium oxide content, the less the CO_2 and the greater the H_2 contents [135,203,207]. Chen et al. and Chireshe et al. explained that these results could be related to the absorption of CO_2 by CaO, which promotes the water-gas shift reaction ($H_2O + CO = CO_2 + H_2$) [135,203]. However, and despite the consumption of CO by this pathway, they still found no decrease in the formation of CO, thus suggesting that CaO addition promotes decarbonylation reactions during biomass pyrolysis. Furthermore, different studies have clearly highlighted increases of CO yields at high temperatures [85,135,173], which can be traced to different mechanisms, including the catalytic cracking of phenols (a process well documented in the case of coal [156,208]), the dissociation of diaryl ether [209] and the Boudouard reaction ($C + CO_2 = 2CO$), which results from the interaction between the CO_2 released from the decomposition of $CaCO_3$ with the carbon in pyrolysis char [210]. With respect to this last route, it is important to note that $CaCO_3$ as well as $Ca(OH)_2$ can be formed at low temperatures due to the absorption of the CO_2 and H_2O molecules released during the pyrolysis by CaO [85,203]. At higher temperatures, these species can, however, be released again through the decomposition of the so formed calcium carbonate and calcium hydroxide. Besides, it has been shown that increasing the CaO loading tends to increase the quantity of water produced due to secondary cracking reactions of the pyrolytic vapors. This release of oxygen in the form of water is in fact quite beneficial to the quality of the organic phase of bio-oils since the water content, which exists mainly in aqueous phase, can be removed by a separation process such as centrifugation, decantation, condensation or solvent extraction [203,211]. Within this framework, Chireshe et al. notably stated that the implementation of a separation process by condensation could decrease the water content in the organic phase of bio-oils to a value as low as 7.8 wt% [203]. Besides, the CO_2 and H_2O produced during CaO-catalyzed pyrolysis will tend to react with the biochar at relatively high temperatures, thus enhancing the biomass conversion [186]. It can also be added that increasing the CaO loading can induce an increase in the CH_4 yields as observed in [135,207], which can be traced to the breakdown of phenol derivates on the CaO catalyst [212].

It is finally noteworthy that the above-mentioned effects induced by the use of CaO as a catalyst on the gas phase composition, as well as on the reduction of tar, can enable the production of high-quality gaseous fuels suitable for gas turbine applications. This has been illustrated in [207], where the CaO-catalyzed conversion of sawdust in a pyrolyzed moving bed coupled with a fluid bed combustor allowed producing a fuel having a lower heating value higher than 16 MJ/m^3 with a tar content lower than 50 mg/Nm^3. Similarly, Chireshe et al. found that the use of CaO as a catalyst during the pyrolysis of forest residues led to the production of a gas having a calorific value of 13.7 MJ/kg as opposed to 5.2MJ/kg without catalyst [203].

5.1.2.2. Magnesium oxide. Magnesium oxide is industrially produced from the calcination of magnesium carbonate ($MgCO_3$), which is the main component of magnesite. It can also be produced via the calcination of magnesium hydroxide ($Mg(OH)_2$) precipitated from seawater [177]. Like calcium oxide (see Section 5.1.2.1), MgO is thermally stable and has a good reactivity with acids. It is therefore considered as an interesting chemical for use in the ex situ catalytic pyrolysis of biomass as it can improve the quality of pyrolytic oils in different ways. It indeed increases the aromatics yields at the expense of oxygenated compounds [213]. Bio-oils with higher monoaromatic, cyclic and aliphatic hydrocarbons contents that are characterized by high stability and heating values can thus be obtained. This aromatic yield increase originates from the glycosidic bond decomposition occurring during the pyrolysis of cellulose. This leads to the formation of oxygen-containing chemicals (acids, aldehydes, alcohols, esters, furans and ketones) by dehydration and rearrangement, whose conversion into aromatic hydrocarbons can subsequently occur through additional deoxygenation and aromatization processes [183,214]. Besides, MgO also favors deacidification via ketonization and aldol condensation reactions over the basic sites of the catalyst [146]. Overall, the aliphatic hydrocarbons, furans, ketones, phenolics and aromatics contents in pyrolytic oils tend to increase under MgO-catalyzed pyrolysis at the expense of acids, alcohols and esters [146,176]. As far as gaseous species are concerned, MgO does not exhibit a significant influence on H_2, CH_4 and CO, while it tends to increase the CO_2 yield by ketonization [203].

In terms of physicochemical characteristics, MgO is characterized by basic sites and negligible (mainly Lewis) acidity. Consequently, the mechanisms at play during MgO-catalyzed pyrolysis are expected to significantly differ from those involved in the case of zeolites exhibiting strong acid sites. When analyzing the structure and morphology of different MgO catalysts produced from the calcination of magnesite mineral with varied durations and temperatures, Stefanidis et al. showed that the higher the number of basic sites, the smaller the crystal size, the larger the surface area of the catalyst, the greater its reactivity with respect to bio-oil deoxygenation, and the greater the reduction of organic bio-oil yields and coke formation [177]. Besides, basic catalysts (as in the case of MgO) are known to enable acid ketonization (as mentioned above) with the simultaneous formation of CO_2 as well as aldol condensation of aldehydes and smaller ketones [215,216]. This can therefore be considered as a preferable route to obtain upgraded bio-oils with a reduced oxygen content as compared to the use of acid catalysts, which favor the production of CO and H_2O as dominant by-products, thus removing only one oxygen atom against two when using MgO. Furthermore, temperature-programmed oxidation analyses carried out in [177] also highlighted that coke formed on MgO oxidizes at lower temperatures (~100 °C) than that issued from the use of acid zeolites, thus making magnesium oxide a catalyst that is easy to regenerate by simple calcination at relatively low temperatures.

MgO is not effective at increasing the yields of aromatics, however, although it tends to increase the production of phenols (principally light and alkylated phenols) [146,177,217]. This explains why the implementation of a dual catalytic approach involving MgO and zeolite can be considered as an interesting option with a view to combining the positive effects of both acid and basic sites in order to upgrade the resulting bio-oil. Doing so indeed allows first converting pyrolytic volatile matters into hydrocarbon fuel precursors, which will then be transformed by the acid catalyst into highly valuable monocyclic aromatics via cracking, dehydration, decarbonylation and aromatization reactions [146]. Ryu et al. notably implemented such an approach within the context of analyses dealing with the catalytic pyrolysis of lignin and the co-pyrolysis of lignin with low-density polyethylene by means of MgO loaded on carbon, aluminum oxide (Al_2O_3) and zirconium dioxide (ZrO_2) [176,218]. The results obtained showed that well-balanced acid/base sites and high surface areas allow to improve the selectivity towards monoaromatic hydrocarbons. This is consistent with the observations reported in [183], noting that the MgO/C catalyst has been demonstrated as being the most effective in terms of deoxygenation and production of valuable chemicals, including aromatics, phenols and furans. Eventually, by comparing the efficiency of four different metal oxides (ZnO, CaO, Fe_2O_3 and MgO) during the fast pyrolysis of a poplar wood-polypropylene composite, Lin et al. found that MgO and CaO globally exhibit similar catalytic activities in upgrading the pyrolysis vapors [204]. Nevertheless, CaO has still been found to be more effective in removing oxygen (thus eliminating carboxylic acids and phenols) due to its strong basicity as compared to MgO, which demonstrated a weaker deoxygenation efficiency [204]. Chireshe et al. confirmed this observation in [203] by comparing the composition and heating value of the products issued from the pyrolysis of eucalyptus wood catalyzed by MgO and CaO. On the other hand, while CaO promotes coke formation and slightly increases cyclopentanones and alkenes, MgO exhibits a much stronger chain scission activity, which allows to significantly enhance the alkene yields [204].

5.1.3. Inherent AAEMs present in biomass

Since the accumulation of alkali and alkaline earth metals is likely to influence the product distribution from catalytic pyrolysis, in addition to being a major reason for catalyst deactivation [192,219], deashing pretreatment may thus be applied to reduce adverse impacts of inherent AAEMs [19]. As an example, Nowakowski et al. used hydrochloric acid to remove salts and most of the inherent metals present in samples of short rotation willow coppice and synthetic biomass [160]. In both cases, the HCl pretreatment led to a significant decrease of the char yields, which could be related to the suppression of inorganic species promoting char formation. However, Nowakowski. et al. still observed that such an effect was more prominent in the case of willow coppice having a higher initial metal content than in the case of the synthetic biomass, thus demonstrating here again that inherent metals play an important role in the mechanisms governing catalytic pyrolysis. As explained by Mourant et al. who analyzed the impacts of AAEMs on the yield and composition of bio-oil derived from the fast pyrolysis of mallee wood, these species (especially divalent Mg and Ca) act as cross-linking points allowing the junction between the biomass biopolymers [92]. Their presence can thus play an important role in the pyrolysis reactions as the bonds between AAEMs and lignin-originated fragments tend to be continuously cleaved and reformed. This process thus extends the residence time of organic fragments within the biomass particles, which in turn induces further cracking reactions. This mechanism is in fact quite similar to the one occurring due to the presence of inherent AAEMs in coal, as described in Sections 5.2.2 and 5.2.3. That being said, and as far as the composition of pyrolytic products is concerned, it is noteworthy that deashing pretreatments usually favor the formation of heavier liquid oligomers [80,92] as well as aromatic hydrocarbon yields. This has been illustrated, for instance, by Wang et al., who analyzed the effect of AAEMs on the yields of hydrocarbons from the catalytic pyrolysis of red oak [91]. Results obtained with raw biomass and acid-washed or acid-infused samples showed that pretreatments, which allow alleviating the influences of inherent AAEMs, induce an increase of aromatics yields at the expense of char and non-condensable gases, whose yields are generally enhanced by the presence of AAEMs. Similarly, by comparing the aromatics and olefins yields produced during the pyrolysis of raw and HCl-washed sugarcane bagasse, Likun et al. concluded that inorganic matter contained in the raw biomass sample inhibits the production of hydrocarbons, in addition to inducing catalyst deactivation by blocking the catalyst pores [220]. Hu et al. notably explained these phenomena by the promoting effect of AAEMs on the breakage and decarboxylation/decarbonylation reactions of thermally labile hetero atoms of tars as well as on the thermal decomposition of heavier aromatics [9]. During this study dealing with the effects of AAEMs on the pyrolysis of rice husk, Hu et al. also noted that inherent metals accelerate the decomposition of levoglucosan and enhance solid and gaseous products yields through the thermal decomposition and polymerization of tars according to [221]. In this respect, it should be noted that the

catalytic effect of inherent AAEMs on the cracking of tar is more significant at low temperatures because of the decomposition of thermally labile groups, whereas the polycyclic aromatic hydrocarbons formed at high temperatures are much more stable. Hu et al. finally added that the presence of inherent AAEMs also enhances the production of H_2 and CO_2 via Boudouard, water-gas shift or hydrocarbon reforming reactions, among others [9]. Alternatively, the demineralization of biomass through acid washing has been shown to increase the levoglucosan yields and to reduce the acidity of bio-oils, in addition to the above-mentioned decrease of the char yields [9,48,193]. Due to the enhanced production of sugars and sugar derivatives issued from the pyrolysis of leached biomass, Persson et al. concluded that such a procedure could represent a promising route for the utilization of pyrolytic liquids in fermentation-based biorefineries [71].

Another important point to be raised regarding the pyrolysis of biomass in industrial systems concerns the presence of inherent AAEMs in the gas phase, which can generate corrosion problems in reactors. The formation of aerosols such as low-melting eutectics containing alkali metal sulfates and chlorines is, moreover, likely to enhance the oxidation of alloys [24,68,222]. To tackle these issues, the AAEM concentration can be removed either by gas cooling or by using adapted sorbent materials, although such processes logically lead to additional and quite significant operating costs [68]. Since these problems are more stringent in the case of biomass (due to the high AAEM content of this type of feedstock as compared to coal), various studies have therefore focused attention on the release and transformation of AAEM species during the thermal treatment of varied biomass feedstocks. In short, it must first be noted that alkali metals are more likely to be released as volatile species during pyrolysis, as compared to alkaline earth metals, since divalent bonds are more thermally stable [24,194,223]. By comparing the pyrolysis of three biomass feedstocks, Jiang et al. observed that the release ratio of alkali metals can reach up to 53–76%, whereas for alkaline earth metals, this upper range is only 27–40%, under the same operating conditions [194]. Besides, the release behavior of potassium and sodium is generally quite similar despite their different initial concentrations in biomass [223]. Furthermore, it has been established that the release of potassium is particularly influenced by the molar ratios with other mineral elements (e.g., K/Si or Cl/K) [222]. As an example, a high level of Cl promotes the formation of KCl, and hence enhances the release of potassium at high temperatures, while Si inversely inhibits the emission of potassium [9,68,224,225]. Another parameter which plays a major role in the release of AAEMs is the pyrolysis temperature. At low temperatures, alkali metals tend to be bonded with silicate and aluminum in the form of solid aluminosilicate, and remain in ultimate ash after pyrolysis. They are, however, released with pyrolytic products at high temperatures, as illustrated in [9,24,222,223]. According to Olsson et al., only a small fraction of the alkali metal content is released below 500 °C, and originates from the decomposition of the organic structure [68]. On the other hand, a significant portion of alkali metals is released from mineral ash into gaseous species at temperatures higher than 500 °C [68]. Chen et al. notably indicated that the optimum temperature for the lowest gaseous release of species containing alkali metals was 900 K (i.e., 627 °C) [222]. Above 1000 K (i.e., 727 °C), the number of gaseous species containing potassium and sodium will decrease, and the species will then transform into $KOH_{(g)}$, $NaCl_{(g)}$ and $NaOH_{(g)}$ [222,223]. In addition to the temperature, environmental conditions also significantly influence the release of AAEMs. As an example, Okuno et al. compared the release of AAEMs during the pyrolysis of pulverized pine and sugarcane bagasse with and without forced gas flow [65]. They concluded that the release of AAEM species was inhibited in the absence of forced gas flow due to the repeated desorption from and adsorption onto the char surface. Zhang et al. also studied the influence of the atmosphere on the transformation of AAEMs and found that oxidizing environments enhance the release of potassium and inhibit the emission of sodium, calcium and magnesium [24]. In addition, oxidizing atmospheres have also been demonstrated to promote the transformation of all AAEM species in the chemical form of silicate.

5.2. Catalytic effects on the pyrolysis of coal

5.2.1. Alkali and alkaline earth metal salts

As in the case of biomass, alkali and alkaline earth metals can have considerable effects on the yields and composition of the products issued from the pyrolysis of coal. In fact, AAEMs are commonly loaded by wet impregnation, and can thus combine with oxygen-containing functional groups (e.g., carboxylic and phenolic groups) that act as virtual cross-linking points [103,226,227]. As a consequence, the catalytic effect of AAEMs is usually more pronounced with low-rank coals than with high-rank fuels since the former are much more abundant in surface oxygen-containing functional groups [35]. The added AAEM cations (X^+) particularly react with -COOH and -OH groups to form -COOX and -OX, as illustrated in Eq. (1) and Eq. (2) [97,103].

$$X^+ + \text{-COOH} = \text{-COOX} + H^+ \quad (1)$$

$$X^+ + \text{-OH} = \text{-OX} + H^+ \quad (2)$$

Although some studies show that AAEM species have little effect on the reactivity of coal pyrolysis, and even tend to inhibit the release of volatiles [97,228], opposite trends have still been highlighted, depending on the considered temperature range [159]. Indeed, and as shown by Liu et al. in a study focusing on the thermal decomposition of lignite in the presence of metal chlorides, the inhibition effect of KCl on pyrolysis is mainly seen between 400 and 720 °C [159]. In fact, carboxylates in coal are known to undergo decomposition at low temperatures, while metal ions initially associated with -COO groups in the coal matrix may be bonded to the coal/char matrix (-CM in Eq. (3)) at higher temperatures [98,159,226,228].

$$\text{-CM} + \text{-COOX} = \text{CM-X} + CO_2 \quad (3)$$

X thus continuously serves as a cross-linking point [38,157,227] and renders the emission of tar fragments more difficult, as exemplified in [159], where chlorides are shown to inhibit the release of volatiles and the pyrolysis rate for temperatures higher than 400 °C. At this stage, char is expected to comprise significant amounts of oxygen-containing groups serving as bonding sites. Nevertheless, the newly formed CM-X bonds, which are not stable enough above 700 °C, will be broken down again to generate gaseous species according to Eq. (4) and Eq. (5).

$$\text{CM-X} = \text{-CM} + \text{X} \quad (4)$$

$$\text{-CM} = \text{-CM'} + \text{gas} \quad (5)$$

AAEMs therefore offer new sites for combining with the char matrix. Furthermore, large quantities of free radicals are produced with increasing temperatures by thermal cracking between AAEMs and the char matrix [98,159,226]. In the case of calcium chloride, Wang et al. demonstrated that a minimum temperature of ~900 °C was required to generate the catalytic effect induced by $CaCl_2$ on the emission of gaseous species [98]. In such conditions, the release of aliphatic gases can be traced to dealkylation and to ring opening reactions of condensed aromatics, together with the cleavage of aliphatic side chains [35]. Wang et al. also noted almost no change in the morphs of KCl before and after pyrolysis, contrary to $CaCl_2$, which for its part, was converted into $CaCO_3$ in coal char [98].

Regarding catalytic mechanisms, AAEMs tend to bond with oxygen-containing groups and to repeatedly connect with the coal/char matrix as described above, which differs from the scheme encountered with transition metals that transform into stable metallic states to catalyze the pyrolysis reactions [98,159,226].

As far as tar formation is concerned, divalent cations, which act as virtual bonds between the carboxylic groups within the coal structure, have often been pinpointed as being responsible for the reduction of the tar yields due to their cross-linking effects [38,229]. Cations can,

moreover, convert tar into char and make the structure of the latter more compact. Consequently, heavy tar molecule release is made more difficult. Metallic cations can also drastically impact the composition of tar products during coal pyrolysis [35]. Depending on the course of the catalytic reaction, tar must first be absorbed by the active sites of the catalyst. Consequently, such a process depends not only on the physical properties of the catalyst, but also on the transfer behavior of the volatile species [156,171].

As regards the impact of AAMs on coal gasification, Skodras et al. showed that the rate of CO_2 gasification of lignite was directly related to the content of inherent inorganic matter, including AAEM species [100]. This phenomenon has also been associated with the significant number of oxygen-containing groups in lignite. These latter indeed facilitate the adsorption of the catalytically active basic elements, which in turn enhances gasification reactions [230]. Bai et al. showed that adding Na and Ca to coal favors the formation of micropores and mesopores during gasification. Moreover, the simultaneous existence of both these compounds results in a more abundant pore structure, more reactions between the carbon matrix of coal char and H_2O, and a higher production of active intermediates (H_2 and CO_2) [231]. When the gasification temperature becomes too high (above 850 °C [103]), the molten catalyst is, however, likely to react with coal ash and form a viscous solid-liquid mixture, thereby drastically changing the catalytic mechanisms [100, 103]. To conclude, the level of catalyst loading should also be considered with caution as the use of an excessive quantity of catalyst may block the inner pores of coal char, thus decreasing the effective contact area of CO_2 with carbon, as well as the efficiency of the gasification process [103].

5.2.1.1. Sodium additives. The addition of Na_2CO_3 has been shown to promote CO and H_2 yields during the pyrolysis of bituminous and anthracite coals [103]. Furthermore, it has been demonstrated that this trend is strengthened by increasing the pyrolysis temperature and the amount of catalyst added to the coals. The so monitored enhanced production of H_2 in the presence of a Na-containing catalyst can be traced to the reaction of Na^+ with the -COOH or -OH groups in coal, which produce -COONa or -ONa, together with the release of H^+ [101]. Concerning the increased production of CO, this can be traced to the reaction between the CO_2 produced during the pyrolysis process and carbon bonded with Na [103].

5.2.1.2. Potassium additives. As mentioned above, the morph of KCl exhibits almost no change before and after the pyrolysis [98,159], which would therefore indicate that KCl experiences decomposition and recombination with coal/char matrix during the whole process, as stated in Section 5.2.1. It has, moreover, been demonstrated that KCl tends to inhibit the yield of CO below 700 °C while promoting it above this temperature. Inherent minerals thus seem to have a good catalytic effect on the breakage of ether, hydroxyl and oxygen-containing heterocyclic compounds, which are the main sources of CO above 700 °C [159]. Inversely, they inhibit the decomposition of aldehyde carbonyl and methoxy groups, as well as secondary reactions of tar, from which CO mainly originates below 700 °C [156,159]. One can add that Liu et al. also showed that KCl and inherent minerals have a great catalytic effect on the production of CH_4 [159], whose formation originates from the cracking of aliphatic chains, aromatic side chains and oxygen methylene containing methyl functional groups [232].

5.2.1.3. Calcium additives. During the pyrolysis process, calcium is likely to catalytically influence cross-linking reactions [117]. At low temperatures (600 – 800 °C), calcium cations can promote the conversion of tar to char and induce a tightening of the coal structure that limits the release of large tar molecules. However, the diffusion of smaller gaseous molecules is not significantly affected [54,55]. Above 800 °C, the secondary cracking of tar molecules prevails, and no measurable effect of calcium on tar yields can be observed [54,55]. In a work focusing on the transformation of sulfur during the pyrolysis of a lignite in a fixed bed reactor, Jia et al. showed that the presence of calcium sulfate ($CaSO_4$) could promote the formation of hydrogen sulfide (H_2S) and carbonyl sulfide (COS) at high temperatures (above 800 °C) and high $CaSO_4$/coal blending ratios (above 20%) by catalyzing the decomposition of organic sulfur [233]. Eventually, when comparing the effects of five metal chlorides (KCl, $CaCl_2$, nickel chloride ($NiCl_2$), manganese chloride ($MnCl_2$), and zinc chloride ($ZnCl_2$)) on the catalytic pyrolysis of lignite, Wang et al. concluded that the yield of CH_4 was only promoted by $CaCl_2$ and that the catalytic effect of this metal chloride was mainly significant above 900 °C, as previously mentioned in Section 5.2.1 [98].

5.2.2. Alkaline earth metal oxides

5.2.2.1. Calcium oxide. As a basic component, calcium oxide has been extensively used in industry as a desulfurization agent [53,233]. The presence of CaO can reduce sulfur-containing compounds (H_2S and sulfur dioxide (SO_2)) by sulfur fixation [234–236]. It can be formed from the decomposition of $CaCO_3$, which is naturally present in coal [237]. In addition, it is known to greatly influence the yields and composition of pyrolytic products, even at low loading ratios (less than 10 wt%) (see Table 6).

Calcium oxide has a catalytic effect on the reactivity of coal pyrolysis. It increases the fuel decomposition rate, decreases the tar yield, and significantly affects the degree and the rate of formation of aromatic compounds. It, moreover, favors the emission of light gaseous species by enhancing the catalytic cracking reactions of larger molecules, including ringed structures, carboxylate and phenolic compounds [26,51–53,97, 156,171]. As such, calcium oxide can be considered as an interesting additive for the removal of tar specifically within the framework of tarry fuel gas issued from biomass and peat gasification [238]. Furthermore, calcium oxide can improve the quality of the tar produced by decreasing their oxygen, nitrogen and sulfur contents. Besides, it also promotes the formation of light alkanes and increase the yields of BTXN compounds (i.e., benzene, toluene, xylene and naphthalene) [35,52–53]. In a study dealing with the effects of AAEMs on the formation of light aromatic hydrocarbons during coal pyrolysis, Yan et al. investigated the pyrolysis of pure fluoranthene in the presence and absence of CaO [35]. In that context, they observed ~280% and ~160% increases in the amounts of benzene and toluene produced, respectively, when adding calcium oxide. Such results thus illustrate the important catalytic effect of CaO, which is able to crack fluoranthene into lighter aromatic hydrocarbons. On the other hand, the yields of some oxygen- or nitrogen-containing species such as phenols, ketones, pyridines and nitriles tend to decrease in the presence of calcium oxide [52,156]. This metal oxide is, moreover, likely to enhance the synergistic effect between coal and biomass during co-pyrolysis experiments. Following Wang et al., this phenomenon would be related to the fact that CaO partly delays the pyrolysis of biomass and promotes the decomposition of coal, thus providing an overlapping pyrolysis range that enhances interactions between both feedstocks [52]. Consequently, more high-valued aromatic compounds such as benzene and naphthalene can be formed.

As far as gaseous species are concerned, their formation is favored by calcium oxide, which is able to effectively catalyze the secondary reactions of primary products. Indeed, as the polarity of the active sites of calcium oxide can affect the π-electron cloud's stability of primary products (which especially include condensed aromatic compounds) and since CaO has a cracking active site on both inner and outer surfaces, it is therefore supposed to enhance the cracking of heavy alkanes and polycyclic aromatic compounds to form light alkanes and gaseous species, while consequently reducing the tar yield [52,53,156,171]. A higher production of CH_4 can actually be traced to the demethylation of methyl substituted groups present in primary products [53,156,234].

With regards to the increase in the CO yields, that is mainly due to the accelerated cracking of oxygenated functional groups present in phenolic compounds and carboxylic acids [97,156,171,237]. According to Skodras et al., the greater the Ca content, the greater the CO_2 gasification, which would be due to the ability of CO_2 to be chemisorbed on alkaline earth metal oxides to form reactive oxygen-containing complexes that act as oxygen transfer media enhancing CO_2 gasification [100]. It has still been noted in [156] that no CO_2 was detected during the CaO catalyzed pyrolysis of a Binxian bituminous coal due to the formation of $CaCO_3$ resulting from the reaction between CO_2 and calcium oxide [156]. As for the formation of H_2, it mainly originates from the cracking of long-chain hydrocarbons at low temperature and from polymerization, cyclization, and aromatization at higher temperatures [156,171]. The higher yields of CO and H_2 during CaO catalyzed pyrolysis can, alternatively, also result from the following reactions:

$$C + H_2O \rightarrow H_2 + CO \quad (6)$$

$$CO + H_2O \rightarrow H_2 + CO_2 \quad (7)$$

$$C + CO_2 \rightarrow 2CO \quad (8)$$

in which the reactants H_2O and CO_2 come from the decomposition of $CaCO_3$ and $Ca(OH)_2$ previously formed at a relatively low temperature range [26,51].

To conclude, is should be noted that the catalytic effects associated with calcium on coal pyrolysis can also be highlighted by means of kinetic analyses (see Section 5.3 for more information on this). This can be exemplified by referring to a study by Jia et al., who expressed the tar cracking rate by means of a simple first-order model. That work allowed estimates of 30% and 45% decreases in the activation energy when adding 6% and 12% of calcium oxide to coal, respectively [156]. Similarly, Liu et al. decomposed the coal pyrolysis process into three independent first-order reactions whose activation energies, determined by means of an integral method [239], have been found to decrease when adding CaO [97] thus, here again, demonstrating the catalytic effect induced by calcium oxide.

5.2.2.2. Magnesium oxide. As far as MgO is concerned, the literature dedicated to the analysis of the catalytic effects induced by this metal oxide on coal pyrolysis is quite limited. In combustion studies, it has been shown that the addition of MgO to a brown coal could decrease the molten slag fraction of ash (that may enhance the oxidation of alloys, as discussed in Section 5.1.3) and of the ash deposition within furnaces due to the production of solid phase aluminosilicates [240]. Besides, Xu et al. also demonstrated through thermodynamic calculations that adding MgO tends to increase the fusion temperature of high-calcium coal ash [241]. Nevertheless, and in the context of pyrolysis analyses, attention has been more particularly devoted to the effect of dolomite as a source of MgO and CaO due to its related effects on the removal of sulfur and the reduction of CO_2 and heavy molecules (tar components and PAHs), among others [234,242,243]. Sciazko and Kubica indeed showed that adding dolomite to bituminous and brown coals allows decreasing the amount of tarous components, PAHs and sulfur in the gaseous products generated during high temperature pyrolysis in a circulating fluid-bed reactor [242]. Ma et al. also observed increased yields of hydrogen (from 52.9 to 55.5 g/kg-fuel) and decreased yields of tar (from 5.4 to 0.4 g/Nm^3) when adding dolomite in the 3.0–12.0 wt% range to mixtures of pine sawdust and brown coal during gasification tests performed in a bubbling fluidized bed [243]. Nevertheless, and even though the sulfur removal efficiency of dolomite in gas emissions has been well documented, Zhang et al. still indicated that MgO seems to have a limited ability to fix sulfur as compared to CaO [236], thus prompting the need for additional investigations to better elucidate the intrinsic role of MgO on the above-mentioned trends.

5.2.3. Inherent AAEMs present in coal

Overall, the yield of tar issued from the pyrolysis of raw coal is less than that obtained in the case of demineralized fuels. This is due to the presence of inherent AAEMs, which are likely to reduce the amount of high molecular weight volatiles by promoting cross-linking and decomposition reactions [35,54,55,117]. This point was illustrated in [35], where the demineralization of a lignite and a subbituminous coal was found to decrease the yields of BTXN, a trend related to the role of inherent AAEM species that enhance the cracking of phenols and condensed aromatics into lighter aromatic hydrocarbons. The intrinsic AAEMs present in coals may also act as cross-linking points (see Section 5.2.1), allowing large free radicals, issued from the cleavage of the chemical bonds connecting carboxyl groups with the char matrix, to recombine repeatedly with the residual matrix of coal. This process expands the residence time of released fragment structures in the particles, and thus promotes thermal decomposition and partial carbonation reactions [27,38,117,118]. On the other hand, it was shown in [35] that the catalytic effect of AAEMs was highly dependent on the metal content of the base fuel. Indeed, Yan et al. showed that the impact of demineralizing a bituminous coal on the yields of BTXN was quite negligible since this fuel type contains very low AAEM concentrations as compared to lignite and subbituminous coals [35]. Besides, and while the amount of tar released is known to be influenced by the fuel heating rate, it has been demonstrated that AAEM species can inhibit this effect and thus reduce the sensitivity of the tar yield to this important operating parameter [38,157]. Coal ash, which contains a wide variety of minerals, as illustrated in Table 4, can moreover, play a significant role in the promotion of gaseous species by inhibiting the tar yields [171,234] while contributing to remove organic sulfur pollutants by cleavage reactions and sulfur fixation [233,234]. Nevertheless, it is important to highlight that the release of AAEMs during pyrolysis can be associated with deleterious effects as it may induce slagging and fouling problems, the agglomeration of fluidized-bed materials, as well as erosion and corrosion of industrial system components [39]. As compared to biomass, whose alkali metals are essentially found in water-soluble and ion-exchangeable forms, alkali metals present in coal are partly dispersed in the mineral phase, thus limiting their vaporization during the pyrolysis process [68]. The volatilization of monovalent cations (e.g., sodium and potassium) is, however, easier than that of divalent cations (e.g., calcium and magnesium) under similar pyrolysis conditions [38,98]. This is due to the fact that divalent cations may connect to the coal matrix via two bonds requiring more energy in order to break the Ca/Mg-char bonds, which in turn restrains the release of such alkaline earth metal ions [98]. Although some intrinsic AAEMs can begin to devolatilize at temperatures as low as 300 °C [38,39], the higher the temperature, the greater the extent of AAEM species released [38,39]. Li et al. indeed noted that the volatilization of Na and Ca during the pyrolysis of a brown coal becomes truly drastic at high temperatures (i.e., between 900 and 1200 °C) with volatilization levels as high as 80% and 40%, respectively [38]. Wang et al. also observed an intensification of the volatilization of K and Ca over a temperature range comprised between 800 and 1200 °C [98]. These authors notably reported increases of the volatilization levels from ~29 to ~88% and from ~37 to ~64% for K and Ca, respectively. Wang et al., moreover, indicated that the release of AAEMs was closely related to the volatilization of free H* radicals via a reaction of the type:

$$R + CM\text{-}X \rightarrow CM\text{-}R + X \quad (9)$$

where R, CM and X denote the radical, the char matrix and the metal, respectively [98]. Of course, the volatilization rate, as well as the amount of AAEMs released during pyrolysis, also largely depends on the heating rate. To illustrate this point, one can refer to a study by Quyn et al. who showed that the volatilization of Na can reach nearly 100% at 900 °C during the fast heating rate pyrolysis of a brown coal, whereas it decreases to less than 20% at the same temperature under low heating

rate conditions [39]. On the other hand, the release of AAEMs can be inhibited by reactions involving SiO_2 and Al_2O_3, as illustrated in Eq. (10) and Eq. (11) [244]:

$$Al_2O_3(s) + 6SiO_2(s) + 2KCl(g) + H_2O(g) \rightarrow 2KAlSi_3O_8(s) + 2HCl(g) \quad (10)$$

$$Al_2O_3(s) + 6SiO_2(s) + 2NaCl(g) + H_2O(g) \rightarrow 2NaAlSi_3O_8(s) + 2HCl(g) \quad (11)$$

5.3. Kinetic analysis of the catalytic effects induced by AAEMs

Kinetic analyses are commonly performed in the context of studies focusing on biomass and coal pyrolysis. These investigations allow to predict the decomposition behavior of a wide variety of feedstocks, while contributing to providing a better grasp of the reaction pathways at play, which is a must for the proper design and optimization of pyrolysis reactors [23,245]. The apparent kinetic parameters of pyrolysis reactions can be calculated based on experimental results issued from thermal analyses. These include the activation energy (E_a) and the pre-exponential factor (A) used in the formulation of the reaction rate constant k(T), where T and R represent the temperature and the universal gas constant, respectively (see Eq. (12)). Based on the reaction model f(α) associated with k(T) in Eq. (13), one can then estimate the fuel's conversion degree as a function of time ($\frac{d\alpha}{dt}$) [245].

$$k(T) = A \bullet \exp\left(-\frac{E_a}{R \bullet T}\right) \quad (12)$$

$$\frac{d\alpha}{dt} = k(T) \bullet f(\alpha) \quad (13)$$

Non-isothermal thermogravimetric analyses (TGA) are among the most commonly employed techniques used to investigate the variation of the residual mass of pyrolyzed materials as a function of the temperature. Many kinetic models have indeed been developed based on fitting procedures aimed at reproducing experimentally monitored data using such an approach. In this case, Eq. (13) has to be reformulated, however, to integrate the heating rate β, as depicted in Eq. (14).

$$\frac{d\alpha}{dT} = \frac{1}{\beta} \bullet k(T) \bullet f(\alpha) \quad (14)$$

Among the existing modeling approaches which have been developed over the years (see [8] and references therein), one can cite the model-fitting and isoconversional (also called model-independent) methods (which are the most commonly implemented methods [246]), the distributed activation energy model (DAEM) [247,248], as well as the lumped kinetic model [249–251], the chemical percolation devolatilization model [116], etc. These can roughly be classified into two categories, depending on whether they aim to simulate the rate of mass loss of the fuel or the distribution of pyrolytic products. In order to illustrate how the use of such modeling tools can be of interest, Table 7 gives a few examples of results obtained within the framework of studies dealing with the impact of AAEM catalysts on pyrolysis kinetics. It should, nevertheless, be noted that this list, which is not intended to be exhaustive, only focuses on analyses conducted with AAEM additives. The reader is thus referred to reviews from Wang et al. [8] or Solomon et al. [32], among others, for more information regarding kinetic parameters related to the pyrolysis of raw biomass and coal samples. In terms of major trends, the results issued from the references reported in Table 7 show that the addition of impregnated AAEMs tends to decrease the activation energy for the main pyrolysis temperature range, as noted in [85,160,244,252,253]. Alternatively, the implementation of water- or acid-washing pretreatments which remove the mineral matters in biomass tends to increase the so derived E_a values [160]. These results therefore corroborate the observations made in previous sections regarding the ability of AAEMs to enhance the degradation of biomass. Some contrary trends can nonetheless be pointed out, as is the case in [58], where it was not possible to identify any significant correlation between the catalyst loading and the variation of the activation energy. On the other hand, the kinetic analyses reported therein still allowed to demonstrate that the pyrolysis process could be divided into two separate steps when adding AAEMs [58,252], which is in agreement with the main mechanisms described in Section 5.1 regarding the AAEM catalyzed decomposition of biomass. Discrepancies in calculated kinetic parameters can actually originate from a series of factors, including differences in investigated operating conditions and temperature ranges, the selection of a wide variety of feedstocks, the use of different catalyst loadings, the implementation of distinct modeling approaches, etc. [8]. In addition, Table 7 also shows that model-fitting approaches have almost exclusively been selected, while the four main isoconversional models commonly used in the literature to study the pyrolysis of raw biomass and its components have not truly been considered yet to simulate data obtained during AAEM catalyzed experiments. This gap is particularly of concern when considering that the linear fitting of TG data to derive kinetic parameters based on common model-fitting methods is mainly suitable within a narrow range of conversion degrees. It is therefore quite difficult to simulate the mass loss for the initial and final stages of the pyrolysis process with a good precision. Furthermore, the so assessed kinetic parameters might not be reliable and consistent as the whole procedure directly depends on the choice of the reaction model f(α), which is also subject to large uncertainties [8]. Compared to model-fitting approaches, isoconversional methods have the advantage of not requiring prior assumptions regarding the form of the f(α) function, thus leading to the estimation of more reliable and consistent kinetic parameters [254]. Isoconversional methods can, moreover, be used to determine reliable kinetic parameters or to define adapted reaction models when complemented with model-fitting methods, as done in [11,245,255,256]. On the other hand, isoconversional models also present some disadvantages. For instance, fluctuations in data measured at different heating rates may result in substantial errors related to the assessed kinetic parameters. Consequently, and even though coefficients of determination (R^2) above 0.9 are often considered as satisfactory when comparing simulated and measured data, some researchers still hold that isoconversional methods are mainly applicable for a rather narrow conversion degree (up to 60–70%) [77,84,175]. It should, moreover, be recalled that since E_a represents the minimum amount of energy required to activate a given chemical reaction, the lower the activation energy, the lower the temperature at which the reaction will generally occur, and vice versa. Nevertheless, the evolution of the activation energy obtained by isoconversional models in the literature does not always depict a monotonous rise with increasing degrees of conversion, as exemplified in [253]. This unexpected trend which is reported in different studies may, here again, be related to fluctuations in data measured for high degrees of conversion, as stated above. Besides, only the activation energy can be estimated when implementing most isoconversional methods. While kinetic parameters are usually used to reproduce or simulate experimentally monitored data with a view to validating the consistency of proposed model parameters [257], this type of procedure is, however, quite rare (if not inexistent) in the context of analyses dealing with the catalytic effects induced by AAEMs. The reliability of kinetic constants obtained can thus often not be assessed. Further analyses are therefore needed.

To conclude, this brief overview of works conducted to lay out the impact of AAEM additives on pyrolysis kinetics shines the light on some fundamental shortfalls regarding the use of model-fitting and isoconversional methods. The disadvantages listed above regarding both these modeling approaches thus prompt the need for additional investigations based on the use of a wide variety of kinetic models (such as phenomenological ones, for instance) in order to refine calculations and propose more accurate and reliable kinetic parameters and modeling tools.

Table 7
Summary of kinetic analysis methods together with examples of related results.

Model	Category	Expression	Sample	Catalyst	Loading ratio	Notes	Reference
Coats-Redfern	Model-fitting	$\ln\left[\frac{g_{(\alpha)}}{T^2}\right] = \ln\left[\frac{AR}{\beta E_a}\left(1-\frac{2RT}{E_a}\right)\right] - \frac{E_a}{RT}$	Pine wood	CH_3COOK	1.25 wt%, 2.5 wt%, 3.75 wt% and 5 wt%	1. The pyrolysis process is divided into two stages, with a limit between bot stages fixed at around 290 °C or 70% of the degree of conversion2. No significant change in E_a has been observed with the impregnation by CH_3COOK	[58]
			Wheat straw	CaO	n(C):n(Ca) = 0.8, 1 and 2	With the addition of CaO, E_a decreases slightly from 70.1 to 76.6 kJ/mol (raw) to 67.3–73.5 kJ/mol	[85]
			Willow wood	CH_3COOK	1 wt%	1. Acid washing by HCl increases E_a from 89.0 to 178.4 kJ/mol2. With the impregnation by CH_3COOK, E_a decreases from 178.4 kJ/mol (HCl treated) to around 132 kJ/mol	[160]
			Corn straw	Coal ash	5 wt%, 10 wt %, 20 wt% and 100 wt%	1. The pyrolysis process is divided into three stages for all samples2. With the addition of coal ash, E_a at the second stage decreases from 19.6 kJ/mol to 13.1–15.7 kJ/mol (at different catalyst loading ratios)	[244]
			Cellulose	NaCl	0.01, 0.1 and 0.5 mol/L	With the impregnation by NaCl, E_a decreases from 248.9 kJ/mol to 144.6 kJ/mol (at 0.1 mol/L NaCl)	[252]
			Cellulose	CH_3COONa	0.01, 0.1 and 0.5 mol/L	1. The pyrolysis process is divided into two stages with the impregnation by CH_3COONa2. With the impregnation by CH_3COONa, E_a decreases from 248.9 kJ/mol to 89.6 kJ/mol (step 1) and 42.5 kJ/mol (step 2) (at 0.5 mol/L CH_3COONa)	[252]
			Cellulose	$(CH_3COO)_2Ca$	0.01, 0.1 and 0.5 mol/L	With the impregnation by the Ca-based catalyst, E_a decreases from 248.9 kJ/mol to 93.6 kJ/mol (at 0.5 mol/L $(CH_3COO)_2Ca$)	[252]
			Cellulose	$(CH_3COO)_2Mg$	0.01, 0.1 and 0.5 mol/L	With the impregnation by the Ca-based catalyst, E_a decreases from 248.9 kJ/mol to 101.9 kJ/mol (at 0.5 mol/L $(CH_3COO)_2Mg$)	[252]
DAEM	Model-fitting	$1-\alpha = \int_0^\infty \exp\left[1-(1-n)\int_{T_0}^{T}\frac{A}{\beta}\exp\left(-\frac{E_a}{RT}\right)dT\right]^{\frac{1}{1-n}} f_{(E_a)}dE \quad \text{for } n \neq 1$ $1-\alpha = \int_0^\infty \exp\left[-\int_{T_0}^{T}\frac{A}{\beta}\exp\left(-\frac{E_a}{RT}\right)dT\right] f_{(E_a)}dE \quad \text{for } n = 1$ $f_{(E_a)} = \frac{1}{\sigma\sqrt{2\pi}}\exp\left[-\frac{(E_a-E_{a0})^2}{2\sigma^2}\right]$	–	–	–	–	–
Starink	Isoconversional	$\ln\left(\frac{\beta_i}{T^{1.92}}\right) = \ln\left(\frac{A_\alpha R^{0.92}}{g_{(\alpha)}E_\alpha^{0.92}}\right) - 0.312 - 1.0008\times\frac{E_\alpha}{RT}$	Pine wood	K_2CO_3	5 wt%, 10 wt% and 20 wt%	With the impregnation by K_2CO_3, E_a decreases at lower temperatures and increases at higher temperatures	[253]
Friedman	Isoconversional	$\ln\left(\frac{\beta_i d\alpha}{dt}\right) = \ln\left(A_\alpha f_{(\alpha)}\right) - \frac{E_\alpha}{RT}$	–	–	–	–	–
KAS	Isoconversional	$\ln\left(\frac{\beta_i}{T^2}\right) = \ln\left(\frac{A_\alpha R}{E_\alpha g_{(\alpha)}}\right) - \frac{E_\alpha}{RT}$	–	–	–	–	–
OFW	Isoconversional	$\ln(\beta_i) = \ln\left(\frac{A_\alpha E_\alpha}{R g_{(\alpha)}}\right) - 5.331 - 1.052\times\frac{E_\alpha}{RT}$	–	–	–	–	–

Note: β_i: i^{th} heating rate; E_α: Activation energy at a given conversion degree α; A_α: Pre-exponential factor at a given conversion degree α; σ: Standard deviation of the activation energy; $g_{(\alpha)}$: Integral form of reaction model $f_{(\alpha)}$.

5.4. Co-pyrolysis of biomass and coal

Due to its high oxygen and moisture and low carbon contents, raw biomass is characterized by a relatively low heating value, especially as compared to coal [68] (see Tables 2 and 3). Furthermore, its fluctuating seasonal availability may cause substantial issues in terms of supply, transport and storage. Consequently, a co-processing of biomass with coal can be considered as an interesting option with a view to partially mitigating these problems [74]. Co-pyrolysis can, moreover, contribute to significantly reducing greenhouse gas emissions if the biomass is sustainably available. This aspect is all the more crucial in Asian countries (e.g., China or India) where coal still plays a major role in the production of electricity and heat. In these cases, the addition of biomass to coal can therefore help accelerate the energetic transition from fossil to renewable and low-carbon energy [5,74].

As explained earlier, the decomposition of biomass occurs mainly at lower temperatures than that of coal. This is primarily attributable to the higher energy required to break the strong C-C bonds that hold the highly cross-linked aromatics of coal [258], as compared to the inter- and intra-molecular links in biomass, which easily break under heating [5,78,79,259]. At the end of pyrolysis (i.e., for temperatures above 900 °C), the weight loss associated with the individual pyrolysis of biomass is generally greater than that measured with coal, while the weight loss related to co-pyrolysis stands between the individual pyrolysis of both these feedstocks [42,78,79]. On the other hand, the weight loss measured during the co-pyrolysis of biomass with coal is typically greater than the sum of the weight losses associated with the individual pyrolysis of both these materials [5, 260-262]. This therefore shows that far from being a simple addition of the individual pyrolysis of coal and of biomass, co-pyrolysis clearly involves interactions between the decomposition processes related to each feedstock. In this respect, many works have shown that the co-pyrolysis of biomass with coal can induce a synergistic effect, which consists in decreasing the apparent activation energy of the pyrolysis reactions [78], promoting the yields of volatiles [5,42,78] and decreasing the temperature of the maximum weight loss rate [79]. This synergistic effect essentially appears over a temperature range where the pyrolysis of both biomass and coal occurs at significant rates, so that interactions may arise through chemical reactions and physical action. At higher temperatures (>700 °C), the synergy is largely reduced as most of the volatiles have been released and no obvious interactions between blended solid residues can be observed [78]. The influence of mineral ash containing AAEMs on the synergistic effect has been confirmed in different studies. In fact, and as shown in [79], although the ash content of a low-rank coal may be greater than that of straw, the mass fraction of ash in the biomass char can significantly exceed the ash content of the coal char (~44% against ~14%). Zhao et al., moreover, observed that the specific surface area of biomass char can be up to two times higher than that of lignite char, with an AAEM content much higher in the case of straw [79]. This large amount of alkali metal and alkaline earth oxides on the surface of biomass char can be traced to the absorption of the volatile species by the numerous active sites present on its surface. These AAEM species will then enhance the pyrolysis of coal by catalyzing the cracking reactions of the heavy components in tar due to their contact with the catalytic char bed, which lasts for an extended period, and thus achieves a balance of adsorption and desorption. Consequently, light oil is likely to be produced through the cleavage of a bridge aromatic structure bond in long chain aliphatic hydrocarbons (see Fig. 9). In addition, the yields of gaseous species with small molecular weight will also tend to increase due to the breakup of relatively more stable bonds at high temperatures [52,78,79]. At the end of the catalytic pyrolysis, the specific surface area, total pore volume, average pore size and micropore ratio of biomass and coal chars decrease due to the deposition of carbon on the char surface [79]. During an analysis of the co-pyrolysis of *Miscanthus sacchariflorus* with lignite, bituminous and anthracite coals, Tian et al. pinpointed that the increased yields of volatile species from coal could be traced to the high level of CaO and K_2O which are introduced with the biomass [5]. It has indeed been demonstrated that calcium and potassium chlorides have a significant catalytic effect on the cracking of the long carbon chain as well as on the cleavage of the carbonyl groups of the coal structure, thus increasing the production of volatiles [171,260]. Furthermore, the migration of biomass minerals is an important phenomenon affecting the redistribution of AAEM species during co-pyrolysis. It should be noted that the mineral content of coal and the oxygen content of the coal char are primary factors influencing this process [263]. In addition to the influence of the mineral species contained in ash, it is also widely admitted that the presence of high levels of hydrogen and oxygen elements in the form of free radicals (such as H* and OH*) issued from biomass [264] significantly impacts co-pyrolysis. Indeed, these species will tend to inhibit condensation, recombination, and cross-linking reactions, which will in turn result in decreased secondary char yields and increased production of gaseous species such as H_2, CH_4, CO and CO_2 [5,42,67,78,265]. Nevertheless, Wang et al. [67] alternatively noted that the amounts of CO_2, CO and CH_4 released during the pyrolysis of corncob/lignite blends were less than those estimated by considering an additive behavior of both feedstocks, thus suggesting that the presence of coal inhibits the release of volatile species from biomass. Since biomass generally presents a higher H/C ratio than coal, it can thus act as a hydrogen donor during the co-pyrolysis. The presence of hydrogen-rich light molecules issued from the rapid biomass decomposition will then influence the pyrolysis of coal through volatile-coal interactions modifying its thermal behavior [266].

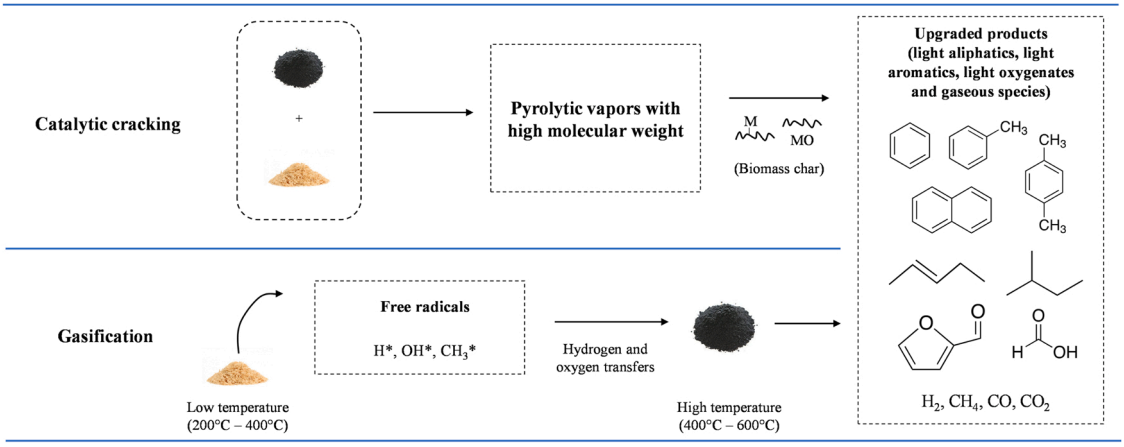

Fig. 9. Possible reaction mechanisms at play during the co-pyrolysis of coal and biomass.

Specifically, the coal cross-linked network is likely to be disturbed during the pyrolysis, thus inducing fragmentation and birthing hydrogen-deficient active sites. Interactions of these latter with the large amount of biomass-derived hydrogen-containing species around the coal will consequently concur to a positive synergistic effect, especially during the co-pyrolysis of biomass with law-rank coals that have a high propensity to capture hydrogen. In addition, the O/C ratio of biomass is generally higher in comparison to coal, which will provide a higher quantity of oxygen during the heating stage, thus increasing the reactivity of the pyrolysis environment and subsequently facilitating coal conversion [42] (see Fig. 9). It should also be noted that biomass char residues can accumulate on the surface of coal during the co-pyrolysis process, thus blocking the coal molecule pores and alternatively inhibiting the thermal decomposition [267]. This provides specific justification for investigations that have been conducted with respect to the reactivity of blended char issued from co-pyrolysis of coal and biomass. In this regard, Ellis et al. concluded that biomass and coal minerals could interact and inhibit gasification [74]. According to the authors, catalytically active calcium species in the biomass may interact with the aluminosilicate species in the coal mineral matter to form $Ca_2Al_2SiO_7$ crystals, which are inert from a catalytic point of view, thus leading to a reduction of the reactivity of the co-pyrolyzed blends. Similarly, in a study focusing on the catalytic effect of coal bottom ash on corn straw pyrolysis, Qin et al. stated that the interactions between AAEMs, Al_2O_3 and SiO_2 inhibit the release of the former (see Eq. (10) and Eq. (11)) from both coal and biomass ash at low temperatures (i.e., 500–600 °C), thereby reducing gas formation until 800 °C [244].

All the above observations illustrate understanding/predicting the

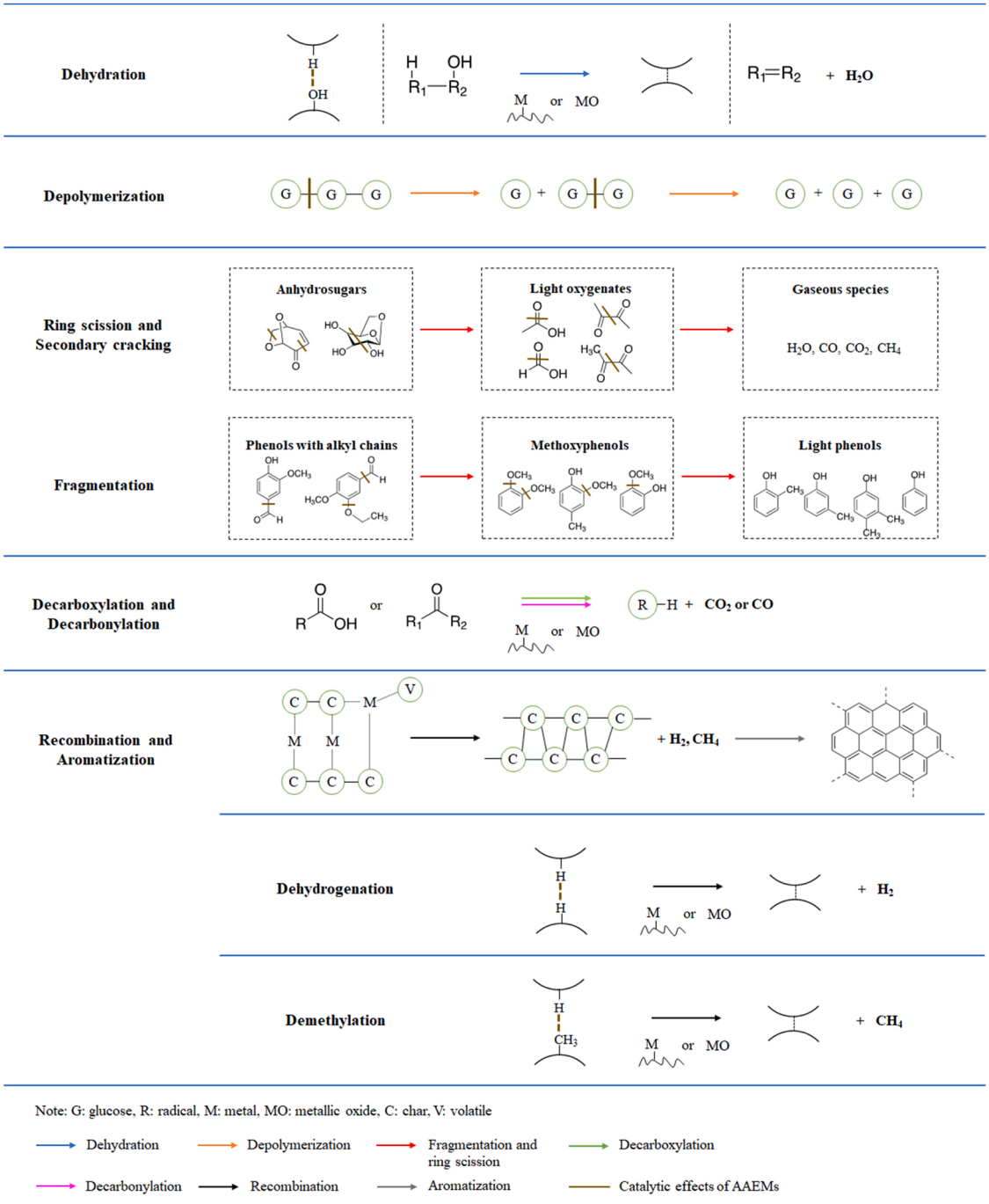

Fig. 10. Summary of some possible pathways at play during the pyrolysis of biomass in the presence of catalysts.

mechanisms at play during the co-pyrolysis of coal and biomass is not a trivial matter as they directly depend on the type of coal and biomass used, the implemented blending ratios and the investigated temperature range. Moreover, the essential role played by the AAEM species contained in biomass in the co-pyrolysis processes has, here again, been clearly underlined, thus illustrating the importance of understanding the impact of such metals on the major decomposition mechanisms, as summarized in the following section.

6. Summary of the decomposition mechanisms at play during AAEM catalyzed pyrolysis

As already mentioned, pyrolysis oils obtained directly from raw biomass are characterized by a high oxygen content. Phenolic compounds derived from the decomposition of lignin are indeed among the main components of bio-oils, thus explaining why they usually present important disadvantages such as a high molecular weight, a high viscosity, a high corrosiveness, a low heating value, and a reduced stability. Consequently, the removal of such compounds through deoxygenation is one of the most important mechanisms to be considered in any process aiming at catalytically upgrading the properties of pyrolytic products [43]. In addition to the possible reaction pathways discussed in Section 3.1, specific mechanisms have been proposed to account for the role of catalysts during in situ or ex situ pyrolysis processes, including dehydration, decarboxylation, decarbonylation and catalytic cracking. (see Fig. 10). All these pathways, which have been discussed in previous sections, involve the removal of oxygen from biomass even though the corresponding mechanisms are different. For instance, dehydration involves the release of a water molecule from the cleavage of a hydroxyl group and of its nearby hydrogen, thus leading to the formation of anhydrosugar and to a charring process due to the so formed unsaturated bond involved. Decarboxylation and decarbonylation yield CO_2

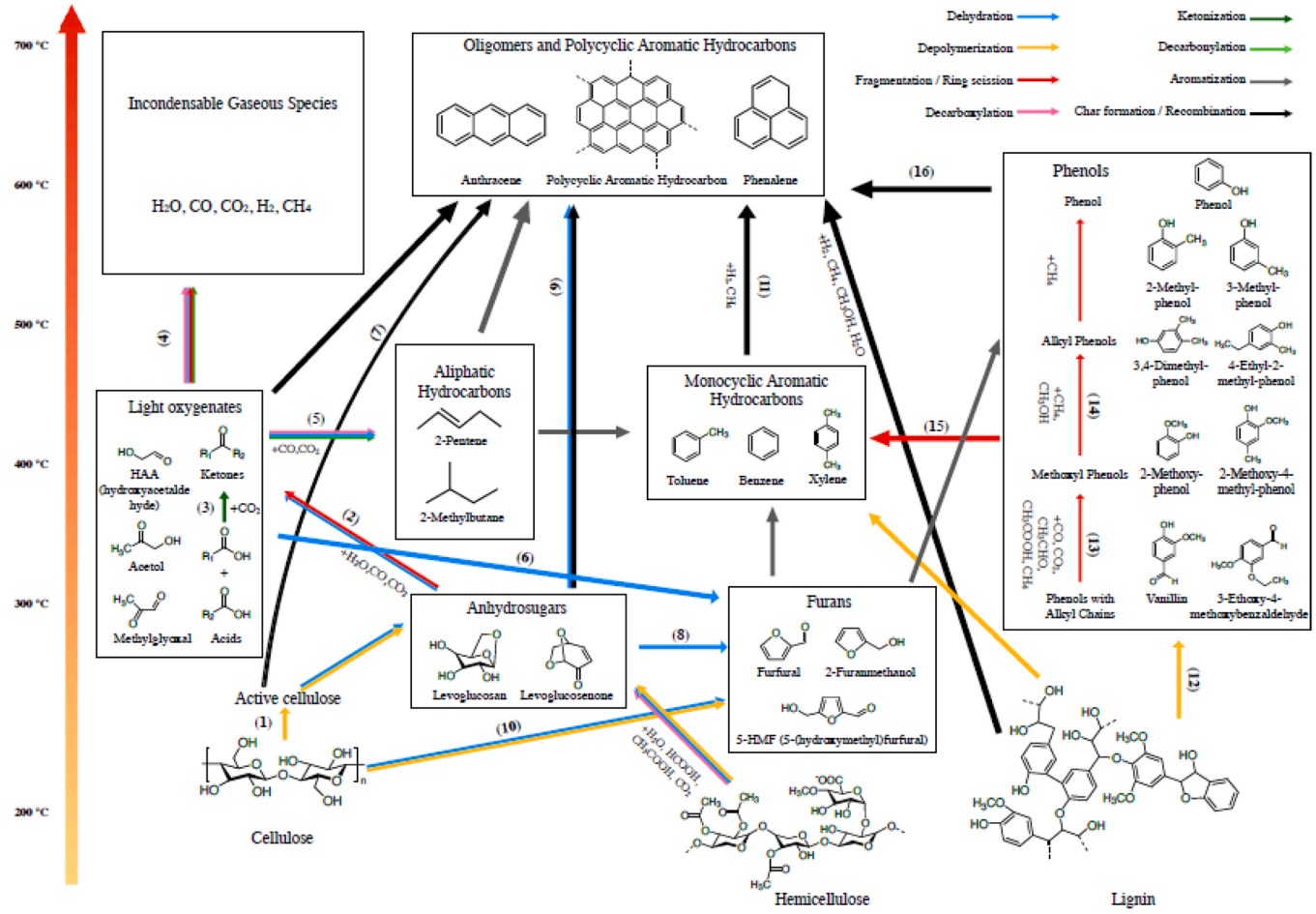

Fig. 11. Summary of the mechanisms at play during AAEM catalyzed pyrolysis. The transformation pathways illustrated herein have been shown to be catalyzed by the following chemical compounds: **Pathway 1**: cellulose – active cellulose => NaCl [75,168], Na_2CO_3 [75], Na_2SiO_3 [75], NaOH [75], KCl [168], K_2CO_3 [57], CH_3COOK [160], $CaCl_2$ [168], $MgCl_2$ [168,188] / **Pathway 2**: anhydrosugars – light oxygenates => NaCl [6,22,82,168], Na_2CO_3 [6], Na_2SiO_3 [6], NaOH [6], KCl [22,49,168,190], K_2CO_3 [191], K_3PO_4 [199], CH_3COOK [160], $CaCl_2$ [22,168], $Ca(NO_3)_2$ [20], $Ca(OH)_2$ [198], CaO [20], $MgCl_2$ [22,161,168,188], $Mg(NO_3)_2$ [20] / **Pathway 3**: acids – ketones => CaO [135], MgO [146,203] / **Pathway 4**: light oxygenates – incondensable gaseous species => NaCl [82], KCl [163,196], K_2CO_3 [191,196] / **Pathway 5**: light oxygenates – aliphatic hydrocarbons => CaO [20,44,85,173,203], MgO [203] / **Pathway 6**: light oxygenates – furans => KNO_3 [50] / **Pathway 7**: active cellulose – oligomers and polycyclic aromatic hydrocarbons => NaCl [75,168], Na_2CO_3 [75], Na_2SiO_3 [75], NaOH [75], KCl [49], K_2CO_3 [57], $CaCl_2$ [49], $MgCl_2$ [188] / **Pathway 8**: anhydrosugars – furans => KNO_3 [50], $Ca(NO_3)_2$ [20], $Mg(NO_3)_2$ [20] / **Pathway 9**: anhydrosugars – oligomers and polycyclic aromatic hydrocarbons => NaCl [10], KCl [10], $CaCl_2$ [10], $Ca(NO_3)_2$ [20], $MgCl_2$ [10,161], $Mg(NO_3)_2$ [20] / **Pathway 10:** cellulose - furans => NaCl [22], KCl [22], K_2CO_3 [167], $CaCl_2$ [22], $MgCl_2$ [22] / **Pathway 11**: monocyclic aromatic hydrocarbons – oligomers and polycyclic aromatic hydrocarbons => $MgCl_2$ [161] / **Pathway 12**: lignin - phenols => NaCl [82], K_3PO_4 [199], CH_3COOK [160] / **Pathway 13**: phenols with alkyl chains – methoxy phenols => NaOH [13], KCl [46], KOH [13], CaO [44] / **Pathway 14**: methoxy Phenols – alkyl Phenols => NaOH [13], KCl [46,190], K_2CO_3 [167], $(HCOO)_2Ca$ [174], CaO [43,44,174], MgO [146] / **Pathway 15**: phenols – monocyclic aromatic hydrocarbons => CaO [44] / **Pathway 16**: phenols – oligomers and polycyclic aromatic hydrocarbons => $MgCl_2$ [161].

and CO, respectively, by cleaving carboxyl and carbonyl bonds, while catalytic cracking allows to enhance smaller molecular weight compounds to be generated (see Section 5 for more details on these mechanisms).

Some of the studies referenced within the present literature review propose diagrams representing some speculated pathways allowing to account for the role of AAEM catalysts on the pyrolysis of biomass [4,20,22,49,50,82,198]. The corresponding figures, however, only depict a limited number of catalytic reactions involving a few additives. In order to summarize recent advances made in the fields of AAEM catalyzed pyrolysis, an extended diagram is proposed in Fig. 11. It notably includes all the aforementioned catalytic mechanisms with a view to helping figure out the role of AAEM catalysts on the pyrolysis of biomass while comparing their respective influence and efficiency levels.

In summary, it can be concluded that the higher the temperature and the greater the catalytic activity level, the smaller the oxygen content of the pyrolytic products. Besides, and as shown in Fig. 11, AAEM catalysts mainly favor deoxygenation reactions by: 1/ enhancing the depolymerization of cellulose through glycosidic bond cleavage, 2/ increasing the formation of char by dehydration and recombination, 3/ favoring the cleavage of anhydrosugar to produce more light oxygenated compounds and incondensable species, and 4/ reducing the oxygenated groups linked to phenols by demethoxylation and rupturing of alkyl chains.

7. Conclusion

Research advances in the fields of biomass pyrolysis and biomass/coal co-pyrolysis have been reviewed in the present paper with a specific emphasis laid on the effects induced by inherent and externally added alkali and alkaline earth metals. In particular, it has been shown that these species, which are essential nutrients for the growth of plants, can cleave existing chemical bonds when added to biomass, thus influencing the whole pyrolysis process. The use of such metal additives can therefore reduce the decomposition temperature, which in turn allows to save energy and promote the yields of specific pyrolytic products, including gaseous products, and improve the selectivity of some aimed chemicals. This therefore explains why ever greater attention has been devoted to AAEM catalysts during the last decades.

After a description of the main properties of lignocellulosic biomass and coal, along with the fundamental mechanisms governing their thermal decomposition, the main experimental strategies adopted in the literature to analyze the impact of AAEMs on pyrolysis processes have been summarized. It is concluded that pretreatment procedures, including water and acid washings, are strongly required prior to conducting any pyrolysis tests. These pretreatments allow isolating the effects of inherent or externally added AAEMs through comparisons of results obtained with raw feedstocks and demineralized control samples. On the other hand, the review has also highlighted that washing procedures could modify the chemical structure of treated samples. This observation therefore prompts the need for specific attention to be paid with respect to the implementation of pretreatment approaches and to the characterization of their impacts on studied feedstocks so as to properly isolate the role of AAEMs on pyrolysis mechanisms.

Regarding the role of alkali and alkaline earth metals, the analysis of the literature led to the illustration of the fact that AAEM salts globally shift the thermal degradation of biomass to lower temperatures while increasing the yields of char and gas, at the expense of bio-oil, whose C/O ratio increases significantly. However, these effects depend strongly on the nature of the metal considered. Conclusions drawn herein especially show that the stronger the basicity of sodium and potassium additives, the stronger the deoxygenation of the so produced bio-oils. As far as potassium additives in particular are concerned, they have been shown to promote the yields of low molecular compounds and gaseous species. Alternatively, magnesium has been demonstrated to promote dehydration reactions, leading to increased water and char yields. For calcium and magnesium oxides that can be physically mixed with biomass, they are known to upgrade the volatile species that are released through deoxygenation and deacidification processes. Nevertheless, and even though the above-mentioned trends are globally admitted, some issues still need to be further investigated and/or clarified. These include, among others, the need for a more comprehensive understanding of the impact of counter anions in AAEM salts on the chemical speciation of pyrolytic products. Furthermore, contrary trends sometimes emerge from the literature regarding the propensity of the different AAEMs to reduce LG, for instance, or concerning the relative strength of alkali metals when it comes to increasing the char yields, as compared to alkaline earth metal oxides. Tackling these issues will require continued efforts in order to ensure a systematic comparison of the impact of AAEMs added to the same feedstocks and under the same operating conditions. Among important avenues needing to be addressed, the promoting role of calcium oxide in terms of PAH formation should be better understood. In addition, it is worth noting that alkali metals, which are more volatile than alkaline earth metals, can be released during pyrolysis and will thus contribute to corrosion problems needing to be addressed. Here are some examples of issues needing to be analyzed in future works with a view to more comprehensively clarifying the numerous effects induced by AAEMs on the pyrolysis of biomass.

In terms of kinetic analysis, it is now admitted that AAEMs enable decreasing the activation energy of the main pyrolysis stage, thus facilitating the conduct of the pyrolysis, that takes place at lower temperatures. A few works have nonetheless been conducted to derive suitable kinetic parameters using advanced isoconversional methods despite the high added value of such analyses which need to be undertaken.

Concerning the co-pyrolysis of biomass with coal, AAEMs have been shown to induce a so-called synergistic effect that leads to a decrease of the apparent activation energy of the pyrolysis reaction, promotes the yields of volatiles, and decreases the temperature of the maximum weight loss rate. The correct interpretation of the role of the AAEMs on these processes here again involves figuring out the detailed mechanisms at play during the co-processing of a wide variety of feedstocks. Consequently, and with this in mind, the present review concludes by proposing a summary diagram gathering the different reaction pathways known to be catalytically influenced by AAEMs, which include dehydration, depolymerization, fragmentation, decarboxylation, decarbonization, etc. Although such a general diagram can benefit from future additional advances, especially regarding the above-mentioned open questions, it can be viewed as an interesting representation of the current knowledge on the role of AAEMs on pyrolysis processes at the molecular level.

Declaration of Competing Interest

The authors declare that they have no known competing financial interests or personal relationships that could have appeared to influence the work reported in this paper.

Acknowledgments

This research was supported by the French Ministry of Higher Education, Research and Innovation (Ministère de l'Enseignement supérieur, de la Recherche et de l'Innovation).

References

[1] F.-X. Collard, A. Bensakhria, M. Drobek, G. Volle, J. Blin, Influence of impregnated iron and nickel on the pyrolysis of cellulose, Biomass Bioenergy 80 (2015) 52–62, https://doi.org/10.1016/j.biombioe.2015.04.032.

[2] F.-X. Collard, J. Blin, A review on pyrolysis of biomass constituents: Mechanisms and composition of the products obtained from the conversion of cellulose,

hemicelluloses and lignin, Renew. Sustain. Energy Rev. 38 (2014) 594–608, https://doi.org/10.1016/j.rser.2014.06.013.
[3] Q. Lu, X. Ye, Z. Zhang, C. Dong, Y. Zhang, Catalytic fast pyrolysis of cellulose and biomass to produce levoglucosenone using magnetic SO_4^{2-}/TiO_2–Fe_3O_4, Bioresour. Technol. 171 (2014) 10–15, https://doi.org/10.1016/j.biortech.2014.08.075.
[4] D. Liu, Y. Yu, Y. Long, H. Wu, Effect of $MgCl_2$ loading on the evolution of reaction intermediates during cellulose fast pyrolysis at 325 °C, Proc. Combust. Inst. 35 (2015) 2381–2388, https://doi.org/10.1016/j.proci.2014.05.026.
[5] H. Tian, H. Jiao, J. Cai, J. Wang, Y. Yang, A.V. Bridgwater, Co-pyrolysis of *Miscanthus sacchariflorus* and coals: a systematic study on the synergies in thermal decomposition, kinetics and vapour phase products, Fuel 262 (2020), 116603, https://doi.org/10.1016/j.fuel.2019.116603.
[6] M.Q. Chen, J. Wang, M.X. Zhang, M.G. Chen, X.F. Zhu, F.F. Min, Z.C. Tan, Catalytic effects of eight inorganic additives on pyrolysis of pine wood sawdust by microwave heating, J. Anal. Appl. Pyrolysis 82 (1) (2008) 145–150, https://doi.org/10.1016/j.jaap.2008.03.001.
[7] M. Van de Velden, J. Baeyens, A. Brems, B. Janssens, R. Dewil, Fundamentals, kinetics and endothermicity of the biomass pyrolysis reaction, Renew. Energy 35 (1) (2010) 232–242, https://doi.org/10.1016/j.renene.2009.04.019.
[8] S. Wang, G. Dai, H. Yang, Z. Luo, Lignocellulosic biomass pyrolysis mechanism: a state-of-the-art review, Prog. Energy Combust. Sci. 62 (2017) 33–86, https://doi.org/10.1016/j.pecs.2017.05.004.
[9] S. Hu, L. Jiang, Y. Wang, S. Su, L. Sun, B. Xu, L. He, J. Xiang, Effects of inherent alkali and alkaline earth metallic species on biomass pyrolysis at different temperatures, Bioresour. Technol. 192 (2015) 23–30, https://doi.org/10.1016/j.biortech.2015.05.042.
[10] H. Kawamoto, D. Yamamoto, S. Saka, Influence of neutral inorganic chlorides on primary and secondary char formation from cellulose, J. Wood Sci. 54 (3) (2008) 242–246, https://doi.org/10.1007/s10086-007-0930-8.
[11] R. Moriana, Y. Zhang, P. Mischnick, J. Li, M. Ek, Thermal degradation behavior and kinetic analysis of spruce glucomannan and its methylated derivatives, Carbohydr. Polym. 106 (2014) 60–70, https://doi.org/10.1016/j.carbpol.2014.01.086.
[12] G. Kabir, B.H. Hameed, Recent progress on catalytic pyrolysis of lignocellulosic biomass to high-grade bio-oil and bio-chemicals, Renew. Sustain. Energy Rev. 70 (2017) 945–967, https://doi.org/10.1016/j.rser.2016.12.001.
[13] C. Peng, G. Zhang, J. Yue, G. Xu, Pyrolysis of lignin for phenols with alkaline additive, Fuel Process. Technol. 124 (2014) 212–221, https://doi.org/10.1016/j.fuproc.2014.02.025.
[14] E.F. Iliopoulou, S.D. Stefanidis, K.G. Kalogiannis, A. Delimitis, A.A. Lappas, K. S. Triantafyllidis, Catalytic upgrading of biomass pyrolysis vapors using transition metal-modified ZSM-5 zeolite, Appl. Catal. B Environ. 127 (2012) 281–290, https://doi.org/10.1016/j.apcatb.2012.08.030.
[15] A. Galadima, O. Muraza, In situ fast pyrolysis of biomass with zeolite catalysts for bioaromatics/gasoline production: a review, Energy Convers. Manag. 105 (2015) 338–354, https://doi.org/10.1016/j.enconman.2015.07.078.
[16] M. Md, R. Rahman, Liu, J. Cai, Catalytic fast pyrolysis of biomass over zeolites for high quality bio-oil – a review, Fuel Process. Technol. 180 (2018) 32–46, https://doi.org/10.1016/j.fuproc.2018.08.002.
[17] J. Liang, G. Shan, Y. Sun, Catalytic fast pyrolysis of lignocellulosic biomass: critical role of zeolite catalysts, Renew. Sustain. Energy Rev. 139 (2021), 110707, https://doi.org/10.1016/j.rser.2021.110707.
[18] X. Zhang, H. Lei, L. Zhu, X. Zhu, M. Qian, G. Yadavalli, J. Wu, S. Chen, Thermal behavior and kinetic study for catalytic co-pyrolysis of biomass with plastics, Bioresour. Technol. 220 (2016) 233–238, https://doi.org/10.1016/j.biortech.2016.08.068.
[19] X. Chen, Q. Che, S. Li, Z. Liu, H. Yang, Y. Chen, X. Wang, J. Shao, H. Chen, Recent developments in lignocellulosic biomass catalytic fast pyrolysis: strategies for the optimization of bio-oil quality and yield, Fuel Process. Technol. 196 (2019), 106180, https://doi.org/10.1016/j.fuproc.2019.106180.
[20] C. Zhu, S. Maduskar, A.D. Paulsen, P.J. Dauenhauer, Alkaline-earth-metal-catalyzed thin-film pyrolysis of cellulose, ChemCatChem 8 (4) (2016) 818–829, https://doi.org/10.1002/cctc.201501235.
[21] I.-Y. Eom, J.Y. Kim, T.S. Kim, S.M. Lee, D. Choi, I.G. Choi, J.W. Choi, Effect of essential inorganic metals on primary thermal degradation of lignocellulosic biomass, Bioresour. Technol. 104 (2012) 687–694, https://doi.org/10.1016/j.biortech.2011.10.035.
[22] P.R. Patwardhan, J.A. Satrio, R.C. Brown, B.H. Shanks, Influence of inorganic salts on the primary pyrolysis products of cellulose, Bioresour. Technol. 101 (12) (2010) 4646–4655, https://doi.org/10.1016/j.biortech.2010.01.112.
[23] S. Hameed, A. Sharma, V. Pareek, H. Wu, Y. Yu, A review on biomass pyrolysis models: kinetic, network and mechanistic models, Biomass Bioenergy 123 (2019) 104–122, https://doi.org/10.1016/j.biombioe.2019.02.008.
[24] Z.-H. Zhang, Q. Song, Q. Yao, R.-M. Yang, Influence of the atmosphere on the transformation of alkali and alkaline earth metallic species during rice straw thermal conversion, Energy Fuels 26 (3) (2012) 1892–1899, https://doi.org/10.1021/ef2011645.
[25] BP Energy Outlook 2020 Edition. ⟨https://www.bp.com/en/global/corporate/energy-economics/energy-outlook/energy-outlook-downloads.html⟩. (Accessed 21 February 2021).
[26] H. Zhang, B. Dou, H. Zhang, J. Li, C. Ruan, C. Wu, Study on non-isothermal kinetics and the influence of calcium oxide on hydrogen production during bituminous coal pyrolysis, J. Anal. Appl. Pyrolysis 150 (2020), 104888, https://doi.org/10.1016/j.jaap.2020.104888.
[27] Y. Zhao, C. Xing, C. Shao, G. Chen, S. Sun, G. Chen, L. Zhang, J. Pei, P. Qiu, S. Guo, Impacts of intrinsic alkali and alkaline earth metals on chemical structure of low-rank coal char: semi-quantitative results based on FT-IR structure parameters, Fuel 278 (2020), 118229, https://doi.org/10.1016/j.fuel.2020.118229.
[28] A. Radenović, Pyrolysis of coal, J. Chem. Chem. Eng. 55 (7–8) (2006) 311–319.
[29] A.O. Odeh, Pyrolysis: pathway to coal clean technologies, in: M. Samer (Ed.), Pyrolysis, InTechOpen, 2017, pp. 305–317, https://doi.org/10.5772/67287.
[30] K.H. van Heek, W. Hodek, Structure and pyrolysis behaviour of different coals and relevant model substances, Fuel 73 (6) (1994) 886–896, https://doi.org/10.1016/0016-2361(94)90283-6.
[31] R. Lemaire, D. Menage, P. Seers, Study of the high heating rate devolatilization of bituminous and subbituminous coals—comparison of experimentally monitored devolatilization profiles with predictions issued from single rate, two-competing rate, distributed activation energy and chemical percolation devolatilization models, J. Anal. Appl. Pyrolysis 123 (2017) 255–268, https://doi.org/10.1016/j.jaap.2016.11.019.
[32] P.R. Solomon, M.A. Serio, E.M. Suuberg, Coal pyrolysis: experiments, kinetic rates and mechanisms, Prog. Energy Combust. Sci. 18 (2) (1992) 133–220, https://doi.org/10.1016/0360-1285(92)90021-R.
[33] P.R. Solomon, T.H. Fletcher, R.J. Pugmire, Progress in coal pyrolysis, Fuel 72 (5) (1993) 587–597, https://doi.org/10.1016/0016-2361(93)90570-R.
[34] K. Murakami, H. Shirato, J. Ozaki, Y. Nishiyama, Effects of metal ions on the thermal decomposition of brown coal, Fuel Process. Technol. 46 (3) (1996) 183–194, https://doi.org/10.1016/0378-3820(95)00056-9.
[35] L.-J. Yan, Y.-H. Bai, X.-J. Kong, F. Li, Effects of alkali and alkaline earth metals on the formation of light aromatic hydrocarbons during coal pyrolysis, J. Anal. Appl. Pyrolysis 122 (2016) 169–174, https://doi.org/10.1016/j.jaap.2016.10.001.
[36] D. Hong, Z. Cao, X. Guo, Effect of calcium on the secondary reactions of tar from Zhundong coal pyrolysis: a molecular dynamics simulation using ReaxFF, J. Anal. Appl. Pyrolysis 137 (2019) 246–252, https://doi.org/10.1016/j.jaap.2018.11.033.
[37] Z. Huang, N. Li, Q. Zhou, D. Wang, H. Yin, A comparative study of the pyrolysis and combustion characteristics of sodium-rich Zhundong coal in slow and rapid processes, Energy Sci. Eng. 7 (1) (2019) 98–107, https://doi.org/10.1002/ese3.242.
[38] C.-Z. Li, C. Sathe, J.R. Kershaw, Y. Pang, Fates and roles of alkali and alkaline earth metals during the pyrolysis of a Victorian brown coal, Fuel 79 (3–4) (2000) 427–438, https://doi.org/10.1016/S0016-2361(99)00178-7.
[39] D.M. Quyn, H. Wu, C.-Z. Li, Volatilisation and catalytic effects of alkali and alkaline earth metallic species during the pyrolysis and gasification of Victorian brown coal. Part I. Volatilisation of Na and Cl from a set of NaCl-loaded samples, Fuel 81 (2002) 143–149, https://doi.org/10.1016/S0016-2361(01)00127-2.
[40] F.F. Adedoyin, M.I. Gumede, F.V. Bekun, M.U. Etokakpan, D. Balsalobre-lorente, Modelling coal rent, economic growth and CO_2 emissions: does regulatory quality matter in BRICS economies? Sci. Total Environ. 710 (2020), 136284 https://doi.org/10.1016/j.scitotenv.2019.136284.
[41] S. O'Neill, Global CO_2 emissions level off in 2019, with a drop predicted in 2020, Engineering 6 (9) (2020) 958–959, https://doi.org/10.1016/j.eng.2020.07.005.
[42] C. Quan, N. Gao, Copyrolysis of biomass and coal: a review of effects of copyrolysis parameters, product properties, and synergistic mechanisms, BioMed. Res. Int. 2016 (2016), 6197867, https://doi.org/10.1155/2016/6197867.
[43] A. Veses, M. Aznar, I. Martínez, J.D. Martínez, J.M. López, M.V. Navarro, M. S. Callén, R. Murillo, T. García, Catalytic pyrolysis of wood biomass in an auger reactor using calcium-based catalysts, Bioresour. Technol. 162 (2014) 250–258, https://doi.org/10.1016/j.biortech.2014.03.146.
[44] X. Zhang, L. Sun, L. Chen, X. Xie, B. Zhao, H. Si, G. Meng, Comparison of catalytic upgrading of biomass fast pyrolysis vapors over CaO and Fe(III)/CaO catalysts, J. Anal. Appl. Pyrolysis 108 (2014) 35–40, https://doi.org/10.1016/j.jaap.2014.05.020.
[45] L. Sun, X. Zhang, L. Chen, B. Zhao, S. Yang, X. Xie, Effects of Fe contents on fast pyrolysis of biomass with Fe/CaO catalysts, J. Anal. Appl. Pyrolysis 119 (2016) 133–138, https://doi.org/10.1016/j.jaap.2016.03.008.
[46] W.-L. Wang, X.-Y. Ren, L.-F. Li, J.-M. Chang, L.-P. Cai, J. Geng, Catalytic effect of metal chlorides on analytical pyrolysis of alkali lignin, Fuel Process. Technol. 134 (2015) 345–351, https://doi.org/10.1016/j.fuproc.2015.02.015.
[47] D.L. Dalluge, K.H. Kim, R.C. Brown, The influence of alkali and alkaline earth metals on char and volatile aromatics from fast pyrolysis of lignin, J. Anal. Appl. Pyrolysis 127 (2017) 385–393, https://doi.org/10.1016/j.jaap.2017.07.011.
[48] L. Deng, J. Ye, X. Jin, D. Che, Transformation and release of potassium during fixed-bed pyrolysis of biomass, J. Energy Inst. 91 (4) (2018) 630–637, https://doi.org/10.1016/j.joei.2017.02.009.
[49] E. Leng, Y. Wang, X. Gong, B. Zhang, Y. Zhang, M. Xu, Effect of KCl and $CaCl_2$ loading on the formation of reaction intermediates during cellulose fast pyrolysis, Proc. Combust. Inst. 36 (2) (2017) 2263–2270, https://doi.org/10.1016/j.proci.2016.06.167.
[50] H. Zhang, Y. Ma, S. Shao, R. Xiao, The effects of potassium on distributions of bio-oils obtained from fast pyrolysis of agricultural and forest biomass in a fluidized bed, Appl. Energy 208 (2017) 867–877, https://doi.org/10.1016/j.apenergy.2017.09.062.
[51] S. Lin, M. Harada, Y. Suzuki, H. Hatano, Comparison of pyrolysis products between coal, Coal/CaO, and Coal/$Ca(OH)_2$ materials, Energy Fuels 17 (3) (2003) 602–607, https://doi.org/10.1021/ef020204w.
[52] J. Wang, M. Ma, Y. Bai, W. Su, X. Song, G. Yu, Effect of CaO additive on co-pyrolysis behavior of bituminous coal and cow dung, Fuel 265 (2020), 116911, https://doi.org/10.1016/j.fuel.2019.116911.

[53] T. Zhu, S. Zhang, J. Huang, Y. Wang, Effect of calcium oxide on pyrolysis of coal in a fluidized bed, Fuel Process. Technol. 64 (1–3) (2000) 271–284, https://doi.org/10.1016/S0378-3820(00)00075-8.

[54] R.J. Tyler, H.N.S. Schafer, Flash pyrolysis of coals: influence of cations on the devolatilization behaviour of brown coals, Fuel 59 (7) (1980) 487–494, https://doi.org/10.1016/0016-2361(80)90175-1.

[55] M.J. Wornat, P.F. Nelson, Effects of ion-exchanged calcium on brown coal tar composition as determined by Fourier transform infrared spectroscopy, Energy Fuels 6 (2) (1992) 136–142, https://doi.org/10.1021/ef00032a004.

[56] H. Yang, R. Yan, H. Chen, D.H. Lee, C. Zheng, Characteristics of hemicellulose, cellulose and lignin pyrolysis, Fuel 86 (12–13) (2007) 1781–1788, https://doi.org/10.1016/j.fuel.2006.12.013.

[57] M. Safar, B.J. Lin, W.H. Chen, D. Langauer, J.S. Chang, H. Raclavska, A. Pétrissans, P. Rousset, M. Pétrissans, Catalytic effects of potassium on biomass pyrolysis, combustion and torrefaction, Appl. Energy 235 (2019) 346–355, https://doi.org/10.1016/j.apenergy.2018.10.065.

[58] L. Zhou, Y. Jia, T.-H. Nguyen, A.A. Adesina, Z. Liu, Hydropyrolysis characteristics and kinetics of potassium-impregnated pine wood, Fuel Process. Technol. 116 (2013) 149–157, https://doi.org/10.1016/j.fuproc.2013.05.005.

[59] M. Poletto, H. Ornaghi, A. Zattera, Native cellulose: structure, characterization and thermal properties, Materials 7 (9) (2014) 6105–6119, https://doi.org/10.3390/ma7096105.

[60] E. Kastanaki, D. Vamvuka, P. Grammelis, E. Kakaras, Thermogravimetric studies of the behavior of lignite–biomass blends during devolatilization, Fuel Process. Technol. 77–78 (2002) 159–166, https://doi.org/10.1016/S0378-3820(02)00049-8.

[61] V. Dhyani, T. Bhaskar, A comprehensive review on the pyrolysis of lignocellulosic biomass, Renew. Energy 129 (2018) 695–716, https://doi.org/10.1016/j.renene.2017.04.035.

[62] Q. Dong, S. Zhang, L. Zhang, K. Ding, Y. Xiong, Effects of four types of dilute acid washing on moso bamboo pyrolysis using Py–GC/MS, Bioresour. Technol. 185 (2015) 62–69, https://doi.org/10.1016/j.biortech.2015.02.076.

[63] I.-Y. Eom, K.H. Kim, J.Y. Kim, S.M. Lee, H.M. Yeo, I.G. Choi, J.W. Choi, Characterization of primary thermal degradation features of lignocellulosic biomass after removal of inorganic metals by diverse solvents, Bioresour. Technol. 102 (3) (2011) 3437–3444, https://doi.org/10.1016/j.biortech.2010.10.056.

[64] A. Trubetskaya, F.H. Larsen, A. Shchukarev, K. Ståhl, K. Umeki, Potassium and soot interaction in fast biomass pyrolysis at high temperatures, Fuel 225 (2018) 89–94, https://doi.org/10.1016/j.fuel.2018.03.140.

[65] T. Okuno, N. Sonoyama, J. Hayashi, C.-Z. Li, C. Sathe, T. Chiba, Primary release of alkali and alkaline earth metallic species during the pyrolysis of pulverized biomass, Energy Fuels 19 (5) (2005) 2164–2171, https://doi.org/10.1021/ef050002a.

[66] S. Xing, H. Yuan, Huhetaoli, Y. Qi, P. Lv, Z. Yuan, Y. Chen, Characterization of the decomposition behaviors of catalytic pyrolysis of wood using copper and potassium over thermogravimetric and Py-GC/MS analysis, Energy 114 (2016) 634–646, https://doi.org/10.1016/j.energy.2016.07.154.

[67] M. Wang, J. Tian, D.G. Roberts, L. Chang, K. Xie, Interactions between corncob and lignite during temperature-programmed co-pyrolysis, Fuel 142 (2015) 102–108, https://doi.org/10.1016/j.fuel.2014.11.003.

[68] J.G. Olsson, U. Jäglid, J.B.C. Pettersson, P. Hald, Alkali metal emission during pyrolysis of biomass, Energy Fuels 11 (1997) 779–784, https://doi.org/10.1021/ef960096b.

[69] A. Trendewicz, R. Evans, A. Dutta, R. Sykes, D. Carpenter, R. Braun, Evaluating the effect of potassium on cellulose pyrolysis reaction kinetics, Biomass Bioenergy 74 (2015) 15–25, https://doi.org/10.1016/j.biombioe.2015.01.001.

[70] L. Jiang, S. Hu, L.S. Sun, S. Su, K. Xu, L.M. He, J. Xiang, Influence of different demineralization treatments on physicochemical structure and thermal degradation of biomass, Bioresour. Technol. 146 (2013) 254–260, https://doi.org/10.1016/j.biortech.2013.07.063.

[71] H. Persson, E. Kantarelis, P. Evangelopoulos, W. Yang, Wood-derived acid leaching of biomass for enhanced production of sugars and sugar derivatives during pyrolysis: Influence of acidity and treatment time, J. Anal. Appl. Pyrolysis 127 (2017) 329–334, https://doi.org/10.1016/j.jaap.2017.07.018.

[72] P. Su, K. Granholm, A. Pranovich, L. Harju, B. Holmbom, A. Ivaska, Metal ion sorption to birch and spruce wood, BioResources 7 (2) (2012) 2141–2155, https://doi.org/10.15376/biores.7.2.2141-2155.

[73] L. Sanchez-Silva, D. López-González, J. Villaseñor, P. Sánchez, J.L. Valverde, Thermogravimetric–mass spectrometric analysis of lignocellulosic and marine biomass pyrolysis, Bioresour. Technol. 109 (2012) 163–172, https://doi.org/10.1016/j.biortech.2012.01.001.

[74] N. Ellis, M.S. Masnadi, D.G. Roberts, M.A. Kochanek, A.Y. Ilyushechkin, Mineral matter interactions during co-pyrolysis of coal and biomass and their impact on intrinsic char co-gasification reactivity, Chem. Eng. J. 279 (2015) 402–408, https://doi.org/10.1016/j.cej.2015.05.057.

[75] J. Wang, M. Zhang, M. Chen, F. Min, S. Zhang, Z. Ren, Y. Yan, Catalytic effects of six inorganic compounds on pyrolysis of three kinds of biomass, Thermochim. Acta 444 (1) (2006) 110–114, https://doi.org/10.1016/j.tca.2006.02.007.

[76] Z. Chen, M. Hu, X. Zhu, D. Guo, S. Liu, Z. Hu, B. Xiao, J. Wang, M. Laghari, Characteristics and kinetic study on pyrolysis of five lignocellulosic biomass via thermogravimetric analysis, Bioresour. Technol. 192 (2015) 441–450, https://doi.org/10.1016/j.biortech.2015.05.062.

[77] R.K. Mishra, K. Mohanty, Pyrolysis kinetics and thermal behavior of waste sawdust biomass using thermogravimetric analysis, Bioresour. Technol. 251 (2018) 63–74, https://doi.org/10.1016/j.biortech.2017.12.029.

[78] S. Qiu, et al., Thermal behavior and organic functional structure of poplar-fat coal blends during co-pyrolysis, Renew, Energy 136 (2019) 308–316, https://doi.org/10.1016/j.renene.2019.01.015.

[79] H. Zhao, Q. Song, S. Liu, Y. Li, X. Wang, X. Shu, Study on catalytic co-pyrolysis of physical mixture/staged pyrolysis characteristics of lignite and straw over an catalytic beds of char and its mechanism, Energy Convers. Manag. 161 (2018) 13–26, https://doi.org/10.1016/j.enconman.2018.01.083.

[80] L. Shi, S. Yu, F.-C. Wang, J. Wang, Pyrolytic characteristics of rice straw and its constituents catalyzed by internal alkali and alkali earth metals, Fuel 96 (2012) 586–594, https://doi.org/10.1016/j.fuel.2012.01.013.

[81] P. Gao, L. Xue, Q. Lu, C. Dong, Effects of alkali and alkaline earth metals on N-containing species release during rice straw pyrolysis, Energies 8 (11) (2015) 13021–13032, https://doi.org/10.3390/en81112356.

[82] N. Zhao, B.-X. Li, The effect of sodium chloride on the pyrolysis of rice husk, Appl. Energy 178 (2016) 346–352, https://doi.org/10.1016/j.apenergy.2016.06.082.

[83] F. Guo, X. Li, Y. Liu, K. Peng, C. Guo, Z. Rao, Catalytic cracking of biomass pyrolysis tar over char-supported catalysts, Energy Convers. Manag. 167 (2018) 81–90, https://doi.org/10.1016/j.enconman.2018.04.094.

[84] A.C. Minh Loy, S. Yusup, B.L. Fui Chin, D.K. Wai Gan, M. Shahbaz, M.N. Acda, P. Unrean, E. Rianawati, Comparative study of in-situ catalytic pyrolysis of rice husk for syngas production: Kinetics modelling and product gas analysis, J. Clean. Prod. 197 (2018) 1231–1243, https://doi.org/10.1016/j.jclepro.2018.06.245.

[85] L. Han, Q. Wang, Q. Ma, C. Yu, Z. Luo, K. Cen, Influence of CaO additives on wheat-straw pyrolysis as determined by TG-FTIR analysis, J. Anal. Appl. Pyrolysis 88 (2) (2010) 199–206, https://doi.org/10.1016/j.jaap.2010.04.007.

[86] T. Bunma, P. Kuchonthara, Synergistic study between CaO and MgO sorbents for hydrogen rich gas production from the pyrolysis-gasification of sugarcane leaves, Process Saf. Environ. Prot. 118 (2018) 188–194, https://doi.org/10.1016/j.psep.2018.06.034.

[87] S.A. Channiwala, P.P. Parikh, A unified correlation for estimating HHV of solid, liquid and gaseous fuels, 1501–1063, Fuel 81 (2002) 1051–1063, https://doi.org/10.1016/S0016-2361(01)00131-4.

[88] D. Tillman, Wood as an Energy resources, Academic Press, New York, 1978, https://doi.org/10.1016/B978-0-12-691260-9.X5001-0.

[89] B. Jenkins, J. Ebeling, Correlation of physical and chemical properties of terrestrial biomass with conversion. Proceedings of Energy from Biomass and Wastes IX, Lake Buena Vista, Florida (January 28 – February 1, 1985), Institute of Gas Technology, 1985, pp. 317–403.

[90] M. Grabosky, R. Bain, Properties of biomass relevant to gasification. A Survey of Biomass Gasification: Principles of gasification, Solar Energy Research Institute, AGRIS, FAO, 1981.

[91] K. Wang, J. Zhang, B.H. Shanks, R.C. Brown, The deleterious effect of inorganic salts on hydrocarbon yields from catalytic pyrolysis of lignocellulosic biomass and its mitigation, Appl. Energy 148 (2015) 115–120, https://doi.org/10.1016/j.apenergy.2015.03.034.

[92] D. Mourant, Z. Wang, M. He, X.S. Wang, M. Garcia-Perez, K. Ling, C.Z. Li, Mallee wood fast pyrolysis: effects of alkali and alkaline earth metallic species on the yield and composition of bio-oil, Fuel 90 (9) (2011) 2915–2922, https://doi.org/10.1016/j.fuel.2011.04.033.

[93] K. Haddad, M. Jeguirim, S. Jellali, C. Guizani, L. Delmotte, S. Bennici, L. Limousy, Combined NMR structural characterization and thermogravimetric analyses for the assessment of the AAEM effect during lignocellulosic biomass pyrolysis, Energy 134 (2017) 10–23, https://doi.org/10.1016/j.energy.2017.06.022.

[94] S. Zhou, D. Liu, Z.T. Karpyn, Y. Cai, Y. Yao, Effect of coalification jumps on petrophysical properties of various metamorphic coals from different coalfields in China, J. Nat. Gas. Sci. Eng. 60 (2018) 63–76, https://doi.org/10.1016/j.jngse.2018.10.004.

[95] S.C. Saxena, Devolatilization and combustion characteristics of coal particles, Prog. Energy Combust. Sci. 16 (1) (1990) 55–94, https://doi.org/10.1016/0360-1285(90)90025-X.

[96] S.V. Vassilev, K. Kitano, C.G. Vassileva, Some relationships between coal rank and chemical and mineral composition, Fuel 75 (13) (1996) 1537–1542, https://doi.org/10.1016/0016-2361(96)00116-0.

[97] Q. Liu, H. Hu, Q. Zhou, S. Zhu, G. Chen, Effect of inorganic matter on reactivity and kinetics of coal pyrolysis, Fuel 83 (6) (2004) 713–718, https://doi.org/10.1016/j.fuel.2003.08.017.

[98] Z. Wang, J. Tan, Y. He, Y. Yuan, L. Liu, Y. Zhu, K. Cen, Catalytic effect of metal chloride additives on the volatile gas release characteristics for high-temperature lignite pyrolysis, Energy Fuels 33 (10) (2019) 9437–9445, https://doi.org/10.1021/acs.energyfuels.9b01342.

[99] T. Cui, W. Fan, Z. Dai, Q. Guo, G. Yu, F. Wang, Variation of the coal chemical structure and determination of the char molecular size at the early stage of rapid pyrolysis, Appl. Energy 179 (2016) 650–659, https://doi.org/10.1016/j.apenergy.2016.06.143.

[100] G. Skodras, G.P. Sakellaropoulos, Mineral matter effects in lignite gasification, Fuel Process. Technol. 77–78 (2002) 151–158, https://doi.org/10.1016/S0378-3820(02)00063-2.

[101] T. Popa, M. Fan, M.D. Argyle, R.B. Slimane, D.A. Bell, B.F. Towler, Catalytic gasification of a Powder River Basin coal, Fuel 103 (2013) 161–170, https://doi.org/10.1016/j.fuel.2012.08.049.

[102] J. Zhang, R. Zhang, J. Bi, Effect of catalyst on coal char structure and its role in catalytic coal gasification, Catal. Commun. 79 (2016) 1–5, https://doi.org/10.1016/j.catcom.2016.01.037.

[103] L. Ding, Z. Zhou, Q. Guo, W. Huo, G. Yu, Catalytic effects of Na_2CO_3 additive on coal pyrolysis and gasification, Fuel 142 (2015) 134–144, https://doi.org/10.1016/j.fuel.2014.11.010.

[104] Q. Li, C. Zhao, X. Chen, W. Wu, Y. Li, Comparison of pulverized coal combustion in air and in O_2/CO_2 mixtures by thermo-gravimetric analysis, J. Anal. Appl. Pyrolysis 85 (1–2) (2009) 521–528, https://doi.org/10.1016/j.jaap.2008.10.018.

[105] J. Riaza, R. Khatami, Y.A. Levendis, L. Álvarez, M.V. Gil, C. Pevida, F. Rubiera, J. J. Pis, Single particle ignition and combustion of anthracite, semi-anthracite and bituminous coals in air and simulated oxy-fuel conditions, Combust. Flame 161 (4) (2014) 1096–1108, https://doi.org/10.1016/j.combustflame.2013.10.004.

[106] R. Khatami, Y.A. Levendis, M.A. Delichatsios, Soot loading, temperature and size of single coal particle envelope flames in conventional- and oxy-combustion conditions (O_2/N_2 and O_2/CO_2), Combust. Flame 162 (6) (2015) 2508–2517, https://doi.org/10.1016/j.combustflame.2015.02.020.

[107] T. Maffei, R. Khatami, S. Pierucci, T. Faravelli, E. Ranzi, Y.A. Levendis, Experimental and modeling study of single coal particle combustion in O_2/N_2 and Oxy-fuel (O_2/CO_2) atmospheres, Combust. Flame. 160 (11) (2013) 2559–2572, https://doi.org/10.1016/j.combustflame.2013.06.002.

[108] R. Lemaire, D. Menage, S. Menanteau, J.-L. Harion, Experimental study and kinetic modeling of pulverized coal devolatilization under air and oxycombustion conditions at a high heating rate, Fuel Process. Technol. 128 (2014) 183–190, https://doi.org/10.1016/j.fuproc.2014.07.020.

[109] D. Menage, R. Lemaire, P. Seers, Experimental study and chemical reactor network modeling of the high heating rate devolatilization and oxidation of pulverized bituminous coals under air, oxygen-enriched combustion (OEC) and oxy-fuel combustion (OFC), Fuel Process. Technol. 177 (2018) 179–193, https://doi.org/10.1016/j.fuproc.2018.04.025.

[110] R. Lemaire, C. Bruhier, D. Menage, E. Therssen, P. Seers, Study of the high heating rate devolatilization of a pulverized bituminous coal under oxygen-containing atmospheres, J. Anal. Appl. Pyrolysis 114 (2015) 22–31, https://doi.org/10.1016/j.jaap.2015.04.008.

[111] W. Selvig, I. Gibson, Calorific value of coal, Chem. Coal Util. 1 (1945) 139.

[112] H. Strache and R. Lant, Kohlenchemie, Akademische Verlags-gesellschaft, Leipzig, 1924, pp.476.

[113] R. Vondracek, Brennst. Chem. 8 (1927) 22–23.

[114] E. Grummel, I. Davis, Fuel 12 (1933) 199–203.

[115] J. Yan, M. Liu, Z. Feng, Z. Bai, H. Shui, Z. Li, Z. Lei, Z. Wang, S. Ren, S. Kang, H. Yan, Study on the pyrolysis kinetics of low-medium rank coals with distributed activation energy model, Fuel 261 (2020), 116359, https://doi.org/10.1016/j.fuel.2019.116359.

[116] D.M. Grant, R.J. Pugmire, Chemical model of coal devolatilization using percolation lattice statistics, Energy Fuels 3 (1989) 175–186, https://doi.org/10.1021/ef00014a011.

[117] P.R. Solomon, M.A. Serio, G.V. Despande, E. Kroo, Cross-linking reactions during coal conversion, Energy Fuels 4 (1) (1990) 42–54, https://doi.org/10.1021/ef00019a009.

[118] Y. Zhao, L. Liu, P.H. Qiu, X. Xie, X.Y. Chen, D. Lin, S.Z. Sun, Impacts of chemical fractionation on Zhundong coal's chemical structure and pyrolysis reactivity, Fuel Process. Technol. 155 (2017) 144–152, https://doi.org/10.1016/j.fuproc.2016.05.011.

[119] K. Śpiewak, G. Czerski, S. Porada, Effect of K, Na and Ca-based catalysts on the steam gasification reactions of coal. Part I: Type and amount of one-component catalysts, Chem. Eng. Sci. 229 (2021), 116024, https://doi.org/10.1016/j.ces.2020.116024.

[120] M. Sakawa, Y. Sakurai, Y. Hara, Influence of coal characteristics on CO_2 gasification, Fuel 61 (8) (1982) 717–720, https://doi.org/10.1016/0016-2361(82)90245-9.

[121] B.B. Hattingh, R.C. Everson, H.W.J.P. Neomagus, J.R. Bunt, Assessing the catalytic effect of coal ash constituents on the CO_2 gasification rate of high ash, South African coal, Fuel Process. Technol. 92 (10) (2011) 2048–2054, https://doi.org/10.1016/j.fuproc.2011.06.003.

[122] M.J. Antal, W.S.L. Mok, G. Varhegyi, T. Szekely, Review of methods for improving the yield of charcoal from biomass, Energy Fuels 4 (1990) 221–225, https://doi.org/10.1021/ef00021a001.

[123] T.E. McGrath, W.G. Chan, M.R. Hajaligol, Low temperature mechanism for the formation of polycyclic aromatic hydrocarbons from the pyrolysis of cellulose, J. Anal. Appl. Pyrolysis 66 (2003) 51–70, https://doi.org/10.1016/S0165-2370(02)00105-5.

[124] M. Somerville, S. Jahanshahi, The effect of temperature and compression during pyrolysis on the density of charcoal made from Australian eucalypt wood, Renew, Energy 80 (2015) 471–478, https://doi.org/10.1016/j.renene.2015.02.013.

[125] J.L. Banyasz, S. Li, J. Lyons-Hart, K.H. Shafer, Gas evolution and the mechanism of cellulose pyrolysis, Fuel 80 (2001) 1757–1763, https://doi.org/10.1016/S0016-2361(01)00060-6.

[126] J. Scheirs, G. Camino, W. Tumiatti, Overview of water evolution during the thermal degradation of cellulose, Eur. Polym. J. 37 (2001) 933–942, https://doi.org/10.1016/S0014-3057(00)00211-1.

[127] Y. Sun, Z. He, R. Tu, Y. Wu, E. Jiang, X. Xu, The mechanism of wet/dry torrefaction pretreatment on the pyrolysis performance of tobacco stalk, Bioresour. Technol. 286 (2019), 121390, https://doi.org/10.1016/j.biortech.2019.121390.

[128] X. Huang, J. Ren, J.-Y. Ran, C.-L. Qin, Z.-Q. Yang, J.-P. Cao, Recent advances in pyrolysis of cellulose to value-added chemicals, Fuel Process. Technol. 229 (2022), 107175, https://doi.org/10.1016/j.fuproc.2022.107175.

[129] Q. Lu, X. Yang, C. Dong, Z. Zhang, X. Zhang, X. Zhu, Influence of pyrolysis temperature and time on the cellulose fast pyrolysis products: analytical Py-GC/MS study, J. Anal. Appl. Pyrolysis 92 (2) (2011) 430–438, https://doi.org/10.1016/j.jaap.2011.08.006.

[130] K.B. Ansari, B. Kamal, S. Beg, M.A. Wakeel Khan, M.S. Khan, M.K. Al Mesfer, M. Danish, Recent developments in investigating reaction chemistry and transport effects in biomass fast pyrolysis: A review, Renew. Sustain. Energy Rev. 150 (2021), 111454, https://doi.org/10.1016/j.rser.2021.111454.

[131] P. Morf, P. Hasler, T. Nussbaumer, Mechanisms and kinetics of homogeneous secondary reactions of tar from continuous pyrolysis of wood chips, Fuel 81 (2002) 843–853, https://doi.org/10.1016/S0016-2361(01)00216-2.

[132] P.R. Patwardhan, R.C. Brown, B.H. Shanks, Product distribution from the fast pyrolysis of hemicellulose, ChemSusChem 4 (2011) 636–643, https://doi.org/10.1002/cssc.201000425.

[133] D.K. Shen, S. Gu, A.V. Bridgwater, Study on the pyrolytic behaviour of xylan-based hemicellulose using TG–FTIR and Py–GC–FTIR, J. Anal. Appl. Pyrolysis 87 (2) (2010) 199–206, https://doi.org/10.1016/j.jaap.2009.12.001.

[134] D.K. Shen, S. Gu, The mechanism for thermal decomposition of cellulose and its main products, Bioresour. Technol. 100 (2009) 6496–6504, https://doi.org/10.1016/j.biortech.2009.06.095.

[135] X. Chen, Y. Chen, H. Yang, W. Chen, X. Wang, H. Chen, Fast pyrolysis of cotton stalk biomass using calcium oxide, Bioresour. Technol. 233 (2017) 15–20, https://doi.org/10.1016/j.biortech.2017.02.070.

[136] S. Wang, X. Guo, K. Wang, Z. Luo, Influence of the interaction of components on the pyrolysis behavior of biomass, J. Anal. Appl. Pyrolysis 91 (1) (2011) 183–189, https://doi.org/10.1016/j.jaap.2011.02.006.

[137] V. Mamleev, S. Bourbigot, J. Yvon, Kinetic analysis of the thermal decomposition of cellulose: the main step of mass loss, J. Anal. Appl. Pyrolysis 80 (1) (2007) 151–165, https://doi.org/10.1016/j.jaap.2007.01.013.

[138] P.W. Arisz, J.J. Boon, Pyrolysis mechanisms of O-(2-hydroxyethyl)celluloses, J. Anal. Appl. Pyrolysis 25 (1993) 371–385, https://doi.org/10.1016/0165-2370(93)80056-6.

[139] P.W. Arisz, G.B. Eijkel, J.J. Boon, Linking of pyrolysis-chemical ionisation mass spectrometric and monomer compositional data of O-(2-hydroxyethyl) celluloses by canonical correlation analysis, J. Anal. Appl. Pyrolysis 33 (1995) 21–28, https://doi.org/10.1016/0165-2370(94)00866-Y.

[140] J.A. Lomax, J.M. Commandeur, P.W. Arisz, and J.J. Boon, Characterisation of oligomers and sugar ring-cleavage products in the pyrolysate of cellulose, Proc. 9th Int. Conf. Fundam. Asp. Anal. Tech. Process. Appl. Pyrolysis. 19 (1991) 65–79. https://www.sciencedirect.com/science/article/abs/pii/0165237091800357.

[141] G.R. Ponder, G.N. Richards, T.T. Stevenson, Influence of linkage position and orientation in pyrolysis of polysaccharides: a study of several glucans, J. Anal. Appl. Pyrolysis 22 (1992) 217–229, https://doi.org/10.1016/0165-2370(92)85015-D.

[142] J. Piskorz, P. Majerski, D. Radlein, A. Vladars-Usas, D.S. Scott, Flash pyrolysis of cellulose for production of anhydro-oligomers, J. Anal. Appl. Pyrolysis 56 (2) (2000) 145–166, https://doi.org/10.1016/S0165-2370(00)00089-9.

[143] M. Widyawati, T.L. Church, N.H. Florin, A.T. Harris, Hydrogen synthesis from biomass pyrolysis with in situ carbon dioxide capture using calcium oxide, Int. J. Hydrog. Energy 36 (2011) 4800–4813, https://doi.org/10.1016/j.ijhydene.2010.11.103.

[144] D. Magalhães, K. Gürel, L. Matsakas, P. Christakopoulos, I. Pisano, J.J. Leahy, F. Kazanç, A. Trubetskaya, Prediction of yields and composition of char from fast pyrolysis of commercial lignocellulosic materials, organosolv fractionated and torrefied olive stones, Fuel 289 (2021), 119862, https://doi.org/10.1016/j.fuel.2020.119862.

[145] T. Hosoya, H. Kawamoto, S. Saka, Pyrolysis behaviors of wood and its constituent polymers at gasification temperature, J. Anal. Appl. Pyrolysis 78 (2) (2007) 328–336, https://doi.org/10.1016/j.jaap.2006.08.008.

[146] J. Wang, B. Zhang, Z. Zhong, K. Ding, A. Deng, M. Min, P. Chen, R. Ruan, Catalytic fast co-pyrolysis of bamboo residual and waste lubricating oil over an ex-situ dual catalytic beds of MgO and HZSM-5: analytical PY-GC/MS study, Energy Convers. Manag. 139 (2017) 222–231, https://doi.org/10.1016/j.enconman.2017.02.047.

[147] H. Kawamoto, S. Horigoshi, S. Saka, Pyrolysis reactions of various lignin model dimers, J. Wood Sci. 53 (2) (2007) 168–174, https://doi.org/10.1007/s10086-006-0834-z.

[148] B. Shrestha, et al., A multitechnique characterization of lignin softening and pyrolysis, ACS Sustain. Chem. Eng. 5 (8) (2017) 6940–6949, https://doi.org/10.1021/acssuschemeng.7b01130.

[149] T. Nakamura, H. Kawamoto, S. Saka, Pyrolysis behavior of Japanese cedar wood lignin studied with various model dimers, J. Anal. Appl. Pyrolysis 81 (2) (2008) 173–182, https://doi.org/10.1016/j.jaap.2007.11.002.

[150] S. Ren, H. Lei, L. Wang, Q. Bu, S. Chen, J. Wu, J. Julson, R. Ruan, Biofuel production and kinetics analysis for microwave pyrolysis of Douglas fir sawdust pellet, J. Anal. Appl. Pyrolysis 94 (2012) 163–169, https://doi.org/10.1016/j.jaap.2011.12.004.

[151] M. Asmadi, H. Kawamoto, S. Saka, Thermal reactions of guaiacol and syringol as lignin model aromatic nuclei, J. Anal. Appl. Pyrolysis 92 (1) (2011) 88–98, https://doi.org/10.1016/j.jaap.2011.04.011.

[152] M. Asmadi, H. Kawamoto, S. Saka, Gas- and solid/liquid-phase reactions during pyrolysis of softwood and hardwood lignins, J. Anal. Appl. Pyrolysis 92 (2) (2011) 417–425, https://doi.org/10.1016/j.jaap.2011.08.003.

[153] C. Liu, J. Hu, H. Zhang, R. Xiao, Thermal conversion of lignin to phenols: Relevance between chemical structure and pyrolysis behaviors, Fuel 182 (2016) 864–870, https://doi.org/10.1016/j.fuel.2016.05.104.

[154] O. Senneca, M. Urciuolo, R. Chirone, A semidetailed model of primary fragmentation of coal, Fuel 104 (2013) 253–261, https://doi.org/10.1016/j.fuel.2012.09.026.

[155] T. Cui, Z. Zhou, Z. Dai, C. Li, G. Yu, F. Wang, Primary fragmentation characteristics of coal particles during rapid pyrolysis, Energy Fuels 29 (10) (2015) 6231–6241, https://doi.org/10.1021/acs.energyfuels.5b01289.

[156] Y. Jia, J. Huang, Y. Wang, Effects of calcium oxide on the cracking of coal tar in the freeboard of a fluidized bed, Energy Fuels 18 (6) (2004) 1625–1632, https://doi.org/10.1021/ef034077v.

[157] C. Sathe, Y. Pang, C.-Z. Li, Effects of heating rate and ion-exchangeable cations on the pyrolysis yields from a victorian brown coal, Energy Fuels 13 (3) (1999) 748–755, https://doi.org/10.1021/ef980240o.

[158] F. Nie, T. Meng, Q. Zhang, Pyrolysis of low-rank coal: from research to practice, in: M. Samer (Ed.), Pyrolysis, InTechOpen, 2017, pp. 319–339, https://doi.org/10.5772/67498.

[159] L. Liu, S. Kumar, Z. Wang, Y. He, J. Liu, K. Cen, Catalytic effect of metal chlorides on coal pyrolysis and gasification part I. Combined TG-FTIR study for coal pyrolysis, Thermochim. Acta 655 (2017) 331–336, https://doi.org/10.1016/j.tca.2017.07.007.

[160] D. Nowakowski, J. Jones, R. Brydson, A. Ross, Potassium catalysis in the pyrolysis behaviour of short rotation willow coppice, Fuel 86 (15) (2007) 2389–2402, https://doi.org/10.1016/j.fuel.2007.01.026.

[161] H. Hwang, S. Oh, I.-G. Choi, J.W. Choi, Catalytic effects of magnesium on the characteristics of fast pyrolysis products – bio-oil, bio-char, and non-condensed pyrolytic gas fractions, J. Anal. Appl. Pyrolysis 113 (2015) 27–34, https://doi.org/10.1016/j.jaap.2014.09.028.

[162] D. Liu, Y. Yu, J. Hayashi, B. Moghtaderi, H. Wu, Contribution of dehydration and depolymerization reactions during the fast pyrolysis of various salt-loaded celluloses at low temperatures, Fuel 136 (2014) 62–68, https://doi.org/10.1016/j.fuel.2014.07.025.

[163] A. Jensen, K. Dam-Johansen, M.A. Wójtowicz, M.A. Serio, TG-FTIR study of the influence of potassium chloride on wheat straw pyrolysis, Energy Fuels 12 (5) (1998) 929–938, https://doi.org/10.1021/ef980008i.

[164] Y. Niu, Y. Lv, X. Zhang, D. Wang, P. Li, S. Hui, Effects of water leaching (simulated rainfall) and additives (KOH, KCl, and SiO_2) on the ash fusion characteristics of corn straw, Appl. Therm. Eng. 154 (2019) 485–492, https://doi.org/10.1016/j.applthermaleng.2019.03.124.

[165] L. Deng, J. Ye, X. Jin, T. Zhu, D. Che, Release and transformation of potassium during combustion of biomass, Energy Procedia 142 (2017) 401–406, https://doi.org/10.1016/j.egypro.2017.12.063.

[166] F. Rubiera, A. Arenillas, C. Pevida, R. García, J.J. Pis, K.M. Steel, J.W. Patrick, Coal structure and reactivity changes induced by chemical demineralisation, Fuel Process. Technol. 79 (3) (2002) 273–279, https://doi.org/10.1016/S0378-3820(02)00185-6.

[167] P. Rutkowski, Pyrolysis of cellulose, xylan and lignin with the K_2CO_3 and $ZnCl_2$ addition for bio-oil production, Fuel Process. Technol. 92 (3) (2011) 517–522, https://doi.org/10.1016/j.fuproc.2010.11.006.

[168] N. Shimada, H. Kawamoto, S. Saka, Different action of alkali/alkaline earth metal chlorides on cellulose pyrolysis, J. Anal. Appl. Pyrolysis 81 (1) (2008) 80–87, https://doi.org/10.1016/j.jaap.2007.09.005.

[169] M. Sun, Q. Wang, C. He, J. Gao, R. Wang, Y. Zhang, L. Xu, Q. Yao, X. Ma, Pyrolysis characteristics of Shendong coal by CH_3OH-THF swelling coupled with in-situ loading of metal ions, Fuel 253 (2019) 409–419, https://doi.org/10.1016/j.fuel.2019.04.154.

[170] K. Śpiewak, G. Czerski, S. Porada, Effect of K, Na and Ca-based catalysts on the steam gasification reactions of coal. Part II: composition and amount of multi-component catalysts, Chem. Eng. Sci. 229 (2021), 116023, https://doi.org/10.1016/j.ces.2020.116023.

[171] Y. Fu, Y. Guo, K. Zhang, Effect of three different catalysts (KCl, CaO, and Fe_2O_3) on the reactivity and mechanism of low-rank coal pyrolysis, Energy Fuels 30 (3) (2016) 2428–2433, https://doi.org/10.1021/acs.energyfuels.5b02720.

[172] C. Zhang, X. Hu, H. Guo, T. Wei, D. Dong, G. Hu, S. Hu, J. Xiang, Q. Liu, Y. Wang, Pyrolysis of poplar, cellulose and lignin: effects of acidity and alkalinity of the metal oxide catalysts, J. Anal. Appl. Pyrolysis 134 (2018) 590–605, https://doi.org/10.1016/j.jaap.2018.08.009.

[173] D. Wang, R. Xiao, H. Zhang, G. He, Comparison of catalytic pyrolysis of biomass with MCM-41 and CaO catalysts by using TGA–FTIR analysis, J. Anal. Appl. Pyrolysis 89 (2) (2010) 171–177, https://doi.org/10.1016/j.jaap.2010.07.008.

[174] P.A. Case, C. Truong, M.C. Wheeler, W.J. DeSisto, Calcium-catalyzed pyrolysis of lignocellulosic biomass components, Bioresour. Technol. 192 (2015) 247–252, https://doi.org/10.1016/j.biortech.2015.05.028.

[175] D.K.W. Gan, A.C.M. Loy, B.L.F. Chin, S. Yusup, P. Unrean, E. Rianawati, M. N. Acda, Kinetics and thermodynamic analysis in one-pot pyrolysis of rice hull using renewable calcium oxide based catalysts, Bioresour. Technol. 265 (2018) 180–190, https://doi.org/10.1016/j.biortech.2018.06.003.

[176] H.W. Ryu, Y.F. Tsang, H.W. Lee, J. Jae, S.C. Jung, S.S. Lam, E.D. Park, Y.K. Park, Catalytic co-pyrolysis of cellulose and linear low-density polyethylene over MgO-impregnated catalysts with different acid-base properties, Chem. Eng. J. 373 (2019) 375–381, https://doi.org/10.1016/j.cej.2019.05.049.

[177] S.D. Stefanidis, S.A. Karakoulia, K.G. Kalogiannis, E.F. Iliopoulou, A. Delimitis, H. Yiannoulakis, T. Zampetakis, A.A. Lappas, K.S. Triantafyllidis, Natural magnesium oxide (MgO) catalysts: a cost-effective sustainable alternative to acid zeolites for the in situ upgrading of biomass fast pyrolysis oil, Appl. Catal. B Environ. 196 (2016) 155–173, https://doi.org/10.1016/j.apcatb.2016.05.031.

[178] R. Yuan, S. Yu, Y. Shen, Pyrolysis and combustion kinetics of lignocellulosic biomass pellets with calcium-rich wastes from agro-forestry residues, Waste Manag 87 (2019) 86–96, https://doi.org/10.1016/j.wasman.2019.02.009.

[179] P. Zhu, Z. Yu, J. Zhang, B. Dai, J. Zhang, P. Liang, Z. Lei, Catalytic pyrolysis of bituminous coal under pyrolysis gas over a Ni/MgO catalyst, Chem. Eng. Technol. 40 (9) (2017) 1605–1610, https://doi.org/10.1002/ceat.201700163.

[180] Y. Li, M.N. Amin, X. Lu, C. Li, F. Ren, S. Zhang, Pyrolysis and catalytic upgrading of low-rank coal using a NiO/MgO–Al_2O_3 catalyst, Chem. Eng. Sci. 155 (2016) 194–200, https://doi.org/10.1016/j.ces.2016.08.003.

[181] J. Rizkiana, G. Guan, W.B. Widayatno, J. Yang, X. Hao, K. Matsuoka, A. Abudula, Mg-modified ultra-stable Y type zeolite for the rapid catalytic co-pyrolysis of low-rank coal and biomass, RSC Adv. 6 (3) (2016) 2096–2105, https://doi.org/10.1039/C5RA24395E.

[182] J. Li, X. Li, G. Zhou, W. Wang, C. Wang, S. Komarneni, Y. Wang, Catalytic fast pyrolysis of biomass with mesoporous ZSM-5 zeolites prepared by desilication with NaOH solutions, Appl. Catal. Gen. 470 (2014) 115–122, https://doi.org/10.1016/j.apcata.2013.10.040.

[183] S. Karnjanakom, T. Suriya-umporn, A. Bayu, S. Kongparakul, C. Samart, C. Fushimi, A. Abudula, G. Guan, High selectivity and stability of Mg-doped Al-MCM-41 for in-situ catalytic upgrading fast pyrolysis bio-oil, Energy Convers. Manag. 142 (2017) 272–285, https://doi.org/10.1016/j.enconman.2017.03.049.

[184] M. Zabeti, T.S. Nguyen, L. Lefferts, H.J. Heeres, K. Seshan, In situ catalytic pyrolysis of lignocellulose using alkali-modified amorphous silica alumina, Bioresour. Technol. 118 (2012) 374–381, https://doi.org/10.1016/j.biortech.2012.05.034.

[185] A. Imran, E.A. Bramer, K. Seshan, G. Brem, High quality bio-oil from catalytic flash pyrolysis of lignocellulosic biomass over alumina-supported sodium carbonate, Fuel Process. Technol. 127 (2014) 72–79, https://doi.org/10.1016/j.fuproc.2014.06.011.

[186] Z. Sun, B. Xu, A.H. Rony, S. Toan, S. Chen, K.A.M. Gasem, H. Adidharma, M. Fan, W. Xiang, Thermogravimetric and kinetics investigation of pine wood pyrolysis catalyzed with alkali-treated CaO/ZSM-5, Energy Convers. Manag. 146 (2017) 182–194, https://doi.org/10.1016/j.enconman.2017.04.104.

[187] E.F. Iliopoulou, K.S. Triantafyllidis, A.A. Lappas, Overview of catalytic upgrading of biomass pyrolysis vapors toward the production of fuels and high-value chemicals, WIREs Energy Environ. 8 (1) (2019), e322, https://doi.org/10.1002/wene.322.

[188] Y. Yu, D. Liu, H. Wu, Formation and Characteristics of Reaction Intermediates from the Fast Pyrolysis of NaCl- and $MgCl_2$- loaded celluloses, Energy Fuels 28 (1) (2014) 245–253, https://doi.org/10.1021/ef401483u.

[189] C. Yang, X. Lu, W. Lin, X. Yang, J. Yao, TG-FTIR study on corn straw pyrolysis-influence of minerals, Chem. Res. Chin. Univ. 22 (4) (2006) 524–532, https://doi.org/10.1016/S1005-9040(06)60155-4.

[190] H. Hwang, S. Oh, T.-S. Cho, I.-G. Choi, J.W. Choi, Fast pyrolysis of potassium impregnated poplar wood and characterization of its influence on the formation as well as properties of pyrolytic products, Bioresour. Technol. 150 (2013) 359–366, https://doi.org/10.1016/j.biortech.2013.09.132.

[191] M. Nishimura, S. Iwasaki, M. Horio, The role of potassium carbonate on cellulose pyrolysis, J. Taiwan Inst. Chem. Eng. 40 (6) (2009) 630–637, https://doi.org/10.1016/j.jtice.2009.05.005.

[192] R. Mahadevan, S. Adhikari, R. Shakya, K. Wang, D. Dayton, M. Lehrich, S. E. Taylor, Effect of alkali and alkaline earth metals on in-situ catalytic fast pyrolysis of lignocellulosic biomass: a microreactor study, Energy Fuels 30 (4) (2016) 3045–3056, https://doi.org/10.1021/acs.energyfuels.5b02984.

[193] C. Yang, J. Yao, W. Lin, Y. Ding, S. Liu, Influence of minerals on biomass pyrolysis and its solution, Chem. Bioeng. 10 (2005) 17–19.

[194] L Jiang, S. Hu, J. Xiang, S. Su, L.S. Sun, K. Xu, Y. Yao, Release characteristics of alkali and alkaline earth metallic species during biomass pyrolysis and steam gasification process, Bioresour. Technol. 116 (2012) 278–284, https://doi.org/10.1016/j.biortech.2012.03.051.

[195] L. Jiang, S. Hu, Y. Wang, S. Su, L. Sun, B. Xu, L. He, J. Xiang, Catalytic effects of inherent alkali and alkaline earth metallic species on steam gasification of biomass, Int. J. Hydrog. Energy 40 (45) (2015) 15460–15469, https://doi.org/10.1016/j.ijhydene.2015.08.111.

[196] M.H. Shah, L. Deng, H. Bennadji, E.M. Fisher, Pyrolysis of potassium-doped wood at the centimeter and submillimeter scales, Energy Fuels 29 (11) (2015) 7350–7357, https://doi.org/10.1021/acs.energyfuels.5b01776.

[197] J.A. Santana, N.G. Sousa, C.R. Cardoso, W.S. Carvalho, C.H. Ataíde, Sodium, zinc and magnesium chlorides as additives for soybean hulls pyrolysis: Influence on the temperature range of reactions and product selectivity, J. Therm. Anal. Calorim. 125 (1) (2016) 471–481, https://doi.org/10.1007/s10973-016-5381-2.

[198] Z. Wang, F. Wang, J. Cao, J. Wang, Pyrolysis of pine wood in a slowly heating fixed-bed reactor: potassium carbonate versus calcium hydroxide as a catalyst, Fuel Process. Technol. 91 (8) (2010) 942–950, https://doi.org/10.1016/j.fuproc.2009.09.015.

[199] Q. Lu, Z. Zhang, X. Yang, C. Dong, X. Zhu, Catalytic fast pyrolysis of biomass impregnated with K_3PO_4 to produce phenolic compounds: analytical Py-GC/MS study, J. Anal. Appl. Pyrolysis 104 (2013) 139–145, https://doi.org/10.1016/j.jaap.2013.08.011.

[200] N. Shimada, H. Kawamoto, S. Saka, Solid-state hydrolysis of cellulose and methyl α- and β-d-glucopyranosides in presence of magnesium chloride, Carbohydr. Res. 342 (10) (2007) 1373–1377, https://doi.org/10.1016/j.carres.2007.04.009.

[201] A. Khelfa, A. Bensakhria, J.V. Weber, Investigations into the pyrolytic behaviour of birch wood and its main components: primary degradation mechanisms, additivity and metallic salt effects, J. Anal. Appl. Pyrolysis 101 (2013) 111–121, https://doi.org/10.1016/j.jaap.2013.02.004.

[202] H. Wu, K. Yip, Z. Kong, C.Z. Li, D. Liu, Y. Yu, X. Gao, Removal and recycling of inherent inorganic nutrient species in mallee biomass and derived biochars by

water leaching, Ind. Eng. Chem. Res. 50 (21) (2011) 12143–12151, https://doi.org/10.1021/ie200679n.
[203] F. Chireshe, F.-X. Collard, J.F. Görgens, Production of an upgraded bio-oil with minimal water content by catalytic pyrolysis: optimisation and comparison of CaO and MgO performances, J. Anal. Appl. Pyrolysis 146 (2020), 104751, https://doi.org/10.1016/j.jaap.2019.104751.
[204] X. Lin, Z. Zhang, Z. Zhang, J. Sun, Q. Wang, C.U. Pittman, Catalytic fast pyrolysis of a wood-plastic composite with metal oxides as catalysts, Waste Manag 79 (2018) 38–47, https://doi.org/10.1016/j.wasman.2018.07.021.
[205] Q. Lu, Z. Tang, Y. Zhang, X. Zhu, Catalytic upgrading of biomass fast pyrolysis vapors with Pd/SBA-15 catalysts, Ind. Eng. Chem. Res. 49 (6) (2010) 2573–2580, https://doi.org/10.1021/ie901198s.
[206] P.A. Case, M.C. Wheeler, W.J. DeSisto, Formate assisted pyrolysis of pine sawdust for in-situ oxygen removal and stabilization of bio-oil, Bioresour. Technol. 173 (2014) 177–184, https://doi.org/10.1016/j.biortech.2014.09.075.
[207] B. Zhao, X. Zhang, L. Chen, L. Sun, H. Si, G. Chen, High quality fuel gas from biomass pyrolysis with calcium oxide, Bioresour. Technol. 156 (2014) 78–83, https://doi.org/10.1016/j.biortech.2014.01.031.
[208] W. Xu, A. Tomita, Effect of metal oxides on the secondary reactions of volatiles from coal, Fuel 68 (5) (1989) 673–676, https://doi.org/10.1016/0016-2361(89)90173-7.
[209] Q. Liu, S. Wang, Y. Zheng, Z. Luo, K. Cen, Mechanism study of wood lignin pyrolysis by using TG–FTIR analysis, J. Anal. Appl. Pyrolysis 82 (1) (2008) 170–177, https://doi.org/10.1016/j.jaap.2008.03.007.
[210] R. Khalil, G. Várhegyi, S. Jäschke, M.G. Grønli, J. Hustad, CO_2 gasification of biomass chars: a kinetic study, Energy Fuels 23 (1) (2009) 94–100, https://doi.org/10.1021/ef800739m.
[211] Y. Lin, C. Zhang, M. Zhang, J. Zhang, Deoxygenation of bio-oil during pyrolysis of biomass in the presence of CaO in a fluidized-bed reactor, Energy Fuels 24 (10) (2010) 5686–5695, https://doi.org/10.1021/ef1009605.
[212] D.L. Ellig, C.K. Lai, D.W. Mead, J.P. Longwell, W.A. Peters, Pyrolysis of volatile aromatic hydrocarbons and n-heptane over calcium oxide and quartz, Ind. Eng. Chem. Process Des. Dev. 24 (4) (1985) 1080–1087, https://doi.org/10.1021/i200031a031.
[213] K. Shi, S. Shao, Q. Huang, X. Liang, L. Jiang, and Y. Li, Review of catalytic pyrolysis of biomass for bio-oil, in 2011 International Conference on Materials for Renewable Energy & Environment, Shanghai, China. (2011) 317–321. https://doi.org/10.1109/ICMREE.2011.5930821.
[214] H.W. Lee, S.H. Park, J.K. Jeon, R. Ryoo, W. Kim, D.J. Suh, Y.K. Park, Upgrading of bio-oil derived from biomass constituents over hierarchical unilamellar mesoporous MFI nanosheets, Catal. Today 232 (2014) 119–126, https://doi.org/10.1016/j.cattod.2013.12.015.
[215] C.A. Gaertner, J.C. Serrano-Ruiz, D.J. Braden, J.A. Dumesic, Catalytic coupling of carboxylic acids by ketonization as a processing step in biomass conversion, J. Catal. 266 (1) (2009) 71–78, https://doi.org/10.1016/j.jcat.2009.05.015.
[216] L. Deng, Y. Fu, Q.-X. Guo, Upgraded acidic components of bio-oil through catalytic ketonic condensation, Energy Fuels 23 (1) (2009) 564–568, https://doi.org/10.1021/ef800692a.
[217] L. Fan, P. Chen, Y. Zhang, S. Liu, Y. Liu, Y. Wang, L. Dai, R. Ruan, Fast microwave-assisted catalytic co-pyrolysis of lignin and low-density polyethylene with HZSM-5 and MgO for improved bio-oil yield and quality, Bioresour. Technol. 225 (2017) 199–205, https://doi.org/10.1016/j.biortech.2016.11.072.
[218] H.W. Ryu, H.W. Lee, J. Jae, Y.-K. Park, Catalytic pyrolysis of lignin for the production of aromatic hydrocarbons: effect of magnesium oxide catalyst, Energy 179 (2019) 669–675, https://doi.org/10.1016/j.energy.2019.05.015.
[219] C.A. Mullen, A.A. Boateng, Accumulation of inorganic impurities on hzsm-5 zeolites during catalytic fast pyrolysis of switchgrass, Ind. Eng. Chem. Res. 52 (48) (2013) 17156–17161, https://doi.org/10.1021/ie4030209.
[220] P.K.W. Likun, H. Zhang, T. Vitidsant, P. Reubroycharoen, R. Xiao, Influence of inorganic matter in biomass on the catalytic production of aromatics and olefins in a fluidized-bed reactor, Energy Fuels 31 (6) (2017) 6120–6131, https://doi.org/10.1021/acs.energyfuels.7b00339.
[221] P. Das, A. Ganesh, P. Wangikar, Influence of pretreatment for deashing of sugarcane bagasse on pyrolysis products, Biomass Bioenergy 27 (5) (2004) 445–457, https://doi.org/10.1016/j.biombioe.2004.04.002.
[222] A. Chen, X. Yang, W. Lin Release, characteristics of chlorine and alkali metals during pyrolysis and gasification of biomass by thermodynamical equilibrium analysis, J. Fuel Chem. Technol. 35 (5) (2007) 539–547, https://doi.org/10.3969/j.issn.0253-2409.2007.05.006.
[223] C. Yu, Z. Luo, W. Zhang, M. Fang, J. Zhou, K. Cen, Inorganic material emission during biomass pyrolysis, J. Fuel Chem. Technol. 28 (5) (2000) 420–425, https://doi.org/10.3969/j.issn.0253-2409.2000.05.009.
[224] H. Zhao, Q. Song, X. Wu, Q. Yao, Study on the transformation of inherent potassium during the fast-pyrolysis process of rice straw, Energy Fuels 29 (10) (2015) 6404–6411, https://doi.org/10.1021/acs.energyfuels.5b00851.
[225] J.N. Knudsen, P.A. Jensen, K. Dam-Johansen, Transformation and release to the gas phase of Cl, K, and S during combustion of annual biomass, Energy Fuels 18 (5) (2004) 1385–1399, https://doi.org/10.1021/ef049944q.
[226] X. Zou, J. Yao, X. Yang, W. Song, W. Lin, Catalytic effects of metal chlorides on the pyrolysis of lignite, Energy Fuels 21 (2) (2007) 619–624, https://doi.org/10.1021/ef060477h.
[227] C.-Z. Li, Some recent advances in the understanding of the pyrolysis and gasification behaviour of Victorian brown coal, Fuel 86 (12–13) (2007) 1664–1683, https://doi.org/10.1016/j.fuel.2007.01.008.
[228] S. Xu, Z. Zhou, J. Xiong, G. Yu, F. Wang, Effects of alkaline metal on coal gasification at pyrolysis and gasification phases, Fuel 90 (5) (2011) 1723–1730, https://doi.org/10.1016/j.fuel.2011.01.033.
[229] M. Shibaoka, Y. Ohtsukat, M.J. Wornat, C.G. Thomas, Application of microscopy to the investigation of brown coal pyrolysis, Fuel 74 (1995) 1648–1653, https://doi.org/10.1016/0016-2361(95)00128-R.
[230] M.R. Martínez-Tarazona, A. Martínez-Alonso, J.M.D. Tascón, Interactions between carboxyl groups and inorganic elements in Spanish brown coals, Fuel 69 (3) (1990) 362–367, https://doi.org/10.1016/0016-2361(90)90101-U.
[231] Y. Bai, P. Lv, F. Li, X. Song, W. Su, G. Yu, Investigation into Ca/Na compounds catalyzed coal pyrolysis and char gasification with steam, Energy Convers. Manag. 184 (2019) 172–179, https://doi.org/10.1016/j.enconman.2019.01.063.
[232] D. Wu, G. Liu, S. Chen, R. Sun, An experimental investigation on heating rate effect in the thermal behavior of perhydrous bituminous coal during pyrolysis, J. Therm. Anal. Calorim. 119 (3) (2015) 2195–2203, https://doi.org/10.1007/s10973-015-4401-y.
[233] X. Jia, Q. Wang, L. Han, L. Cheng, M. Fang, Z. Luo, K. Cen, Sulfur transformation during the pyrolysis of coal with the addition of $CaSO_4$ in a fixed-bed reactor, J. Anal. Appl. Pyrolysis 124 (2017) 319–326, https://doi.org/10.1016/j.jaap.2017.01.016.
[234] J. Gao, Y. Zhang, D. Meng, T. Jiao, X. Qin, G. Bai, P. Liang, Effect of ash and dolomite on the migration of sulfur from coal pyrolysis volatiles, J. Anal. Appl. Pyrolysis 140 (2019) 349–354, https://doi.org/10.1016/j.jaap.2019.04.013.
[235] M. Puig-Gamero, J. Lara-Díaz, J.L. Valverde, L. Sanchez-Silva, P. Sánchez, Dolomite effect on steam co-gasification of olive pomace, coal and petcoke: TGA-MS analysis, reactivity and synergistic effect, Fuel 234 (2018) 142–150, https://doi.org/10.1016/j.fuel.2018.07.014.
[236] Y. Zhang, P. Liang, T. Jiao, J. Wu, H. Zhang, Effect of foreign minerals on sulfur transformation in the step conversion of coal pyrolysis and combustion, J. Anal. Appl. Pyrolysis 127 (2017) 240–245, https://doi.org/10.1016/j.jaap.2017.07.028.
[237] D. Franklin, A. Peters, J.B. Howard, Mineral matter effects on the rapid pyrolysis and hydropyrolysis of a bituminous coal. I. Effects on yields of char, tar and light gaseous volatiles, Fuel 61 (1982) 155–160, https://doi.org/10.1016/0016-2361(82)90227-7.
[238] P.A. Simell, J.K. Leppälahti, J.B. Bredenberg, Catalytic purification of tarry fuel gas with carbonate rocks and ferrous materials, Fuel 71 (2) (1992) 211–218, https://doi.org/10.1016/0016-2361(92)90011-C.
[239] A.W. Coats, J.P. Redfern, Kinetic method from thermogravimetric data, Nature 201 (1964) 68–69, https://doi.org/10.1038/201068a0.
[240] K. Akiyama, H. Pak, Y. Ueki, R. Yoshiie, I. Naruse, Effect of MgO addition to upgraded brown coal on ash-deposition behavior during combustion, Fuel 90 (11) (2011) 3230–3236, https://doi.org/10.1016/j.fuel.2011.06.041.
[241] J. Xu, X. Song, G. Yu, C. Du, Investigating the effect of flux on ash fusibility of high-calcium coal, ACS Omega 5 (20) (2020) 11361–11368, https://doi.org/10.1021/acsomega.0c00320.
[242] M. Sciazko, K. Kubica, The effect of dolomite addition on sulphur, chlorine and hydrocarbons distribution in a fluid-bed mild gasification of coal, Fuel Process. Technol. 77–78 (2002) 95–102, https://doi.org/10.1016/S0378-3820(02)00060-7.
[243] X. Ma, X. Zhao, J. Gu, J. Shi, Co-gasification of coal and biomass blends using dolomite and olivine as catalysts, Renew. Energy 132 (2019) 509–514, https://doi.org/10.1016/j.renene.2018.07.077.
[244] Q. Qin, J. Zhou, B. Lin, C. Xie, L. Zhou, Influence of coal ash on the characteristics of corn straw pyrolysis products, Bioresour. Technol. 318 (2020), 124055, https://doi.org/10.1016/j.biortech.2020.124055.
[245] S. Wang, H. Lin, B. Ru, G. Dai, X. Wang, G. Xiao, Z. Luo, Kinetic modeling of biomass components pyrolysis using a sequential and coupling method, Fuel 185 (2016) 763–771, https://doi.org/10.1016/j.fuel.2016.08.037.
[246] S. Vyazovkin, C.A. Wight, Model-free and model-fitting approaches to kinetic analysis of isothermal and nonisothermal data, Thermochim. Acta 340–341 (1999) 53–68, https://doi.org/10.1016/S0040-6031(99)00253-1.
[247] D.B. Anthony, J.B. Howard, H.C. Hottel, H.P. Meissner, Rapid devolatilization of pulverized coal, Symp. Int. Combust. 15 (1) (1975) 1303–1317, https://doi.org/10.1016/S0082-0784(75)80392-4.
[248] D. Anthony, J. Howard, H. Hottel, H. Meissner, Rapid devolatilization and hydrogasification of bituminous coal, Fuel 55 (2) (1976) 121–128, https://doi.org/10.1016/0016-2361(76)90008-9.
[249] E. Ranzi, A. Cuoci, T. Faravelli, A. Frassoldati, G. Migliavacca, S. Pierucci, S. Sommariva, Chemical kinetics of biomass pyrolysis, Energy Fuels 22 (6) (2008) 4292–4300, https://doi.org/10.1021/ef800551t.
[250] S. Sommariva, T. Maffei, G. Migliavacca, T. Faravelli, E. Ranzi, A predictive multi-step kinetic model of coal devolatilization, Fuel 89 (2) (2010) 318–328, https://doi.org/10.1016/j.fuel.2009.07.023.
[251] T. Maffei, A. Frassoldati, A. Cuoci, E. Ranzi, T. Faravelli, Predictive one step kinetic model of coal pyrolysis for CFD applications, Proc. Combust. Inst. 34 (2) (2013) 2401–2410, https://doi.org/10.1016/j.proci.2012.08.006.
[252] H. Wu, Z. Zhao, W. Zhang, H. Li, F. He, Effects of alkali/alkaline earth metals on pyrolysis characteristics of cellulose, Trans. CSAE 28 (4) (2012) 215–222, https://doi.org/10.3969/j.issn.1002-6819.2012.04.036.
[253] W. Zhou, B. Bai, G. Chen, L. Ma, D. Jing, B. Yan, Study on catalytic properties of potassium carbonate during the process of sawdust pyrolysis, Int. J. Hydrog. Energy 43 (30) (2018) 13829–13841, https://doi.org/10.1016/j.ijhydene.2018.02.002.
[254] S. Vyazovkin, A.K. Burnham, J.M. Criado, L.A. Pérez-Maqueda, C. Popescu, N. Sbirrazzuoli, ICTAC kinetics committee recommendations for performing

kinetic computations on thermal analysis data, Thermochim. Acta 520 (1–2) (2011) 1–19, https://doi.org/10.1016/j.tca.2011.03.034.
[255] A. Khawam, D.R. Flanagan, Complementary use of model-free and modelistic methods in the analysis of solid-state kinetics, J. Phys. Chem. B. 109 (20) (2005) 10073–10080, https://doi.org/10.1021/jp050589u.
[256] A. Anca-Couce, A. Berger, N. Zobel, How to determine consistent biomass pyrolysis kinetics in a parallel reaction scheme, Fuel 123 (2014) 230–240, https://doi.org/10.1016/j.fuel.2014.01.014.
[257] J. Cai, D. Xu, Z. Dong, X. Yu, Y. Yang, S.W. Banks, A.V. Bridgwater, Processing thermogravimetric analysis data for isoconversional kinetic analysis of lignocellulosic biomass pyrolysis: case study of corn stalk, Renew. Sustain. Energy Rev. 82 (2018) 2705–2715, https://doi.org/10.1016/j.rser.2017.09.113.
[258] S. Yi, X. He, H. Lin, H. Zheng, C. Li, C. Li, Synergistic effect in low temperature co-pyrolysis of sugarcane bagasse and lignite, Korean J. Chem. Eng. 33 (10) (2016) 2923–2929, https://doi.org/10.1007/s11814-016-0129-z.
[259] A.K. Sadhukhan, P. Gupta, T. Goyal, R.K. Saha, Modelling of pyrolysis of coal–biomass blends using thermogravimetric analysis, Bioresour. Technol. 99 (17) (2008) 8022–8026, https://doi.org/10.1016/j.biortech.2008.03.047.
[260] Z. Wu, S. Wang, J. Zhao, L. Chen, H. Meng, Thermal behavior and char structure evolution of bituminous coal blends with edible fungi residue during co-pyrolysis, Energy Fuels 28 (2014) 1792–1801, https://doi.org/10.1021/ef500261q.
[261] Y. Song, A. Tahmasebi, J. Yu, Co-pyrolysis of pine sawdust and lignite in a thermogravimetric analyzer and a fixed-bed reactor, Bioresour. Technol. 174 (2014) 204–211, https://doi.org/10.1016/j.biortech.2014.10.027.
[262] M. Ma, Y. Bai, X. Song, J. Wang, W. Su, M. Yao, G. Yu, Investigation into the co-pyrolysis behaviors of cow manure and coal blending by TG–MS, Sci. Total Environ. 728 (2020), 138828, https://doi.org/10.1016/j.scitotenv.2020.138828.
[263] Y. Song, et al., The biomass potassium migration rule during coal biomass co-pyrolysis process, J. Taiyuan Univ. Technol. (2018).
[264] T.J. Morgan, R. Kandiyoti, Pyrolysis of coals and biomass: analysis of thermal breakdown and its products, Chem. Rev. 114 (2014) 1547–1607, https://doi.org/10.1021/cr400194p.
[265] D.K. Park, S.D. Kim, S.H. Lee, J.G. Lee, Co-pyrolysis characteristics of sawdust and coal blend in TGA and a fixed bed reactor, Bioresour. Technol. 101 (2010) 6151–6156, https://doi.org/10.1016/j.biortech.2010.02.087.
[266] Z. Zheng, Y. Huang, J. Pan, J. Jiang, W. Dai, Research progress in co-pyrolysis-liquefaction of coal and biomass, Biomass Chem. Eng. 43 (5) (2009) 55–60.
[267] O. Onay, E. Bayram, O.M. Kockar, Copyrolysis of seyitomer-lignite and safflower seed: influence of the blending ratio and pyrolysis temperature on product yields and oil characterization, Energy Fuels 21 (2007) 3049–3056, https://doi.org/10.1021/ef700230s.